AN ABSTRACT OF THE THESIS OF

Angela K. McDannel for the degree of Master of Science in

Geology presented on January 12, 1989   .

Title: Geology of the Southernmost Deschutes Basin, Tumalo

Quadrangle, Deschutes County, Oregon

Abstract approved: _Edward M Taylor_____

Dr. Edward M. Taylor

    The Tumalo quadrangle lies approximately 30 kilometers behind the

Cascade volcanic arc and marks the southernmost extent of continuously

exposed Deschutes Formation rocks. Deschutes Formation rocks in the

Tumalo quadrangle include late Miocene volcaniclastic sedimentary

rocks, ignimbrites and lapillistones, and late Miocene to early

Pliocene basalts and basaltic andesites. Volcaniclastic sediment and

pyroclastic flows originated from sources west to southwest of the

Tumalo area and were the products of Early High Cascade arc volcanism.

Most pyroclastic flows and falls had silicic compositions and silicic

volcanic material dominated the sedimentary deposits. Intermittent

and apparently widespread, high discharge events onto a back-arc

alluvial plain deposited tuffaceous sediments, much of which became

incipient soils during long periods of subaerial exposure. The close

of sedimentation was coincident with the initiation of local volcanism

at approximately 5.4 Ma. Several small monogenetic shield volcanoes

and cinder cones in the Tumalo area erupted the basalt and basaltic

andesite lavas which cap the sedimentary section. The basalts are typically porphyritic and high in Al_2O_3. Basaltic andesites are aphyric to sparsely porphyritic, are commonly high in FeO and TiO_2, appear younger than the basalts, and are not related to the basalts by simple fractionation. Both lava types have relatively evolved compositions based on their Fe' values.

An inlier of older Tertiary rhyodacite lavas known as Cline Buttes lies near the northern boundary of the study and is the only locally exposed pre-Deschutes Formation unit. The southern part of the Tumalo quadrangle marks the boundary between continuously exposed Deschutes Formation rocks to the north and Late High Cascade volcanic units to the south. After a hiatus of approximately 4 million years, deposition in the Tumalo area resumed at approximately 0.6 Ma when pyroclastic flows from the High Cascade Range flowed east and northeast into the Tumalo area to rest disconformably above the Deschutes Formation. A diktytaxitic basalt from Newberry volcano locally overlies the pyroclastic units. Widespread, thick alluvium obscures some 16 km^2 of bedrock in the study area and appears to be the result of deposition during high discharge events associated with late Pleistocene to Holocene age glaciation of the High Cascade Range.

Some thirty en echelon normal faults of the Tumalo fault zone trend between N15°-35°W and cut Pleistocene and older units in the Tumalo quadrangle. Deschutes Formation basalt and basaltic andesite vents are localized in the fault zone. This suggests volcanism was structurally controlled and that an tensional stress regime with a northeast-southwest least compressive stress orientation prevailed in the Tumalo area between the late Miocene to late Pleistocene.

Geology of the Southernmost Deschutes Basin,
Tumalo Quadrangle, Deschutes County, Oregon

by

Angela K. McDannel

A THESIS

submitted to

Oregon State University

in partial fulfillment of
the requirements for the
degree of

Master of Science

Completed January 12, 1989
Commencement June 1989

APPROVED:

_____
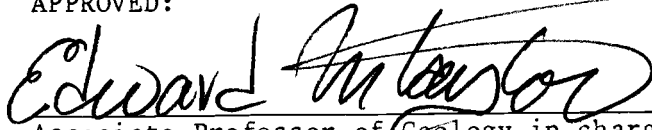
Associate Professor of Geology in charge of major

_____
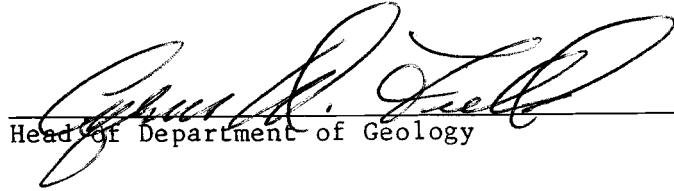
Head of Department of Geology

_____
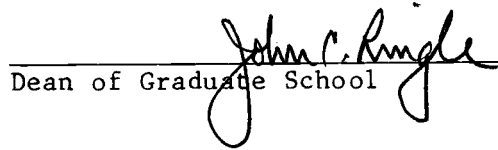
Dean of Graduate School

Date thesis is presented   January 12, 1989

ACKNOWLEDGEMENTS

TABLE OF CONTENTS

LIST OF FIGURES

LIST OF TABLES

Geology of the Southernmost Deschutes Basin, Tumalo Quadrangle, Deschutes County, Oregon

INTRODUCTION

The Tumalo quadrangle marks the southernmost extent of continuously exposed Deschutes Formation rocks. Locally exposed Deschutes Formation lithologies include non marine volcaniclastic sedimentary rocks, pyroclastic flow and fall deposits, and basalt and basaltic andesite lavas. Cline Buttes, an inlier of rhyodacite domes, are the only locally exposed pre-Deschutes Formation rocks. Near Tumalo, the Deschutes Formation disappears beneath Pleistocene pyroclastic deposits of the High Cascades and a lava flow from Newberry volcano. Stratigraphic units of all ages (Figure 1) are cut by north-northwest trending en echelon faults of the Tumalo fault zone.

The objectives of this study were to: 1) characterize the lithology, stratigraphy and major element chemistry of the Deschutes Formation in the Tumalo quadrangle; 2) compare the lithology and stratigraphy of the southernmost Deschutes basin with that of the more northerly parts of the basin; 3) identify local sources for Deschutes Formation lavas; 4) determine the nature of the contact between Deschutes Formation and Quaternary rocks; and 5) investigate the structure of the Tumalo fault zone and its relationship to regional tectonism.

Cascade volcanic episode *	Unit	Tumalo quadrangle stratigraphy	Age	Ma
Late High Cascade	High Cascade	hiatus	Pleistocene / Pliocene	1 2 3 4 5
Early High Cascade	Deschutes Formation		Miocene	6 7 8
Late Western Cascade	Pre-Deschutes Formation	hiatus		9 10 11 12 13 14 15 16 17

Cline Buttes
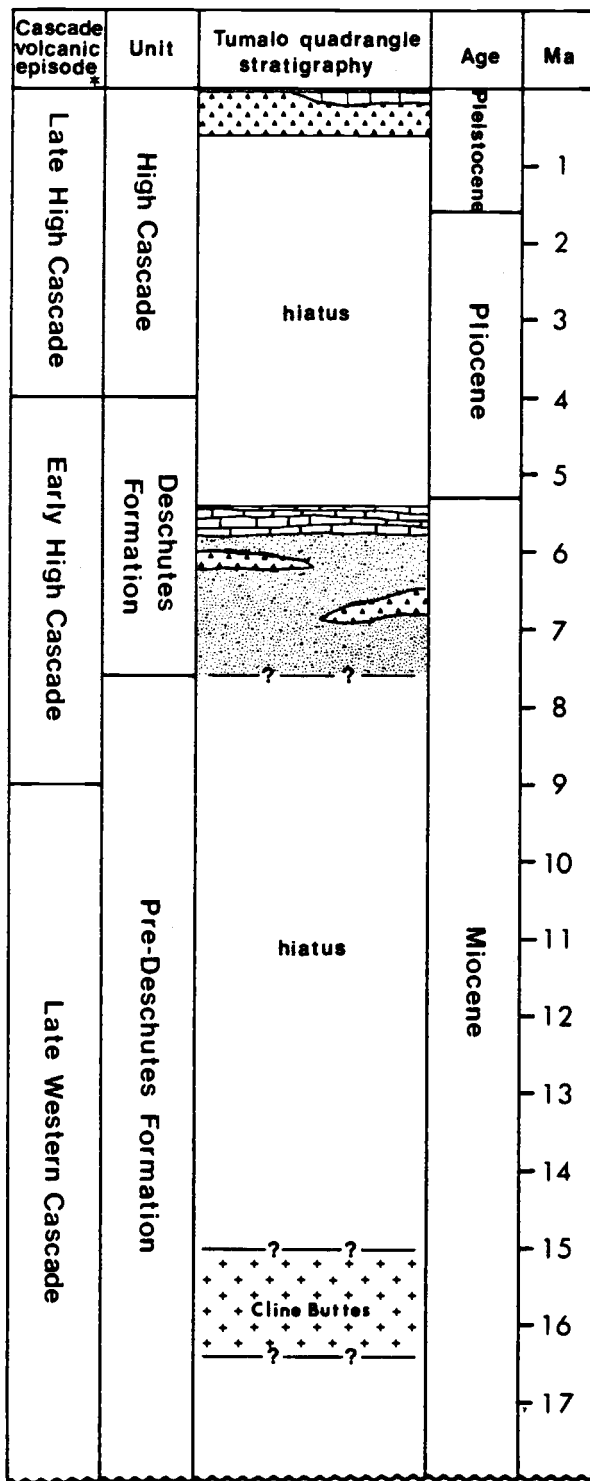
Figure 1.   Stratigraphy of the Tumalo quadrangle. (GSA DNAG 1983 geologic time scale).   * Cascade volcanic episodes after Priest and others, 1983.

LOCATION, ACCESS AND PHYSIOGRAPHY

The setting of this study is on the boundary between the High Lava Plains and the Deschutes-Umatilla Plateau physiographic provinces, approximately 32 km east of the High Cascade Range. The Tumalo quadrangle (Figure 2) lies in western Deschutes County and covers an area of approximately 88 km^2. The hamlet of Tumalo lies in the south part of the quadrangle. Three population centers are located nearby; the town of Sisters lies 23 km to the northwest, and the cities of Bend and Redmond are 10 km to the southeast and 19 km to the northeast, respectively.

The gentle topography of the area facilitates access. Main topographic features are Cline Buttes (1,368 m), low-lying cinder cones and shield volcanoes, and the Deschutes River Canyon. Canyon depth is nowhere greater than 67 m.

PREVIOUS WORK

Interest in the Deschutes Formation began with evaluation of water resources and potential dam sites in central Oregon. Russell (1905) referred to the rocks exposed in the Deschutes River canyon as the "Deschutes Sand." I. Williams (1924) suggested the name Deschutes Formation better described the varied lithology in the canyon. Authors of ensuing publications referred to these rocks by various names: the Madras Formation (Hodge, 1928, 1940; I. Williams,
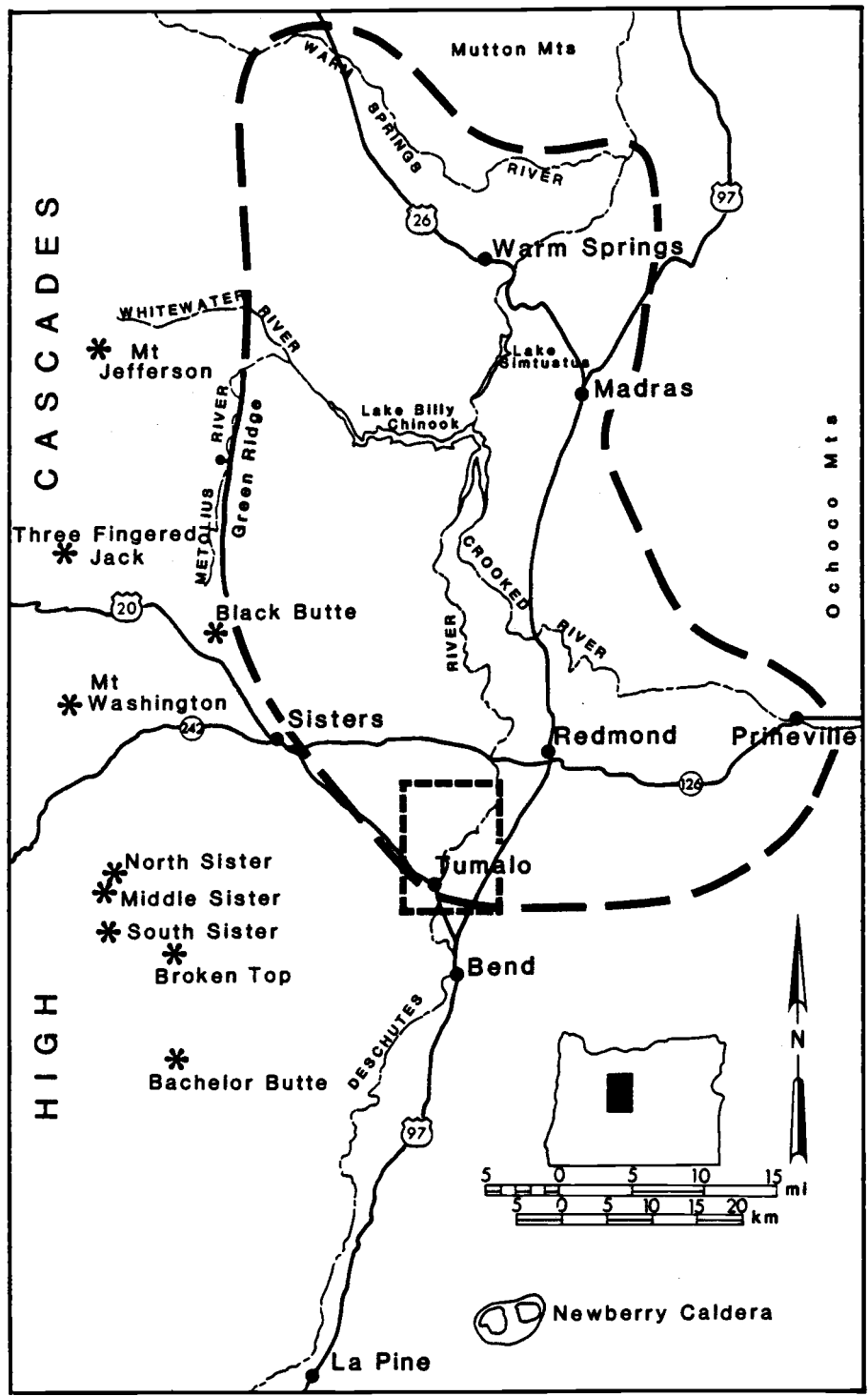
Figure 2. Location map of the Deschutes basin and the Tumalo
quadrangle. Broadly defined boundaries of the Deschutes
basin are represented by long dashes. Shorter dashed
lines at the southern end of the basin enclose the Tumalo
quadrangle.

1957; Robinson and Price, 1963; Hewitt, 1970; Robinson and Stensland, 1979; Walker, 1981), the Dalles Formation (Hodge, 1942; Waters, 1968; Peterson and Groh, 1970; Robinson, 1975; Robison and Laenen, 1976), and the Deschutes Formation (Stearns, 1930; Stensland, 1970; Peterson and others, 1976; Taylor, 1980, 1981a). In an attempt to revise and formalize the nomenclature of correlative deposits within the Neogene basins of north central Oregon, Farooqui and others (1981) proposed restoring the name Deschutes Formation and placed it in the Dalles Group.

Early investigators recognized the Deschutes Formation was of late Tertiary age. Fossil flora in the formation were dated as lower to middle Pliocene by Chaney (1938). This age was later verified by a K-Ar date on plagioclase from the rock encasing the fossils (Evernden and James, 1964). Using K-Ar methods Hales (1974) established the age of the Deschutes Formation at Green Ridge and Armstrong and others (1975) reported dates from rocks throughout the Deschutes basin. Ar-Ar methods have recently been used to improve a previous K-Ar date from the lowest member of the Deschutes Formation (Smith and Snee, 1983).

The first detailed investigations and maps of the Deschutes basin were the products of masters theses (Hewitt, 1970; Stensland, 1970; Hales, 1975). Recent and concurrent thesis projects on the Deschutes basin include Jay (1983), Hayman (1984), Cannon (1985), Conrey (1985), Smith (1986), Yogodzinski (1985), Dill (1989), and Wendland (1989).

Geologic field trip guides provide a good overview of Deschutes basin geology. These guides include Peterson and Groh's (1970) Cove Palisades State Park tour, Taylor's (1980, 1981a) High Cascade and Deschutes basin guides, and Smith and Priest's (1983) guide to the central Oregon Cascades.

Five previous investigations are of particular interest to this study. The 1:125,000 reconnaissance map of the Bend quadrangle (Williams, 1957) was the first geologic map to include the Tumalo area. Peterson and others (1976) subsequently published a more detailed geologic map (1:87,500) of Deschutes County. Taylor (1980, 1981a) described geologic features in the southern part of the Tumalo quadrangle. Stensland's (1970) masters thesis study area adjoins the northern boundary of the Tumalo quadrangle. Two Quaternary pyroclastic units in the Tumalo area were investigated by Hill (1985, 1987).

REGIONAL GEOLOGY

Cenozoic volcanic products have largely buried pre-Tertiary rocks in central Oregon. Pre-Tertiary rocks exposed to the southwest and northeast suggest central Oregon is underlain by fragmented oceanic and continental margin terranes which have been variably metamorphosed and intruded by plutons.

The subduction related calc-alkaline volcanism which formed the Clarno Formation is the first chapter in central Oregon's Tertiary history. Clarno volcanism is considered to be a late stage

of the "Challis volcanism" (Armstrong, 1978) which began at approximately 54 Ma and was active in Montana, Wyoming, Idaho, and Washington. Published dates have placed the lower boundary of the Clarno at 46 Ma (Enlows and Parker, 1972). However, unpublished dates of 48.9 $\pm$ 5.2 Ma (Enlows, Robinson and McKee, pers. comm., in Taylor, 1981b) and 50 Ma (Robinson, pers. comm., in Noblett, 1981) suggest Clarno volcanism may have begun earlier than previously assumed.

The date on the upper boundary of the Clarno Formation is likewise controversial (i.e. see Noblett, 1981; and Taylor, 1981b). In some locations the Clarno Formation is in contact with the overlying John Day Formation, the lowermost member of which is dated at 36.4 Ma (Evernden and James, 1964). In other localities a saprolite and angular unconformity separate the two formations (Waters, 1954; Hay 1962; Swanson, 1969). A date of 41.0 $\pm$ 1.2 Ma was obtained on a rock from one of the youngest flows in the upper Clarno Formation (Swanson and Robinson, 1968).

Clarno vents were widespread across central Oregon; Clarno rocks crop out extensively in the Ochoco Mountains, the Mutton Mountains and north to the Columbia River basalt plateau (Waters, 1968). Thickness of the formation varies greatly, units are discontinuous and correlation between units is difficult. Andesite lavas are the chief Clarno rock type, but compositions range from olivine basalt to rhyolite and include lava flows and domes, volcanic breccias, and tuffaceous sedimentary rocks.

By about 40 Ma arc-related volcanism had migrated westward, initiating the first of four stages of central Oregon Cascade volcanism (Priest and others, 1983). The Western Cascade Range (Peck and others, 1964; Hammond, 1979) developed during the first two stages. The first stage occured during the late Eocene to early Miocene and produced dominantly silicic lithologies. The second stage was characterized by early to middle Miocene basaltic andesite and andesite lavas. Subsequent volcanism shifted slightly to the east, became more mafic in character and heralded the formation of the Oregon High Cascade Range. Early High Cascade volcanism (late Miocene to early Pliocene) produced basalt and basaltic andesite lavas and voluminous andesitic to rhodacitic pyroclastic flows. Beginning with the late Pliocene, basalt and basaltic andesite issued from shield volcanoes, forming the broad mafic platform of the Late High Cascades. Pleistocene and Holocene volcanism has continued to be predominantly mafic but includes localized silicic volcanism. The stratovolcanoes familiar on today's Cascade skyline were developed during the Pleistocene and Holocene.

Early Western Cascade volcanism is recorded in central Oregon by the John Day Formation. The andesitic to dacitic tuffaceous clay-stones and airfall tuffs which form the eastern facies of the John Day Formation were formed from airfall produced by explosive eruptions in the early Western Cascade Range (Robinson and Brem, 1981, Robinson and others, 1984). Based on K-Ar dates, deposition of the John Day Formation occured between 36.4 ± 1.1 Ma (Swanson and Robinson, 1968) and 22.7 ± 2.7 Ma (Dingus, 1979). A vertebrate

fauna found near the top of the formation suggests an age as young as 19 Ma (Woodburne and Robinson, 1977). The western facies of the John Day Formation is characterized by moderately alkalic ignimbrites and lavas erupted from vents east of the Cascades (Robinson and Brem, 1981, Robinson and others,1983). Folding along the Blue Mountain anticline (Rogers, 1966; Fisher, 1967) coincident with deposition of the early John Day Formation produced a barrier which prohibited eastward movement of most ignimbrites and lavas. Small, localized flows of high-titania alkali-olivine basalt and trachyandesite occur in the lower part of the eastern and western facies (Fisher, 1967; Robinson and Brem 1981, Robinson and others, 1983).

During the middle Miocene sheet floods of tholeiitic basalt and basaltic andesite lavas of the Columbia River Basalt Group (Waters, 1961) formed a broad plateau in southeast Washington, western Idaho, and northern Oregon. Continued folding along the Blue Mountain anticline produced an angular unconformity between the John Day Formation and the overlying Columbia River Basalt. Subsequent to deposition of the Columbia River Basalt lavas, much of the plateau they formed was gently folded. The lavas issued from fissures now marked by large north to north-northwest trending dike swarms in the eastern part of the plateau (Waters, 1961; Taubeneck, 1970). The bulk of the lavas were erupted between 16 and 13.5 Ma, decreasing in frequency of eruption and volume until their cessation at 6 Ma (McKee and others, 1977).

Members of the Columbia River Basalt Group are distinguished largely by their chemistry and magnetic polarity. The Prineville

chemical type (Uppuluri, 1974) crops out in the northern part of the Deschutes basin. Its source is conjectured to have been in the Prineville area.

Explosive Cascade volcanism which was contemporaneous with eruptions of the Columbia River basalt led to development of the Simtustus Formation (Smith, 1986a). In the Deschutes basin, the Simtustus Formation is interbedded with and lies conformably above Columbia River basalt. The crossbedded tuffaceous sandstone, mud-stone, minor ignimbrites and lahars which compose the Simtustus Formation had long been assumed to be part of the Deschutes Formation. However, vertebrate fauna discovered in the Simtustus formation place it stratigraphically below the Deschutes Formation. There is also a slight angular unconformity between the Simtustus and Deschutes Formations. The extent of the Simtustus formation is unknown; it occurs as thin, localized outcrops in the northern Deschutes basin. The late Miocene-early Pliocene Deschutes Formation rests unconformably above older Tertiary rocks. Deposition of the Deschutes Formation occured largely between 7.6 m.y. (Smith and Snee, 1983) and 4.7 m.y. (Armstrong and others, 1975). Deschutes Formation lithologies include lava flows ranging in composition from basalt to rhyodacite, andesitic to rhyodacitic pyroclastic flow and fall deposits, non marine volcaniclastic sedimentary rocks, and lahars. Rocks similar in age and composition to the Deschutes Formation (i.e. the Outerson Formation of Thayer, 1936) are found in the Western Cascades, near the High Cascade-Western Cascade Range boundary.

High Cascade volcanism (the "late High Cascade" of Priest and others, 1983) began at approximately 5.4 Ma (Smith, Snee, and Taylor, 1987) and has continued into the Holocene. Eruptions of basalt and basaltic andesite produced a north-south trending volcanic platform 12-18 km wide characterized by shield volcanoes (Taylor, 1980). Some of the basaltic andesite volcanoes developed composite cones upon their shield bases. Localized High Cascade silicic volcanism has been active west of Bend, in the vicinity of South Sister volcano. Newberry volcano, a large shield volcano which lies in the High Lava Plains province east of the High Cascade axis, produced large quantities of basaltic to rhyolitic lavas during Pleistocene and Holocene age eruptions.

ROCK CLASSIFICATION AND TERMINOLOGY

The volcanic rock classification adopted for use in this study is based on weight percent silica from H_2O-free chemical analyses (Taylor, 1978). Similar classification schemes are used by numerous Cascade geologists (White, 1980a, 1980b; MacLeod and others, 1982; Priest and others, 1983).

48 - 53% SiO_2 . . . . basalt

53 - 58% SiO_2 . . . . basaltic andesite

58 - 63% SiO_2 . . . . .andesite

63 - 68% SiO_2 . . . . .dacite

> 68% SiO_2. . . . . .rhyodacite

> 73% SiO_2 and > 4% K_2O . . . . . . .rhyolite

The terminology used to describe volcaniclastic sedimentary rocks is less straightforward. The term volcaniclastic (Fisher, 1961, 1966) refers to clastic rocks composed of volcanic fragments formed by any mechanism or origin, emplaced in any environment or mixed with any other non volcanic fragments in any proportion. All sedimentary rocks in the thesis area are composed of volcanic rock fragments and therefore are volcaniclastic. Two different fragmentation processes contribute to the creation of volcaniclastic sediments: 1) pyroclastic fragments, or pyroclasts, are particles "generated by disruption as a direct result of volcanic action" (Schmid, 1981); 2) epiclastic fragments are produced by weathering or erosion of pre-existing rocks. The particles of unconsolidated pyroclastic deposits remain pyroclasts regardless of later processes that may disrupt and redeposit them. However, lithified pyroclastic deposits such as ignimbrites may be eroded to produce epiclasts which are indistinguishable from pyroclasts in volcaniclastic sediment. For this reason, naming volcaniclastic sedimentary rocks based on percentages of pyroclastic verses epiclastic constituents (i.e. Schmid, 1981) are difficult to apply. For the purposes of this study the adjective "tuffaceous" is used to modify any sedimentary rock type which is composed of between 25 and 75% pyroclastic material regardless of its prior depositional history.

Terminology used to describe most pyroclastic deposits is based on clast size (Table 1). The term ignimbrite refers to a

TABLE 1. TERMINOLOGY AND CLASSIFICATION OF VOLCANICLASTIC ROCKS
(after Schmid, 1981)

Clast size	Pyroclast	Pyroclastic deposit	Clastic sedimentary rock w/ 25-75% pyroclastic material
	block, bomb	agglomerate, pyroclastic breccia	
64mm	---	---	tuffaceous conglomerate tuffaceous breccia
	lapillus	lapillistone	
2mm	---	---	---
	coarse ash	coarse tuff	tuffaceous sandstone
1/16mm	---	---	---
	fine ash	fine tuff	tuffaceous siltstone tuffaceous mudstone

pyroclastic-flow deposit and, as used in this study, is synonymous

with the term ash-flow tuff.

STRATIGRAPHY AND LITHOLOGY OF MAP UNITS

PRE-DESCHUTES FORMATION ROCKS

The eroded conical peaks of Cline Buttes (Figure 3) mark a center of silicic volcanism which was active prior to deposition of the Deschutes Formation. The rhyodacitic lavas of Cline Buttes are the oldest exposed rocks in the area and cover approximately 13 km^2. Only the southern flanks of Cline Buttes lie within the study area.

CLINE BUTTES

Two high-silica rhyodacite lavas and a basalt lava form the southern part of Cline Buttes; a single rhyodacite forms the bulk of exposed rock. The subordinate rhyodacite crops out over an area of less than 0.25 km^2 in the northeastern corner of section 30, T15S, R12E. Contacts between the two rhyodacites are covered, obscuring their relationship.

The rhyodacite lavas are typically platy and rarely massive (Figure 4). Rock color ranges from light gray on fresh surfaces to tan and reddish brown on weathered surfaces. Banded, varicolored examples are locally present. The lavas have sparse (less than 2%) phenocrysts of oligoclase (approximately An20) and the oxidized

Figure 3. Cline Buttes looking west toward the Cascade Range. Deschutes River canyon in foreground.

Figure 4. Platy Cline Buttes rhyodacite. Hammer left of center for scale.

skeletal outlines of an elongate mafic mineral in a hypocrystalline, trachytic groundmass of plagioclase, devitrifed glass, and iron oxide. Some samples have a microcrystalline groundmass of quartz(?) and feldspar, a texture common to silicic domes.

Locally, the rhyodacites exhibit lithophysal or spherulitic textures (Figure 5). Features identified in handsample as spheru-lites lacked the characteristic radiating devitrification texture when examined in thin section (Figure 6). In plane light the spherulites appear as round, dark spots with slightly reddish, oxidized margins, in an otherwise light colored, glassy rock. The dark color may be due to fine iron oxide, as suggested by the slightly reddish margins. Under crossed nicols the dark spots show only slightly more devitrification and are barely distinguishable from the remainder of the rock. An uninterrupted trachytic texture is pervasive in both the light colored, glassy part of the rock and the dark spots, indicating that development of the dark spots, or spherulites, is post-depositional and not a feature of compositional inhomogenities in the magma.

A weathered porphyritic basalt lava forms a small hill on the west side of Cline Buttes. The basalt appears to have erupted subsequent to the rhyodacite as it is not overlain by it, despite its lower elevation and juxtaposition against the rhyodacite. Because the basalt appears younger than the rhyodacites and is similar in appearance and composition to Deschutes Formation basalts, it is included in the discussion of Deschutes Formation lavas.

Figure 5.   Spherulites in Cline Buttes rhyodacite.

Figure 6.   Thin section of spherulites in plane light at 40X.

No radiometric age for Cline Buttes has been determined. It has been mapped as both Clarno Formation (Stensland, 1970) and John Day Formation (Williams, 1957). Field identification of the platy rhyodacite as andesite seems to have been the basis for Stensland's (1970) interpretation of Cline Buttes as part of the Clarno Formation. Its eroded appearance, thick soil cover, and the younger Deschutes Formation rocks which encircle its base indicate that Cline Buttes is no younger, and is likely much older, than late Miocene.

DISCUSSION

Cline Buttes is but one of the Tertiary age silicic volcanic centers (e.g., see Peck, 1964; Robinson, 1975; Swanson, 1969; Williams, 1957; Obermiller, 1987) that projects through the cover of younger rocks in or near the margin of the Deschutes basin (Figure 7). Rocks from some of these centers, such as Powell Buttes (Weidenheim, 1980), Juniper Buttes, and unnamed domes near Ashwood and in the Mutton Mountains, yield isotopic ages (Fiebelkorn et al., 1982) coincident with deposition of the John Day Formation (between 36 - 22 Ma) and have chemical compositions similar to western facies John Day rocks (Robinson and Brem, 1981, 1984). These domes were probably sources for western facies John Day Formation lavas and ignimbrites. The ignimbrites and lavas of the western facies John Day Formation (Table 2) are moderately alkali rhyolites with silica contents on the order of 75% to 76% (Robinson and Brem, 1981, 1984).
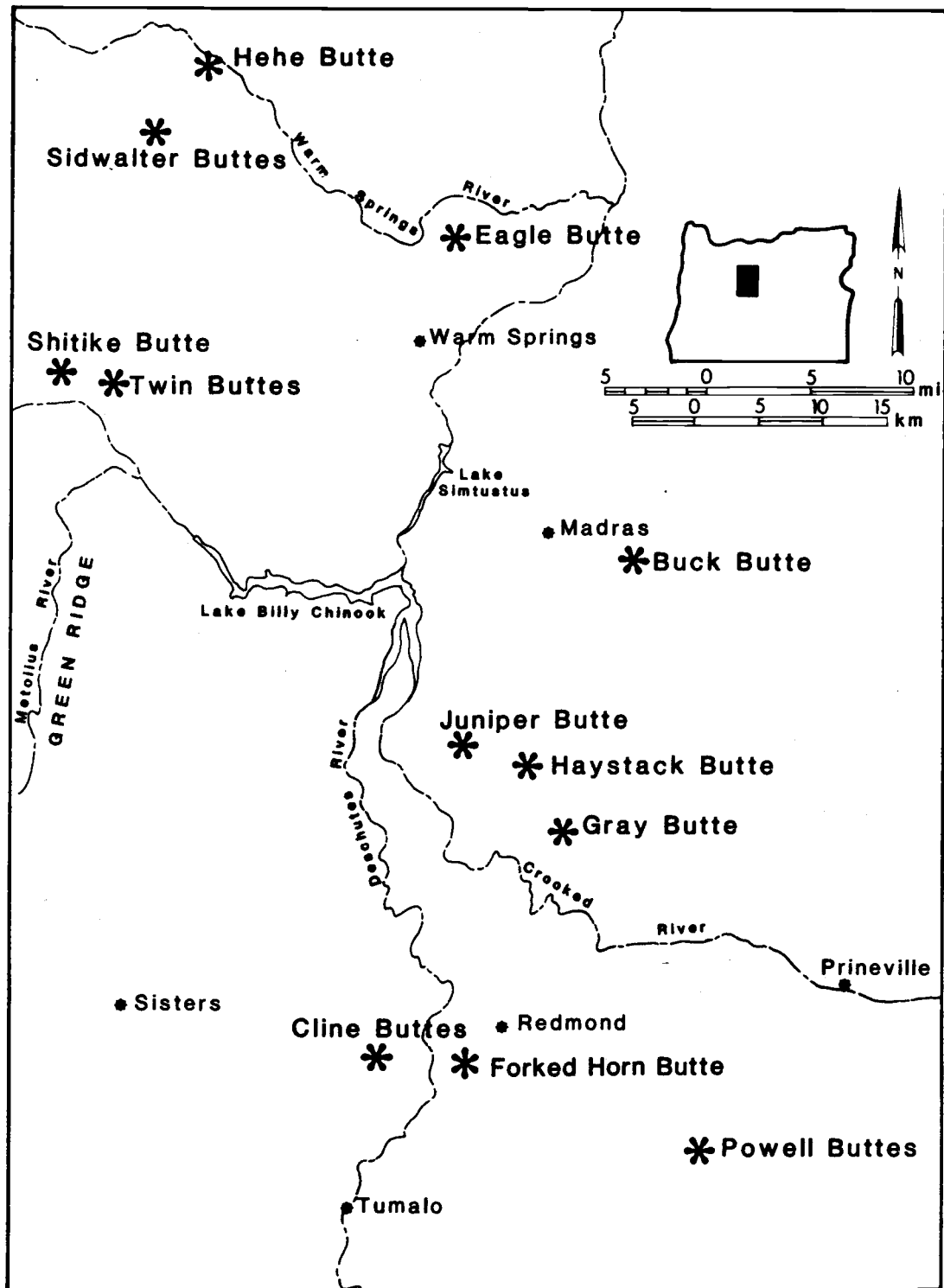
Figure 7.   Oligocene to mid-Miocene(?) silicic volcanic centers
in the Deschutes basin.

Table 2. AVERAGE ANALYSES OF WESTERN FACIES JOHN DAY FORMATION ROCKS

	JD1	JD2
SiO2	75.47	77.9
Al2O3	12.7	11.8
TiO2	0.3	0.3
FeO*	2.3	1.7
CaO	0.7	0.4
MgO	0.2	0.05
Na2O	3.2	3.1
K2O	5.1	4.7
P2O5	0.05	0.02
MnO	0.05	0.03

JD1   Average of 9 analyses of unaltered ignimbrites, from Robinson and Brem (1984).

JD2   Average of 5 analyses of silcic lava flows, from Robinson and Brem (1984).

* Total iron as FeO

Major element analyses of samples from Cline Buttes and a number of other silicic centers (Table 3) were performed as a part of this study and contemporaneous studies (Yogodzinski, 1985; Smith, 1986; Obermiller, 1987; E. M. Taylor, unpublished data). The analyses indicate that the rocks are predominately dacites and rhyodacites, and less commonly rhyolites, with variable alkali content. This compositional variability suggests that there is greater chemical diversity among western facies John Day Formation rocks than previously recognized, or that some of the domes (including Cline Buttes) are not part of the John Day Formation as it is presently defined.

K-Ar age dates from a Gray Butte rhyolite and an ignimbrite which unconformably overlies tuffaceous beds at the summit of Gray Butte,

Table 3.   REPRESENTATIVE ANALYSES OF SILICIC VOLCANIC CENTERS
IN THE DESCHUTES BASIN

Sample	EB	FHB	SHB	SB	TB	CB	PB	BB	GB
SiO_2	63.8	67.1	69.5	71.9	72.5	72.8	75.9	77.2	77.8
Al_2O_3	18.0	14.4	16.0	15.1	15.4	14.5	11.4	11.64	12.1
TiO_2	0.77	0.96	0.47	0.36	0.35	0.19	0.25	0.17	0.20
$FeO*$	5.0	5.9	3.1	2.7	2.8	2.3	3.4	1.9	1.4
MgO	2.4	1.0	0.9	0.0	0.5	0.2	0.0	0.0	0.0
CaO	5.4	3.2	2.6	0.8	1.4	0.9	0.3	0.5	0.2
Na_2O	3.6	4.2	5.0	4.6	4.7	5.1	5.0	5.4	4.1
K_2O	1.14	3.15	2.00	3.47	2.92	3.06	3.95	3.12	4.45
Total	100.11	99.91	99.57	98.93	100.57	99.05	100.20	99.93	100.25

EB   Eagle Butte dacite, from Smith (1986).

FHB   Forked Horn Butte dacite, from Smith (1986).

SHB   Shitike Butte rhyodacite, from Yogodzinski (1985).

SB   Sidwalter Buttes rhyodacite, from Smith (1986).

TB   Twin Buttes rhyodacite, from Yogodzinski (1985).

CB   Cline Buttes rhyodacite, sample AM290 from Appendix IIa.

PB   Powell Butte rhyodacite, sample JPW-117 from Weidenhiem, (1981).

BB   Buck Butte rhyodacite, sample BBRH2 from Obermiller, (1987).

GB   Gray Butte rhyolite, sample SRRH1 from Obermiller, (1987).

* Total iron as FeO

are 17.8 and 10.4 Ma, respectively (Obermiller, 1987). These dates suggests that silicic volcanism in the Deschutes basin was active into the mid-Miocene. Further isotopic dating and comprehensive chemical investigations of the silicic domes in the Deschutes basin are needed to determine their relationship to one another, the John Day Formation, and Cascade volcanism.

DESCHUTES FORMATION ROCKS

The late Miocene to early Pliocene Deschutes Formation
(Figure 8) is a nearly flat-lying sequence of volcanic and non
marine sedimentary rocks which are separated from older Tertiary rocks
by angular and erosional unconformities. The bulk of Deschutes Forma-
tion rocks was deposited between approximately 7.5 and 5.3 Ma,
although volcanism at Round Butte, east of the Cascade Range, with an
age of approximately 4.0 Ma has been included as part of the formation
(Smith, 1986a, Smith and others, 1987).

Deschutes Formation rocks (Figure 9) define and lie within an
area known as the Deschutes basin. To the west, the Deschutes basin
is bounded by the High Cascade Range. To the north and east the basin
is bounded by older Tertiary rocks which form the Mutton Mountains and
the Blue Mountains. The southern boundary of the basin is defined not
by a topographic high, but by the contact between Deschutes Formation
rocks and late Pliocene and Pleistocene lavas from the High Cascade
Range, Newberry volcano, and sources southeast of the basin.

Composition of the formation varies from east to west at the
latitude of Green Ridge and represents proximal and distal records of
Early High Cascade arc volcanism. Basaltic andesite and andesite lava
flows dominate the western part of the formation at Green Ridge
(Conrey, 1985) but are interbedded with basalt and dacite lavas,
andesitic to rhyodacitic ignimbrites, debris-flow deposits, and minor
sedimentary rocks. East and southeast of Green Ridge the formation

Figure 8. Outcrop of Deschutes Formation near Lake Billy Chinook.
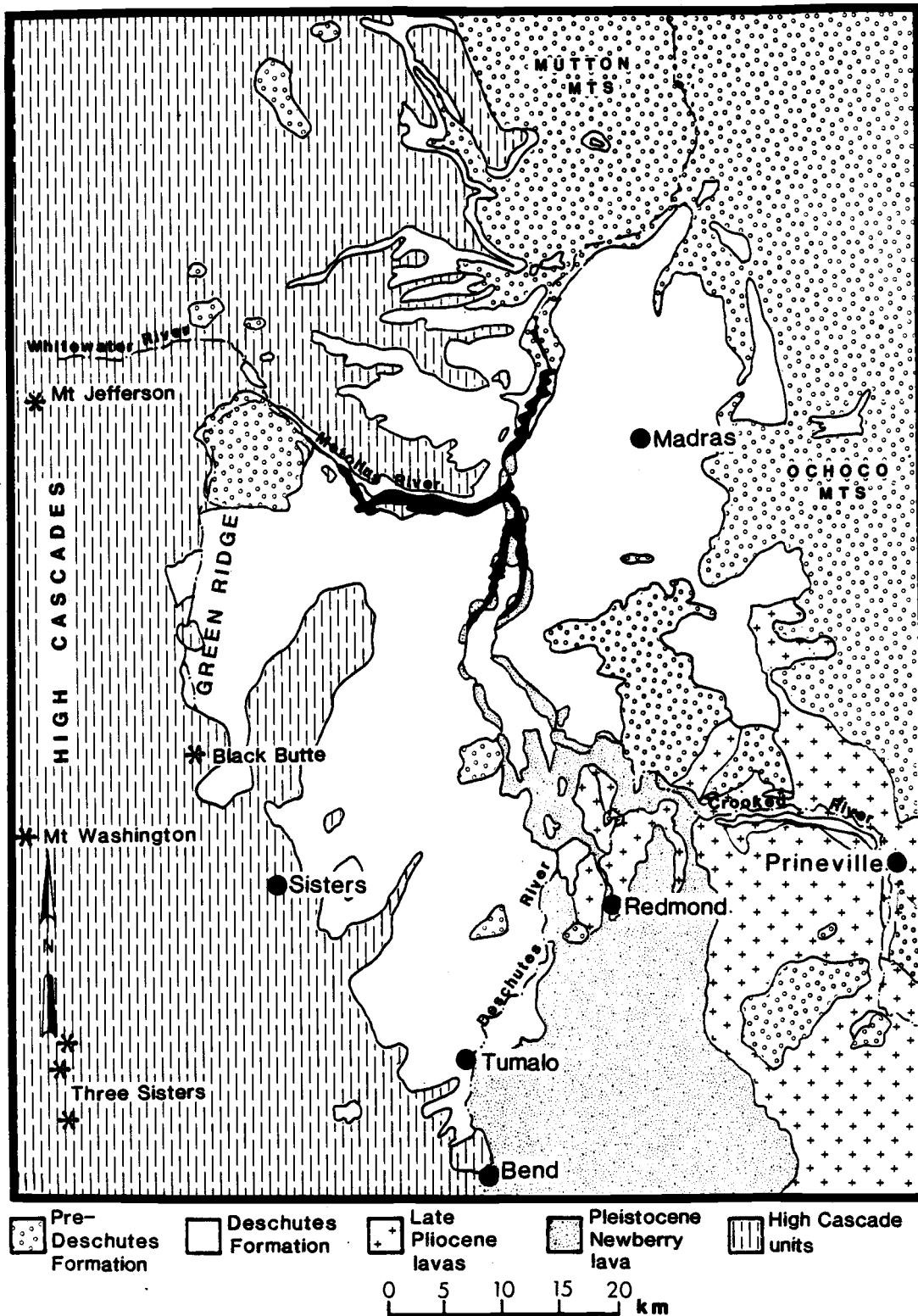
Figure 9. General geology of the Deschutes basin and adjoining
areas.

is dominated by volcaniclastic sedimentary rocks with interbedded
ignimbrites, pumice lapillistones, and mafic lavas. Sedimentary
lithologies are dominated by sandstones and conglomerates, with
lesser siltstones and mudstones. Thickness variations and flow
directions of lavas and ignimbrites, and paleocurrent data indicate
that the lavas and sediments which combined to form the Deschutes
Formation entered the basin from the west and southwest.

Sedimentation in the Deschutes basin ended at approximately
5.3 - 5.4 Ma. Subsequently, lavas from small intrabasinal volcanoes
erupted to form the top of the formation. The end of sedimentation
and eruption of intrabasinal lavas coincided with the development of
faulting at Green Ridge. Offset along the down-to-the-west normal
faults at Green Ridge represents more than 600 m of motion and
locally forms the Deschutes Formation-High Cascade Range boundary.
The dominance of lavas among the lithologies at Green Ridge and their
gentle eastward dip suggest that Deschutes Formation source volcanoes
lay to the west. However, Deschutes Formation sources are not found
among the late Pliocene and Quaternary age volcanoes which charac-
terize the present High Cascade Range. The abrupt termination of the
Deschutes Formation at Green Ridge and the large amount of offset
along the Green Ridge fault suggest that Deschutes Formation source
volcanoes were downdropped along the fault and buried by younger
lavas (Taylor 1981a). The depression into which the Deschutes
Formation volcanoes subsided is known as the central Oregon High
Cascade graben (Smith and Taylor, 1983).

Deschutes Formation volcanoes also lay south of the latitude of
Green Ridge and introduced numerous pyroclastic flows into the

basin. The absence of Deschutes Formation volcanoes south of Green Ridge is somewhat more enigmatic than the absence of volcanoes west of Green Ridge, as there is no topographic expression of graben faulting to explain their disappearance.

Late Pliocene and Pleistocene basaltic lavas from the High Cascade Range, Newberry volcano, and sources southeast of the basin flowed over much of the Deschutes Formation and filled deep channels cut into the sedimentary pile. Today the formation is best exposed along canyons cut by the Deschutes, Crooked, and Metolius Rivers and their tributaries.

In the Tumalo area the Deschutes Formation is represented by volcaniclastic sedimentary rocks and ignimbrites capped by basalt and basaltic andesite lavas which were erupted from local, small volcanoes.

SEDIMENTARY ROCKS

Deschutes Formation sedimentary rocks in the Tumalo quadrangle are generally poorly exposed. Small, isolated outcrops of sedimentary rocks in the talus-strewn walls of the Deschutes River canyon confirm that they underlie the widespread plateau-forming basaltic andesites. An exceptionally well-exposed section (Figure 10) approximately 30 m thick and 0.5 km long in the southwest corner of section 10, T16S, R12E, is the best preserved and most complete record of sedimentary rocks and their depositional environment. The
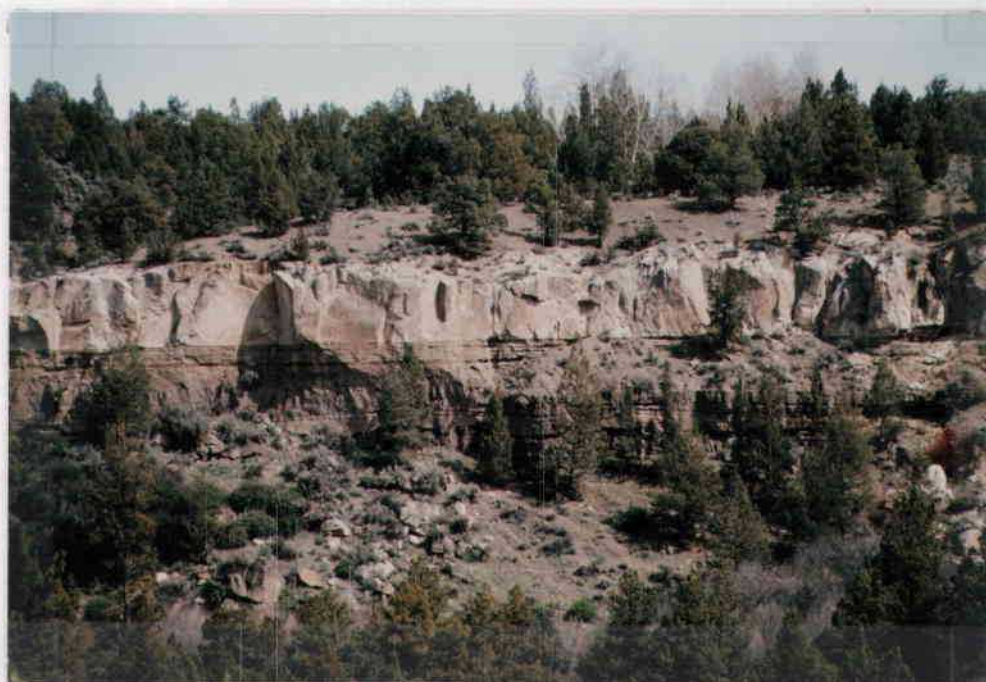
Figure 10. Deschutes Formation volcaniclastic rocks exposed in the
wall of the Deschutes River canyon. Lithologies include a
light grey ignimbrite (at top of section), sandstone,
minor mudstone, siltstone and conglomerate, and pumice
lapillistones.

sedimentary and pyroclastic units are generally stratiform and hori-
zontal. Many units are laterally continuous over a distance of 0.5
km or more and thin gradually toward what appears to have been the
margins of broad, shallow channels. A strike of N 23°E was measured
along one channel margin. Measurements of sedimentary structures
throughout the central basin (Smith, 1986a) and the flow direction of
lavas and ignimbrites indicate a northeast paleoslope prevailed
during deposition of the Deschutes Formation.

Outside of the canyon, exposures of sedimentary rocks are
scarce. Sandy, pebbly soil and rare, small outcrops of sandstones
and ignimbrites underlie the plateau-forming lavas at the west
central edge of the study area and limited exposures lie in the canal
at the south base of Cline Buttes (Plate 1).

Lithology

Sandstone is the dominate lithology in the area, with lesser
conglomerate, siltstone and mudstone. All units are volcaniclastic
and contain both pyroclastic and epiclastic fragments. Most units
contain a sufficient amount of pyroclastic material to carry the
modifier "tuffaceous." Sedimentary units are interbedded with thick
pumice lapillistones and ignimbrites.

Constituents of the sandstones (Figures 11a and 11b) include
varying amounts of rounded pumice lapilli, volcanic rock fragments,
volcanic glass, and crystal fragments of feldspar, clinopyroxene,
orthopyroxene and magnetite. Common, pebble-size clasts are dark- to
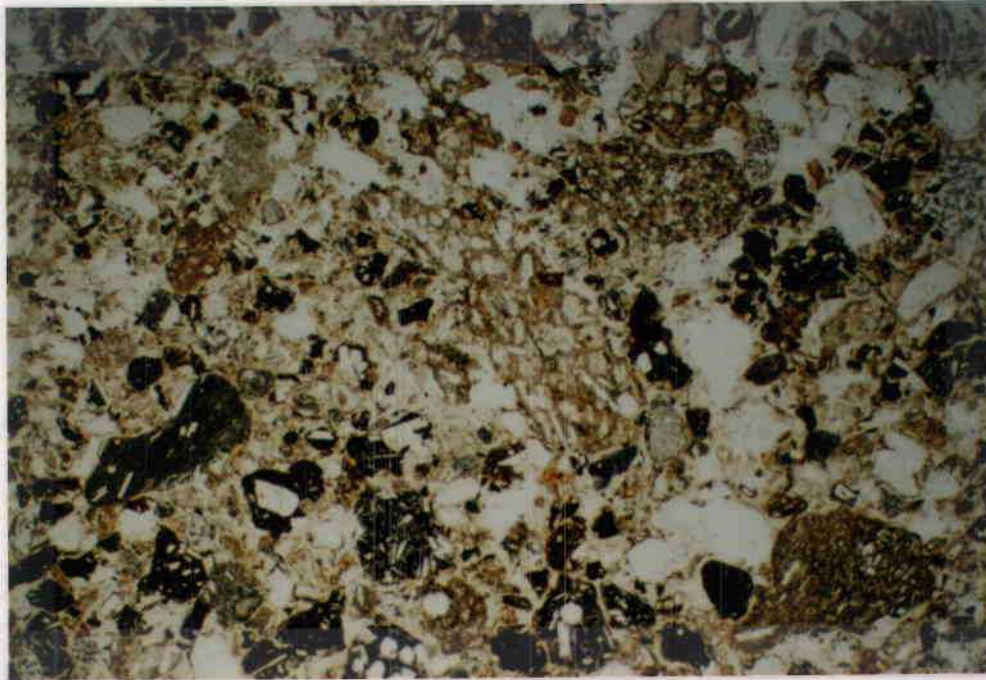
Figure 11a. Photomicrograph of massive sandstone. Constituents
            include pumice fragments, fine grained basaltic clasts,
            and crystal fragments. Photograph at 40x.
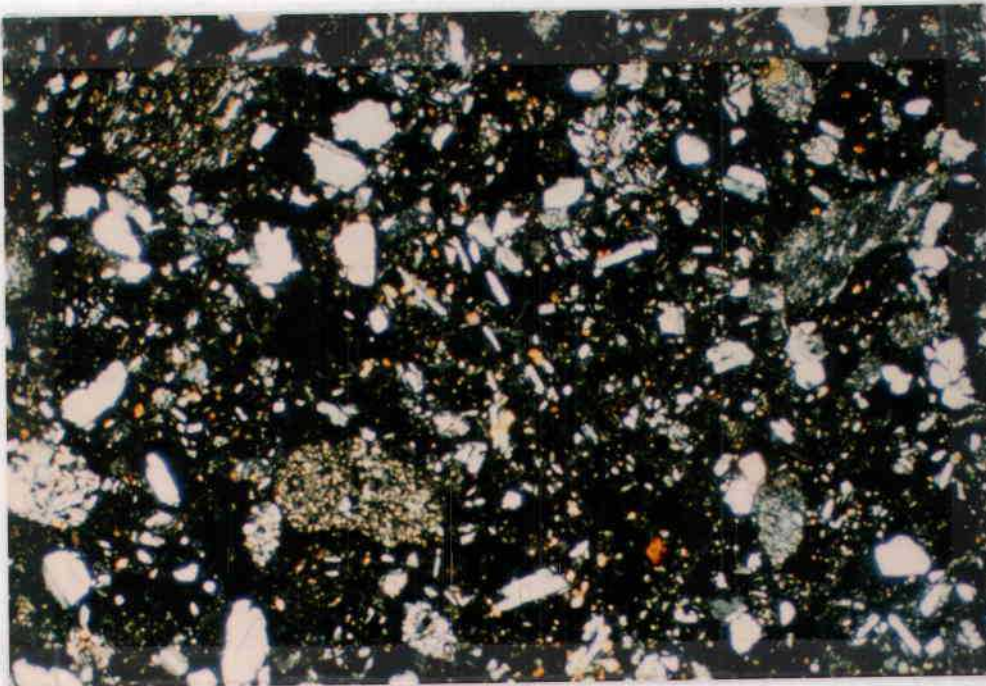
Figure 11b. As above, crossed nichols.

medium-gray to reddish brown and fine-grained, similar to Deschutes
Formation basic to intermediate lavas. Induration of the sandstones
is variable. Typically, tuffaceous units are friable. Better
indurated units contain a smaller amount of pyroclastic material and
have a soft, white, opaline coating on the grains that acts as a
cement. Secondary alteration of the sandstone components is variable
but is usually minor and includes clay development around the rims of
some grains. Plagioclase crystals and ash-size glass fragments, the
components of volcaniclastic sandstones most susceptable to alter-
ation (Surdam and Boles, 1979), appear relatively fresh.

Color of the sandstones ranges from light gray and tan to
darker shades of brown and gray; subtle orange or reddish tints
suggesting oxidation are common. Thick, massive beds may vary in
color from dark near the bottom to light near the top, reflecting a
slight change in composition or development of incipient soil.

Siltstones and mudstones are relatively uncommon. They are
typically tuffaceous, light gray to tan and occur as horizontal
ylaminae interbedded with sandstone. Conglomerates are most commonly
composed of angular to subangular, pebble-sized clasts. A single,
very coarse grained conglomerate is composed of cobble- to boulder-
size clasts supported in a tuffaceous matrix.

Facies

Based on lithology and structure, seven facies (Table 4) are
identified in the sedimentary rocks of the Tumalo area:

TABLE 4. SUMMARY OF FACIES IDENTIFIED IN DESCHUTES FORMATION
SEDIMENTARY ROCKS, TUMALO QUADRANGLE

Facies	Description	Interpretation
A	**Massive sandstone,** fine- to coarse grained, normal grading, poorly to moderately sorted.	paleosols, high sediment concentration flood deposit?
B	**Horizontally bedded sandstone,** fine- to medium-grained, poorly to moderately sorted, crude beds and lenses of gravel and pumice, rare laminations, diffuse contacts.	incipient paleosols
C	**Laminated sandstone,** fine- to coarse-grained, horizontal laminae, often in beds 0.3 m thick, rare convolute bedding and parting lineation	ephemeral, high-energy flood deposit
D	**Interlaminated sandstone, siltstone, mudstone,** lenses of pebble conglomerate, horizontal laminae, low-angle crossbeds, scour-fill.	sheet-flood/channel-flood deposit
E	**Pebble conglomerate,** crudely stratified beds to 0.3 m, and 2.65 cm thick, laterally continuous beds.	sheet-flood/channel-flood deposit
F	**Massive conglomerate,** matrix supported, massive.	debris flow deposit
G	**Lapillistones** and ash beds, horizontal to gently undulating and unstratified beds, angular pumice.	air-fall tephra, predominately as primary deposits.

Facies A: Massive Sandstone

Massive sandstone (Figure 12) is the most abundant facies. The sandstones are fine to coarse grained, poorly to moderately sorted, and commonly contain dispersed pumice lapilli. Other constituents are sand size particles of mafic lavas, glass shards, crystal fragments, and small pebbles. Some units have subtle normal or coarse-tail grading. Thickness ranges from 0.3 to 2 m. Contacts with other facies are usually sharp and roughly planar. Pumice lapillistones overlain by massive sandstones show only minor disturbance, suggesting minimal erosion accompanied sandstone deposition.

There is no evidence of extensive bioturbation or other process which could have so thoroughly destroyed primary structures and homogenized the sandstones to give them a massive character. Vessel and Davies (1981) report obliteration of bedding in contemporary deposits of volcaniclastic sediment due to diagenesis and weathering in humid environments. The semi-arid paleoclimate of the Deschutes basin would result in less weathering and clay alteration of sediments than that common in humid areas.

Although charcteristics common to paleosols such as bioturbation and root casts are not obvious, the reddish oxidation color of many
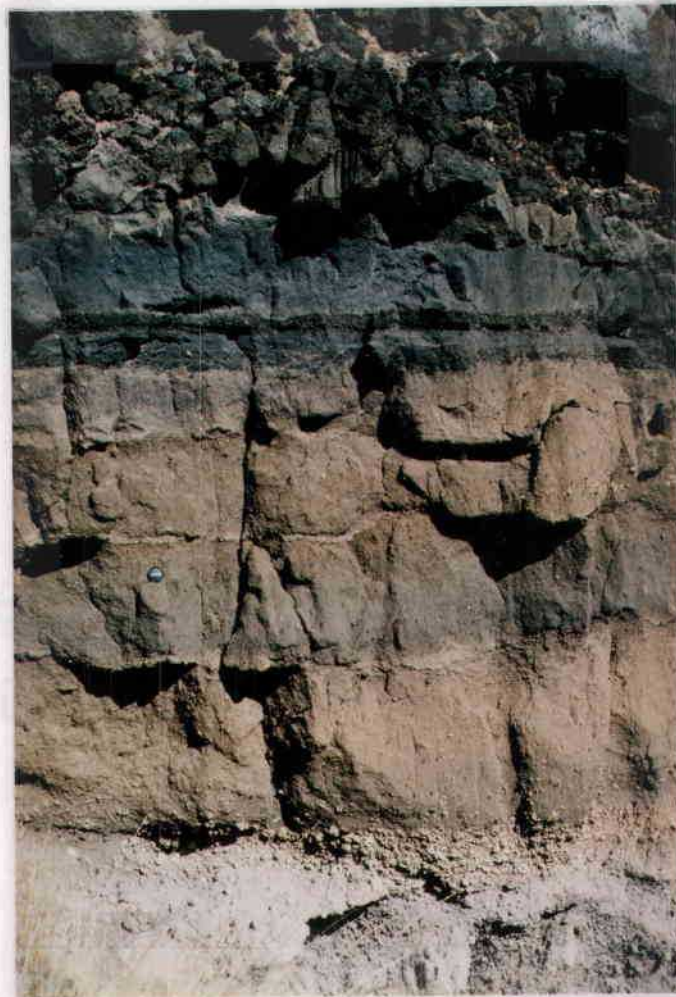
Figure 12. Massive sandstone of Facies A. Reworked pumice lapilli
lie at the contact between sandstone and ignimbrite at
bottom of photo. Cinder-rich tuffaceous sandstones and a
cinder lapillistone lie below the plateau-capping lava.

beds suggests that they have been subaerially exposed for long periods of time. The well preserved air-fall lapillistones that are interbedded with the sandstones suggest that subaerial exposure was common. Many of the massive sandstones probably represent incipient soils.

The unoxidized, dark grey, massive sandstones may represent units deposited from high sediment concentration fluids which restricted settling out of particles. Rapid, en masse deposition from debris flows (Johnson, 1970) and lab studies of high concentration, subaqueous turbidity flows (Middleton, 1967) result in massive units. Fisher (1971) suggested that massive ancient marine and nonmarine sandstones were the product of high concentration dispersions intermediate in water/sediment concentration to normal, dilute stream flow and debris flow and results in rapid transport and deposition of sediment. Smith (1986a, 1986c) interpreted massive, poorly sorted, pebbly sandstones in the central part of the Deschutes as deposits from hyperconcentrated flood-flows. Hyperconcentrated flood-flow is a high-sediment and high-water discharge event inter- mediate in water/sediment concentration to normal, dilute stream flow and debris flow and results in rapid transport and deposition of sediment.

Facies B: Horizontally bedded sandstone

A 1.3 m thick, weathered sandstone unit is characterized by lenses and beds of gravel and reworked pumice that give it a crudely stratified appearance (Figure 13). The sandstone beds are generally
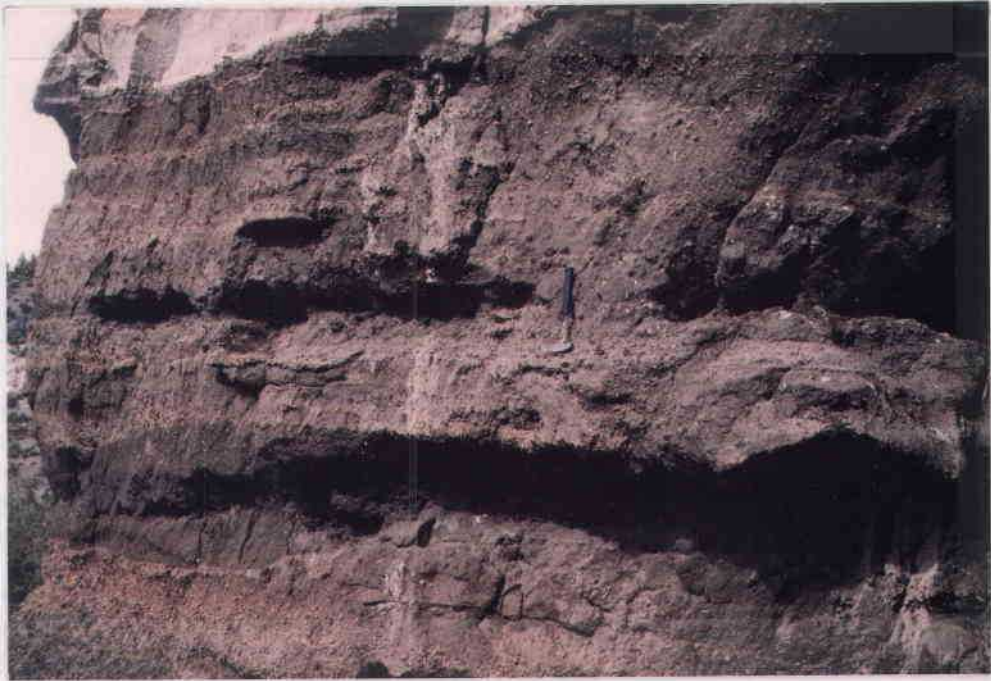
Figure 13. Crudely bedded sandstone of Facies B. Note laminations
below and to the right of hammer.

massive, fine to medium grained, poorly sorted, poorly graded, and pumiceous. The lenses and beds are 5 to 15 cm thick and are usually laterally discontinuous over distances of 0.5 to 5 m. Thin, discontinuous, horizontal laminae are found between the poorly defined beds. This unit grades down into massive sandstone.

The diffuse contact between pumice beds and sandstone beds and the laterally discontinuous character of beds suggests the original deposits have been altered by subaerial processes. Pumice beds and lenses appear to be reworked air-fall tephra rather than primary deposits. However, most individual units retain their integrity and have not been homogenized as is common during formation of paleosols. The massive character of the sandstones may be the result of pedogenic processes or may represent the original, structureless character of the deposits as suggested for some units in facies A. The relatively rare horizontal laminae in facies B suggest episodic high-energy fluvial events.

Facies C: Laminated sandstone

Thick sets of horizontally laminated sandstone are commonly exposed at the top of the sedimentary section. Beds of laminated sandstone up to 1 m thick lie immediately below the plateau-forming lavas (Figure 14) and may exhibit baking or load deformation. Facies C sandstones are fine to medium grained and horizontal, and may show parting lineation. Lateral continuity of individual laminae varies

Figure 14. Laminated sandstone of Facies C is baked by overlying
basaltic andesite lava.

from 1 m or more in medium to fine grained sandstone, to 20 cm or less in medium to coarse grained, pumiceous laminae only a few grains thick. Beds of laminated sandstone at the same stratigraphic level are exposed over distances as great as 0.5 km, suggesting widespread deposition during the same event.

Horizontally laminated sandstones have been attributed to shallow plane-bed transport in both the upper- and the lower-flow regimes (Picard and High, 1973; Harms and others, 1975). Thick laminae sets and absence of lower-flow regime bedforms suggest Facies C originated in the upper-flow regime. Thick beds of parallel-laminated sands are characteristic of sedimentation during high-energy floods in ephemeral streams (Frostick and Reid, 1977; McKee and others, 1967; Williams, 1971) and sheet floods (Tunbridge, 1981). In contrast, parallel laminated sands are not a major feature in perennial streams (Harms and Fahnstock, 1965), where they most commonly occur as thin deposits atop channel bars.

A high-energy depositional environment, the absence of perennial stream deposits and lower-flow regime structures, and the extensive lateral continuity of some units, suggest Facies C represents sedimentation during broadly confined or unconfined, rapidly waning, ephemeral floods.

Facies D: Interlaminated sandstone, siltstone, and mudstone

Medium to fine grained and often pebbly sandstone laminae are interlaminated with less abundant siltstone and mudstone laminae and lenses of pebble conglomerate in a unit 1.3 m thick (Figure 15).

Figure 15. Interlaminated sandstone, siltstone and mudstone of
            Facies D, with prominent cut-and-fill structures.
            Massive tuffaceous sandstones of Facies A underlie and
            overlie the unit. Distance between black bands on stick
            is 0.3 m.

Laminae are generally horizontal but may form broad, low-angle crossbeds at scour sites. Some scours are filled with poorly sorted, massive sandstone which is generally coarser grained than the surrounding laminae. Individual horizontal laminae may be laterally continuous over a distance of many meters.

Models of ephemeral streams dominated by catastrophic flooding (McKee and others 1967; Miall, 1977, 1978; Rust, 1978) are characterized by deposits similar to Facies D. Horizontal laminae and crosscutting networks of small, shallow channels suggest deposition in a shallow, high-energy, braided stream. Sand and pebbles were deposited during high-energy flow, and precipitation of finer material occured as flow energy waned. Waning flow or subsequent high-energy flow scoured and channelized earlier deposits. Scour-fill of massive, poorly sorted sandstone suggests rapid deposition from high sediment concentration flow. Laterally continuous laminated units suggest flow over a broad, flat area as in sheet-floods or broadly confined channel-floods.

Facies E: Pebble conglomerate

Facies E is rare and poorly exposed. Most commonly, it is represented by horizontal beds 2 to 3 cm thick of moderately sorted clast to matrix supported pebble conglomerate (Figure 16). These thin conglomerates are interbedded with faintly laminated, pebbly

Figure 16. Facies E pebble conglomerate (C) lies below top of
stick and is overlain by interbedded pebble conglomerate
and laminated sandstone beds (D). Units at top (E) and
bottom (A) of photo are air-fall pumice lapillistones.
Lower lapillistone is overlain by fine tuff (B)
containing accretionary lapilli.
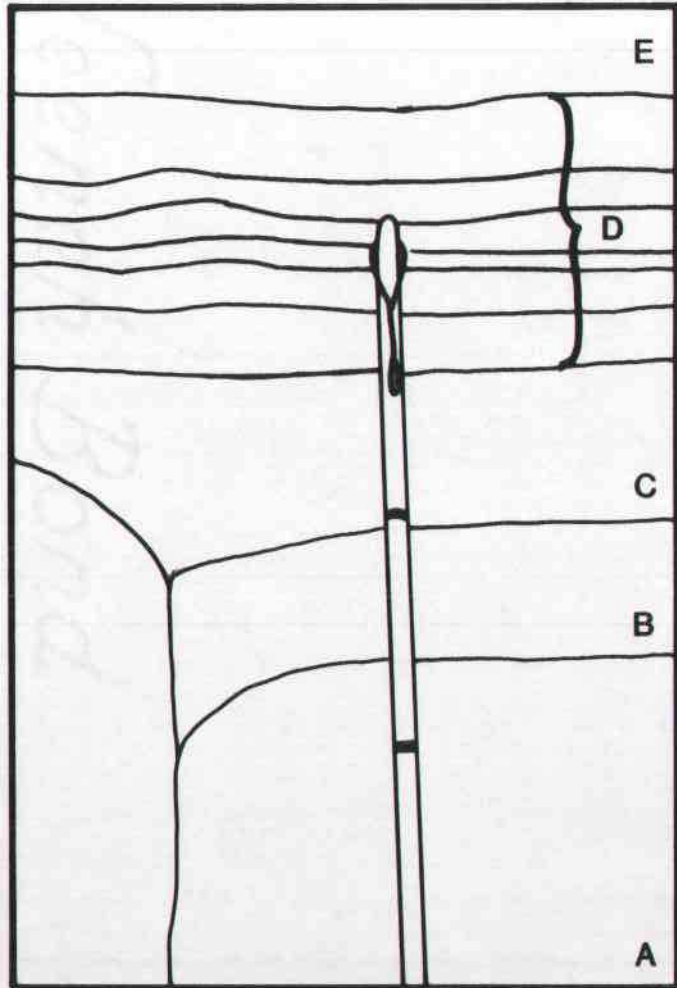
Figure 16. (Figure caption on preceding page).

sandstones of approximately the same thickness as the conglomerates. Together they form a unit with a lateral continuity tens of meters long. Localized, crudely stratified, non-imbricated, horizontal beds of conglomerate 0.3 m thick underlie the conglomerate and sandstone interbeds. A well-indurated fine tuff which lies below a conglomerate exhibits minor erosion.

Lack of imbrication suggests that individual clasts did not move freely with respect to each other. The gravel was probably rapidly deposited and was not reworked. Interbeds of pebble conglomerate and laminated sandstone, and crude stratification based on slight changes in clast size in the thicker conglomerate units suggest deposition under fluctuating high-energy flow. Rapid deposition, thin, laterally extensive beds of conglomerate and sandstone interbeds, the absence of perennial stream deposits, and the close stratigraphic position to facies attributed to flood deposition, suggest Facies E originated with broad, ephemeral floods.

Facies F: Massive conglomerate

Facies F is represented by a 30 m thick, unsorted, massive, matrix supported conglomerate of cobble- to boulder-sized volcanic clasts with a sandy to tuffaceous matrix (Figure 17). Some exposures of the conglomerate suggest reverse grading. The characteristics of this deposit indicate en masse deposition from a debris-flow (Johnson, 1970). The Tetherow debris-flow deposit discussed in a following section is representative of Facies F.
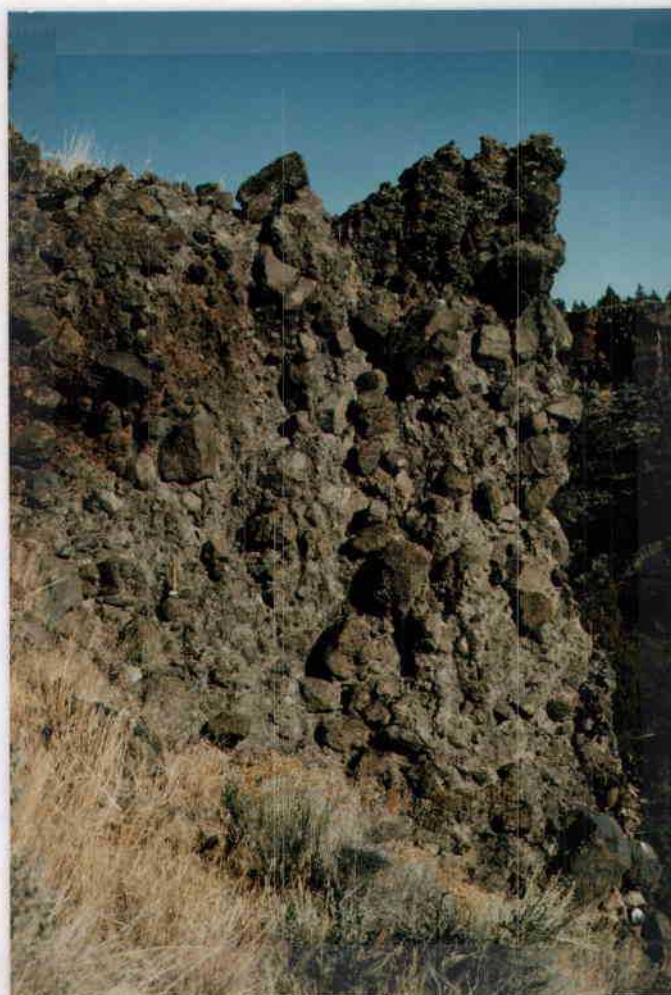
Figure 17. Massive conglomerate of Facies F. Hammer for scale is left of center.

Facies G: Lapillistones

Pumice lapillistones (Figure 18) are common in the study area.
They range in thickness from 5 cm to 2 m; larger lapilli usually form
thicker beds than smaller lapilli. Beds are horizontal and are of
uniform thickness except where they drape over minor irregularites
in the depositional surface. Fine cinder lapillistone beds to 5 cm
thick are exposed between sandstones that lie beneath plateau-capping
basaltic andesites.

Pumice lapilli from a lapillistone bed are typically incor-
porated into the lower 8 to 15 cm of an overlying sandstone. In most
cases, this is the maximum extent of reworking of a lapillistone bed.
Generally, pumice lapilli are angular and lapillistone beds are
not stratified. Fine tuffs interpreted as air-fall ash deposits are
often associated with lapillistones and are included in Facies G.
Lapillistones may be overlain or underlain by the fine tuffs, some of
which contain accretionary lapilli.

The minimal reworking of most lapillistones and their common
association with fine tuffs of airfall origin suggests that most
lapillistones are primary deposits of airfall tephra.

Depositional Environment

For the purposes of this study, the six facies described above
are regarded as a single facies assemblage. The facies do not appear
in a systematic or cyclical sequence nor is there a progressive
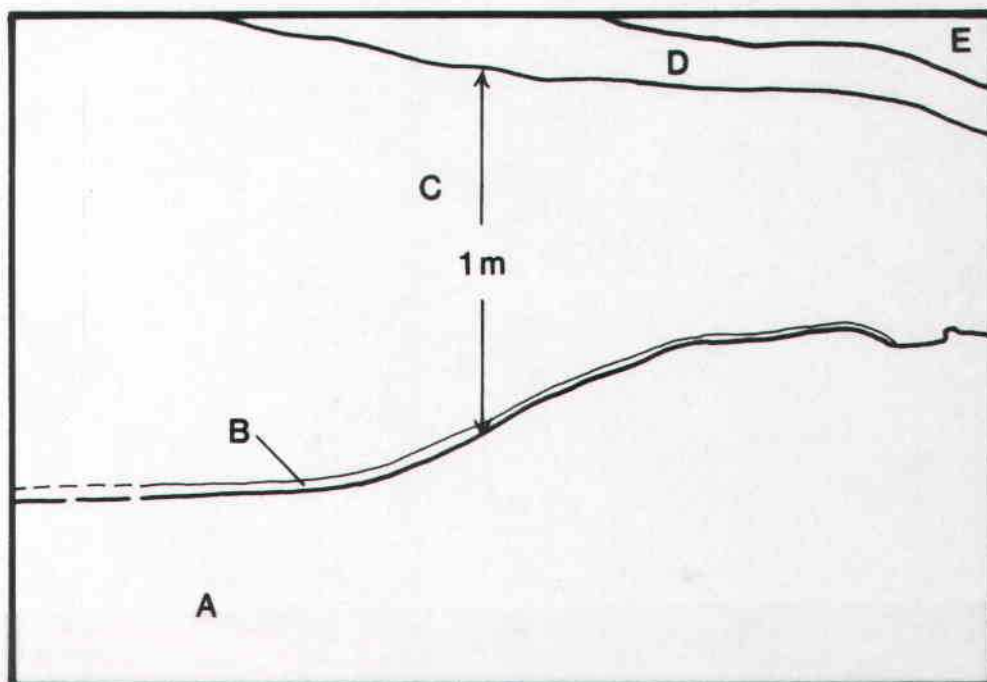
Figure 18. Primary lapillistone of Facies F (C) drapes over gently
undulating depositional surface. Note slight reworking
at top of unit. The lapillistone is underlain (B) and
overlain (D) by fine tuffs formed from air-fall ash.
Unit at bottom of photo (A) is a massive sandstone.
Interbedded sandy conglomerate and laminated sandstone
(E) is at top of photo.

stratigraphic change or trend. The localized and limited exposure of sedimentary rocks in the area make it unlikely that the deposits and processes represented by these facies reflect all of those in the larger, and possibly more diverse, local depositional environment.

Most sedimentation was during three types of events: 1) debris flows, 2) shallow, high-energy, broadly confined floods, and 3) subaerial fall-out of tephra. The absence of normal stream and overbank deposits indicates that sediment deposition was not influenced by processes associated with perennial streams. The numerous tephra beds and thick paleosols suggest the depositional surface was subaerially exposed for long periods of time. Subaerial exposure was punctuated by wide-spread shallow floods which did not significantly rework underlying units. A broad, flat depositional surface is suggested by the horizontal continuity of the units. The abundance of silicic material in the deposits suggests that deposition was controlled by processes associated with nearby silicic volcanism. A broad, low-lying alluvial plain adjacent to an active volcanic arc seems the most likely depositional setting. Assuming a northeast paleodrainage as suggested by paleocurrent data and flow direction of lavas, the material deposited in the Tumalo area originated from sources southwest of Tumalo in the vicinity of the contemporary High Cascade arc.

Tetherow debris-flow deposit

Remains of a distinctive Deschutes Formation debris-flow deposit (Facies F, Figure 17) form localized outcrops in the northeast part of the Deschutes River canyon. This unit is part of Stensland's (1970) "Tetherow mudflow breccia," a debris-flow deposit exposed northwest of Redmond in the vicinity of Tetherow Buttes. As mapped by Stensland (1970), the debris-flow deposit crops out over a 9 km distance, trending roughly north-south. Maximum exposed thickness of the deposit is 60 m. Actual thickness is unknown because the base of the unit is not exposed. The deposit overlies Deschutes Formation sedimentary rocks and lava flows and is overlain by Deschutes Formation and younger lavas (Robinson and Stensland, 1970).

Lithologies in the deposit include pebble- to boulder-sized clasts of black, gray, or red perlitic dacite vitrophyre, banded rhyolite, basaltic andesite lavas, and blocks of unwelded ignimbrite, supported in a tan tuffaceous sandstone matrix. Black, perlitic dacite vitrophyre clasts predominate over other lithologies, giving some outcrops an almost monolithologic appearance. Compositional and petrographic analyses of dacite vitrophyre boulders which litter the lower southwest flank of Cline Buttes indicate they also are remnants of the debris-flow deposit.

Assuming the debris flow was not an intra canyon flow, the debris-flow deposit is the oldest exposed unit in the sedimentary rock section in the Tumalo area. The base of the deposit lies below river level and is not exposed; maximum exposed thickness is 30 m.

At one location the top of the unit is in contact with a light grey to pink ignimbrite which contains dacitic clasts identical to those in the debris-flow deposit. The genetic relationship between the two units is unknown. It is possible that clasts were entrained in the pyroclastic flow as it swept over the surface of the debris-flow deposit. Alternatively, the debris-flow deposit and the ignimbrite may have originated from the same eruption or closely spaced eruptions of the same source.

Origin of the Tetherow debris-flow deposit remains enigmatic. Using thickness variations to determine flow direction is precluded because the base of the deposit is not exposed. Stensland (1970) suggested that the deposit thinned to the north, and that topographic relationships indicated at least one lobe of the deposit terminated to the north. Smith (1985) suggested that dacitic clasts prominent in the deposit originated from Forked Horn Butte, a pre-Deschutes Formation volcanic highland immediately southwest of Redmond. If the dacite vitrophyre prevalent in the deposit originated from Forked Horn Butte, south and east directed flow components are required to explain the distribution of the debris-flow deposit in the Tumalo quadrangle. Such a flow direction would have been contrary to the north to northeast paleoslope that was prevalent during deposition of the Deschutes Formation.

There are no known Deschutes Formation silicic vents in the basin which could have served as the source for the Tetherow debris flow. Silicic volcanism along the Cascade highland to the southwest of the Tumalo area produced numerous Deschutes Formation ignimbrites

and is the most likely source region for a debris-flow dominated by silicic lithologies. A 30 km travel distance and a thickness of 60 m at the deposit's northernmost edge, suggest that the volume of the debris flow was enormous.

Discussion

Studies of contemporary volcaniclastic sedimentation (Kuenzi and others, 1979; Vessel and Davies, 1981; Mathisen and Vondra, 1983) document the control of volcanic processes on nonmarine sedimentation in arc-adjacent basins. Eruptions produce high-relief terrain covered with loose, erodable material and introduce poorly consolidated pyroclastic flow and fall deposits into nearby canyons and onto adjacent plains. This material is reworked and transported by streams to adjacent lowlands. If sediment quantity exceeds the transporting capacity of the streams, aggradation results. Typically, large eruptions are necessary to produce a sediment volume sufficient to initiate alluvial plain flooding and sedimentation. Hence, alluvial plain sedimentation is characterized by episodic deposition and subaerial exposure, the length of which depends upon the frequency and magnitude of volcanic activity.

Because its base is not exposed, total thickness of the sedimentary section in the southernmost part of the Deschutes basin is unknown. Incision into the sedimentary pile in the southern reaches of the basin is much shallower than in central and northern parts of the basin where maximum vertical exposures are greater than

250 m. The original southward extent of Deschutes Formation deposits is also unknown as it has been concealed by younger lavas and pyroclastic flows. Gravity data (Couch and others, 1982) suggests that the gravity low which characterizes the Deschutes basin extends some 17 km south of Bend, beneath the cover of High Cascade units. A $6km^2$ inlier of Deschutes Formation rocks (Taylor, 1987) crops out among High Cascade lithologies at an elevation of approximately 1470 m, some 20 km east of the High Cascade Range between the latitudes of Tumalo and Bend. This confirms that Deschutes Formation deposition extended at least this far south and west of the present day boundaries of the Deschutes basin.

The close of sedimentation in the Tumalo area appears to have been coincident with the initiation of local basaltic andesite volcanism. Black cinder lapillistones and grey tuffaceous sandstones with cinder fragments are restricted to the top of the sedimentary section and record the inception of local volcanism. The reason aggradation in the Deschutes basin ceased is a subject of specu- lation. Termination of sedimentation throughout the basin is generally attributed to restricted passage of sediment and pyro- clastic flows by the development of the High Cascade graben as expressed by the Green Ridge fault scarp. This hypothesis is more difficult to apply for the Deschutes basin south of the latitude of Green Ridge as there is no topographic expression of north-south trending graben faults south of Green Ridge. Widespread laminated tuffaceous sandstones at the top of the sedimentary section in the Tumalo area show only minor bioturbation, suggesting their subaerial

exposure was relatively brief before being covered by basaltic andesite lavas. Soft sediment deformation in the laminated sandstones at their contact with the lavas suggest that they were still moist enough to be plastically deformed. Ignimbrites near or at the top of the sedimentary section also suggest that the southern part of the basin remained accessible at the latest stages of sedimentation.

The dominance of silicic tuffaceous material in the sedimentary rocks, the presence of rhyodacitic ignimbrites, and a large volume debris-flow deposit dominated by dacite clasts, suggests deposition in the southern Deschutes basin was largely controlled by processes associated with silicic volcanism. A temporary decline in silicic volcanism should be considered as a possible factor in the termination of Deschutes Formation sedimentation in the southern basin. A decline in silicic volcanism is supported by the lack of ignimbrites at the top of the Deschutes Formation section at Green Ridge (Conrey, 1985) and the absence of pyroclastic flow deposits above the plateau-capping basaltic andesite lavas. The mid- to late Pliocene volcanic activity of the central High Cascade Range which proceeded the Deschutes Formation is characterized by basalt to basaltic andesite lavas.

IGNIMBRITES

The remains of five Deschutes Formation ignimbrites are found in the Tumalo quadrangle (Table 5). They range in composition from andesite to rhyodacite. With the exception of one, the White Rock

TABLE 5. SUMMARY OF DESCHUTES FORMATION IGNIMBRITES IN THE
TUMALO QUADRANGLE

Ignimbrite unit	color	pumice color	SiO$_2$ wt.%	Mineralogy			
				plag	cpx	opx	other
White Rock ignimbrite	white-pink	lt gray rare med gray	68% 71%	X		X	mag, il
Unnamed ignimbrite, west wall, north canyon	white-pink	white	71%	X	X		ol, mag
Unnamed andesitic ignimbrite	orange	black gray	63%	X	X	X	mag, il
Unnamed ignimbrite, Dayton Road	pink	white pink	67%	X	X	X	mag
Unnamed ignimbrite, S. of Long Butte	white-lt gray	white brown dk gray	no analytical data				

ignimbrite, the ignimbrites are represented by small, poorly exposed, localized outcrops.

White Rock Ignimbrite

White Rock ignimbrite (Figure 19) is the informal name given to a rhyodacitic ignimbrite exposed in the canyon wall at the White Rock Ranch (SE 1/4 section 10, T16S, R12E), where it conformably caps a horizontally stratified section of sedimentary rocks. Maximum thickness of the ignimbrite is 13 m. River gravel and sand overlie the unit, indicating that the top of the ignimbrite was subject to erosion. The ignimbrite thins at its northern edge and terminates at what appears to have been the margin of a broad, shallow northeast-southwest trending paleochannel. The ignimbrite also appears to thin to the south before it becomes obscured by talus.

The White Rock ignimbrite is not welded and represents a single flow unit. Its overall color is white to light gray with pale pink weathered surfaces. The unit is massive, very poorly sorted and matrix supported, which are characteristics common to the main body (i.e. the 2b layer of the standard ignimbrite unit of Sparks et al., 1973, and Sparks, 1976) (Figure 20). Pumice lapilli and rock fragments are estimated to compose 35% and 5% of the unit, respectively. Pumice is largest at the northern margin of the flow, where blocks up to 12 cm are found. Small, isolated pockets of pumice up to a few lapilli thick lie at the base of the flow. A layer of structureless, white ash approximately 3 cm thick rests
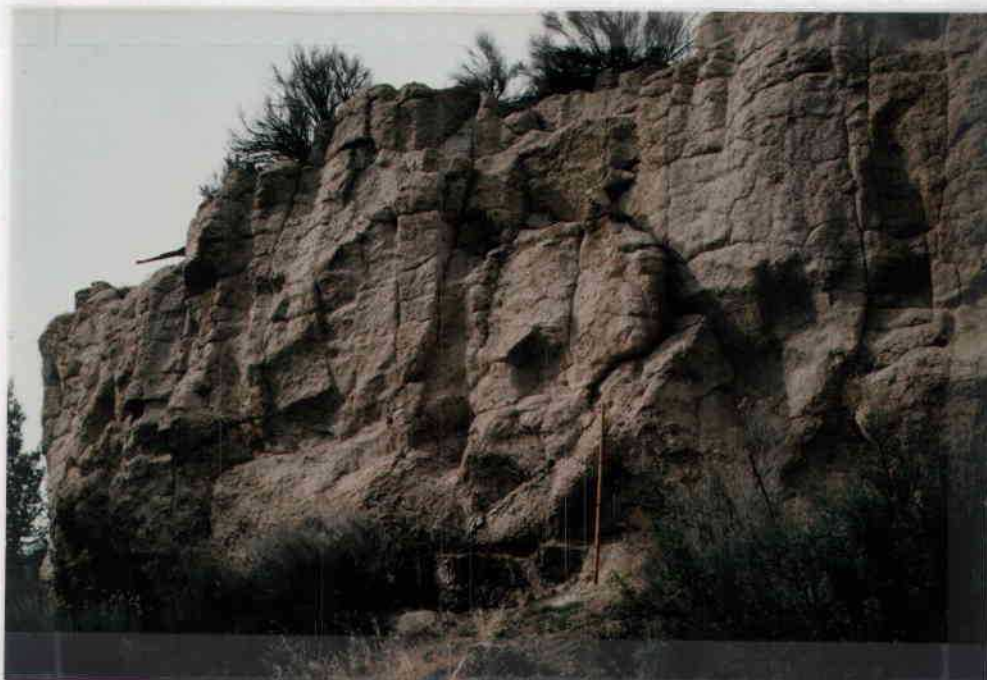
Figure 19. White Rock ignimbrite near its northern margin.
Ignimbrite overlies tuffaceous sandstone seen at base of
outcrop. Distance between black lines on stick is 0.3 m.

IDEALIZED SEQUENCE

WHITE ROCK IGNIMBRITE

3 fine ash deposit

2b

pyroclastic flow deposit

2a

1 pyroclastic-surge deposit

precursor air-fall deposit

alluvium

pyroclastic flow deposit

ash deposit
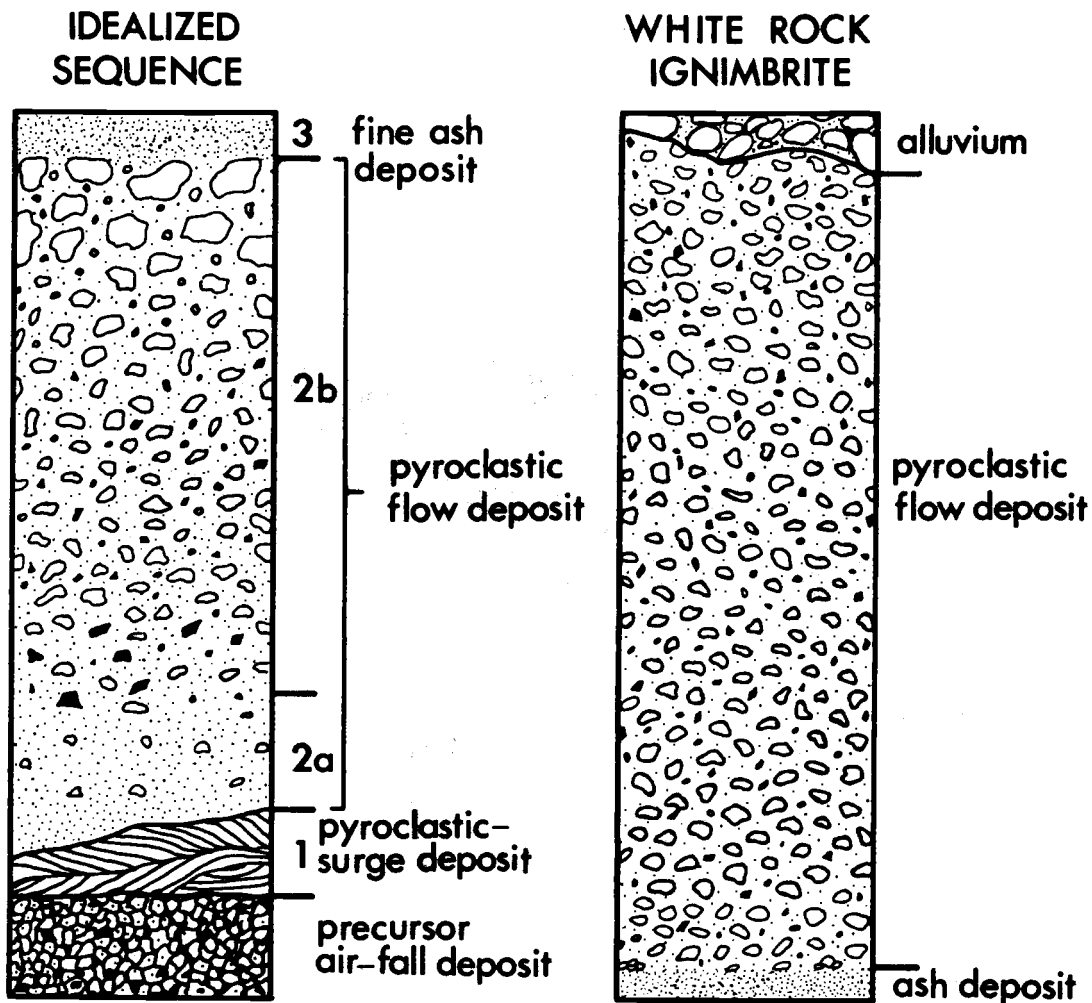
Figure 20. Vertical sections representative of the idealized "standard ignimbrite flow unit" (after Sparks and others, 1973) and the White Rock ignimbrite. The White Rock ignimbrite is a structureless, homogeneous unit equivalent to the main body (2b) of the idealized sequence. Deposits commonly associated with ignimbrites are a precursor air-fall lapillistone, a pyroclastic surge deposit (layer 1) and a fine ash-fall deposit (layer 3).

below the ignimbrite (Figure 21). The ash is uniform in thickness
and the contact with the overlying ignimbrite is sharp and planar
rather than gradational. Such characteristics do not suggest that
the ash deposit is a fine-grained basal ignimbrite layer (2a), but
that it is an air-fall ash deposit which preceeded the pyroclastic
flow. The uniform thickness and composition, and the undisturbed
appearance of the ash layer suggest that the subsequent pyroclastic
flow was not erosive and that only a short period of time elapsed
between deposition of the air-fall ash and the overlying ignimbrite.

Most pumice is light gray, but oxidized pale pink examples
are common. Rarely, a medium gray or light and medium gray mixed
pumice lapillus is found. These dark gray or mixed lapilli are
randomly dispersed throughout the unit and are not characteristic of
any particular horizon. In the main body of the ignimbrite, pumice
sizes range from 6.5 cm to 0.5 cm with the 2 cm to 4 cm size most
common. Dark gray, vitreous lithic fragments range up to 2 cm
in size, but are commonly 1 cm or less.

Chemical analyses (Appendix IIc) of the light gray pumice
indicate that it has a rhyodacite composition. Phenocrysts in the
pumice are sparse and include plagioclase, orthopyroxene, platy
crystals of ilmenite, and octahedra of magnetite which are often
intergrown with orthopyroxene. The rare, medium gray pumice is also
rhyodacite and has sparse phenocrysts. Insufficient samples of the
medium gray pumice were collected to determine its mineralogy.

The White Rock ignimbrite has not been correlated with any
other Deschutes Formation ignimbrite(s) in the basin. Data from
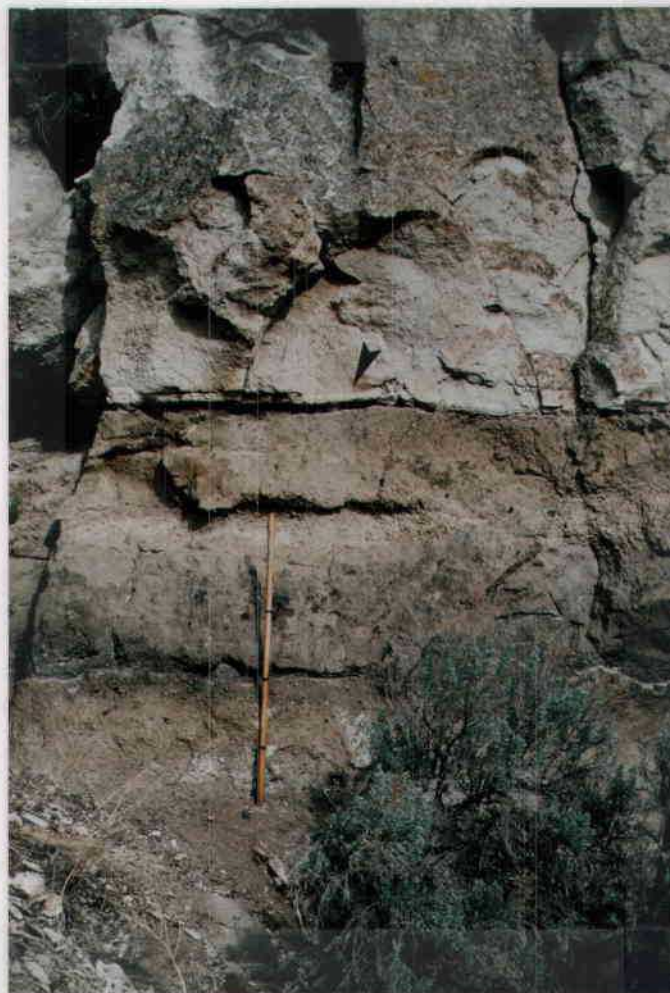
Figure 21.   Fine ash layer (below arrow) at base of White Rock
             ignimbrite.   Tuffaceous sandstone (paleosol) lies below
             ash layer.

other workers (Smith, 1986a) reveal that nearby, unnamed ignimbrites exposed north of the thesis area have major element compositions and a stratigraphic position very similar to that of the White Rock ignimbrite (Table 6). The similar compositions suggest that if the ignimbrites are not products of the same pyroclastic flow, they originated from a similar source. Unfortunately, there are no mineralogical or trace element data to take these comparisons further at this time.

Other Ignimbrites

A white-to light-pink rhyodacitic ignimbrite (Figure 22) is exposed in at least three locations in the west wall of the Deschutes canyon, section 35, T 15 S, R 12 E. Its maximum exposed thickness is slightly less than 4 m. The unit is typically overlain by sandstone and appears to be reworked in its uppermost part. Sorting is poor, but grading in the unit is distinctly normal. Pumice lapilli and blocks up to 15.5 cm in diameter make up approximately 40% of the unit. Pumice is crystal poor but contains phenocrysts of plagio-clase, olivine, clinopyroxene and minor magnetite. Petrographic analyses of the olivine reveal that it has a low optic angle and a high index of refraction, suggesting a fayalitic composition.

Lithic fragments of banded rhyodacite, black vitrophyre, lithophysal rhyolite, and perlitic glass in a pink, glassy matrix, range to boulder size in the lower part of the unit. Some of these clasts appear identical to those in the Tetherow debris-flow deposit

TABLE 6. COMPARATIVE ANALYSES OF TUMALO QUADRANGLE IGNIMBRITES AND
OTHER DESCHUTES FORMATION IGNIMBRITES

	AM282	SF132b	H400b	AM57	CF38g	CF38w
SiO_2	62.6	62.9	63.1	68.2	68.0	67.1
Al_2O_3	16.5	16.6	17.6	16.2	15.9	17.0
TiO_2	1.14	1.12	1.18	0.79	0.74	0.72
FeO*	5.4	5.9	5.6	3.9	4.1	4.1
MgO	1.8	2.8	2.2	1.0	1.0	1.0
CaO	4.3	4.5	4.0	2.6	2.5	2.5
K_2O	1.74	1.88	1.58	2.21	2.12	2.12
Na_2O	5.0	4.4	5.0	4.6	5.4	5.4
Total	98.48	100.10	100.26	99.50	99.76	99.94

AM282   Black pumice from Hollywood ignimbrite (?). Tumalo
quadrangle, SE 1/4, NE 1/4, sec. 23, T16S, R11E
(Appendix IIc).

SF132b   Black pumice from Hollywood ignimbrite, Crooked River
canyon, 2260', SE 1/4, SW1/4, sec. 3, T13S, R12E,
from Smith (1986a).

H400b   Black pumice from Hollywood ignimbrite (?), cuttings from
400' depth in the State Highway #1 geothermal gradient well
north of Powell Buttes, SE 1/4, SE 1/4, sec. 17, T16S,
R12E, from Smith (1986a).

AM57   Light gray pumice from White Rock ignimbrite, NW 1/4,
SE 1/4, T16S, R12E (Appendix IIc).

CF38g   Gray pumice from pink ignimbrite in roadcuts north of
highway 126 and west of Cline Falls, 2835', SW 1/4, NW 1/4,
T15S, R15S, from Smith (1986a).

CF38w   White pumice from above described ignimbrite, from Smith
(1986a).

* Total iron as FeO
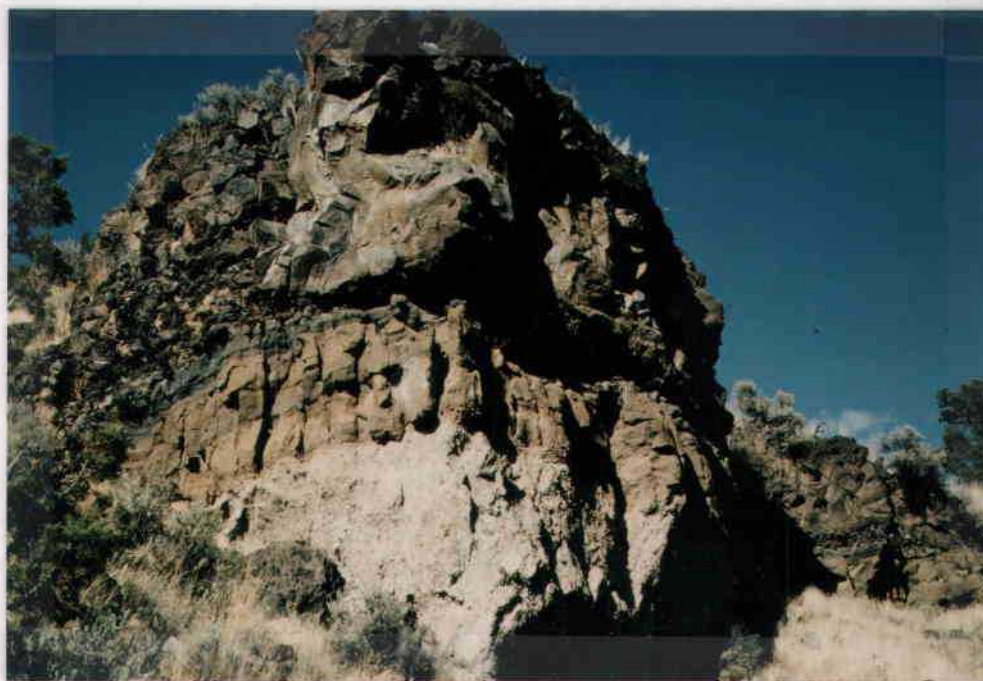
Figure 22. Unnamed pink Deschutes Formation ignimbrite is exposed at the base of this outcrop in the Deschutes River canyon (see text for location). The ignimbrite is overlain by tuffaceous sandstone, a thin, black cinder lapillistone, and aphyric basaltic andesite lava.

which lies immediately below the ignimbrite. The clasts may be accidental fragments entrained in the pyroclastic flow as it passed over the surface of the debris-flow deposit. Alternatively, the pyroclastic flow and debris flow may have been genetically associated, perhaps having their origins in the same eruptive event or in closely spaced eruptions of the same source. Debris flows or "mudflows" are a common product of ignimbrite eruptions and have been observed to form from or at the same time as pyroclastic flows (Moore and Melson, 1969; Zen and Hadikusumo, 1964).

An andesitic ignimbrite is found in sections 13, 14, 23, and 24, T 16 S, R 11 E, on the south and east sides of the lava-capped plateau. The ignimbrite is not welded and forms scarce outcrops near the south base of the plateau where it is in close association with volcaniclastic sediments. Most often its presence is marked by loose, black to oxidized orange pumice lapilli and a reddish soil. Outcrops are usually low lying and have a knobby texture caused by differential weathering of the pumice and ashy matrix. Black, dark gray and mixed pumice lapilli and bombs ranging in size from 2.5 to 15 cm are common. The pumice is typically dense and less inflated than that of the more silicic ignimbrites. Plagioclase phenocrysts in the pumice are common and are accompanied by orthopyroxene, clinopyroxene, magnetite and minor ilmenite. Lithic fragments in the unit are typically dark gray, and are usually less than 1 cm. The ashy matrix is tan to reddish brown or orange. Phenocryst mineralogy and major element composition of black pumice from this unit closely resemble those from black pumice in the

compositionally heterogenous Hollywood ignimbrite in the Crooked River gorge. Both are similar in composition and mineralogy to cuttings from an ignimbrite intercepted in a geothermal gradient well north of Powell Butte (Smith, 1986a) (Table 6). Lack of stratigraphic control between the areas makes correlation between the ignimbrite units tenuous, but their similarity in composition and mineralogy implies a similar if not the same source.

A light pink, dacitic ignimbrite crops out along a narrow roadcut on Dayton Road (section 23, T 16 S, R 11 E). An ignimbrite of similar appearance forms an exposure less than 0.3 m high at the west base of the lava plateau in center of section 14, T 16 S, R 11 E, and is assumed to be the same unit. The ignimbrite is not welded and contains light gray to white pumice lapilli with sparse phenocrysts of plagioclase, orthopyroxene, clinopyroxene, and magnetite. This ignimbrite is assumed to be a member of the Deschutes Formation although its stratigraphic relationship is uncertain due to its limited exposure. The hydrated appearance of the pumice suggests that it is not a Quaternary pyroclastic deposit.

Shallow roadside excavation immediately south of Long Butte in the NW 1/4 of section 27, T 16 S, R 12 E, revealed a white to light gray ignimbrite. The unit is overlain by up to 0.3 m of soil and cinder and is not exposed at the surface. Pumice lapilli are predominately white but include brown to dark gray and mixed varieties. Available pumice clasts were too weathered for chemical analysis.

Discussion

Numerous ignimbrites ranging in composition from andesite to rhyolite are interlayered with the sedimentary rocks and lavas of the Deschutes Formation. Approximately 30 ignimbrites have been recognized at Green Ridge (Conrey, 1985) and others are exposed northeast of Green Ridge in the Whitewater canyon (Yogodzinski, 1986). Within the Deschutes basin, ignimbrites often formed widespread sheets. Remains of at least 15 ignimbrites in the basin are extensive enough to serve as stratigraphic markers (Stensland, 1970; Cannon, 1984; Smith, 1986a).

By contrast, the number and volume of Deschutes Formation ignimbrites in the Tumalo area appear small. None have been positively correlated with ignimbrites identified elsewhere in the basin. The ignimbrites exposed in the Tumalo area appear to have been small, localized deposits. Numerous, primary pumice lapillistones, the air-fall deposits of Plinian eruptions, are exposed locally in the walls of the Deschutes canyon, which suggests that nearby pyroclastic volcanism was more active than indicated by the number of exposed ignimbrites. Assuming these Plinian eruptions had concomitant pyroclastic flows, few of the pyroclastic flows appear to have reached the Tumalo area. Numerous, thick lapillistones near the top of the Deschutes Formation have been suggested to represent continuing pyroclastic eruption of Deschutes Formation volcanoes after their subsidence into the High Cascade graben prevented the movement of pyroclastic flows into the basin.

The sparse number of ignimbrites exposed in the Tumalo area may be attributable in part to the tendency of unwelded ignimbrites to erode and form slopes, reducing the liklihood that they would have surface expression or be exposed in an area of low topographic relief. Deeper dissection of the Tumalo area would likely reveal other Deschutes Formation ignimbrites.

Lack of welding and absence of paleomagnetic signatures among the ignmibrites in the Tumalo area suggest relatively cool emplacement. Cool emplacement and relatively thin, localized ignimbrite units suggest the ignimbrites exposed in the Tumalo area represent the distal parts of pyroclastic flows.

Many pyroclastic flows entered the Deschutes basin via the flanks of volcanoes at the latitude of Green Ridge. Other ignimbrites, including those in the Tumalo area, followed the northeast paleoslope into the basin from sources far south of Green Ridge. The source volcanoes for these pyroclastic flows are hypothesized to have been in the topographic highland known as the Tumalo Volcanic Center (TVC) (Hill, 1988) approximately 15 km east of the Three Sisters (Figure 23). The TVC marks an area of localized silicic volcanism which has been active throughout the Pleistocene and has been identified as the source of numerous Pleistocene ignimbrites in the Tumalo-Bend vicinity.
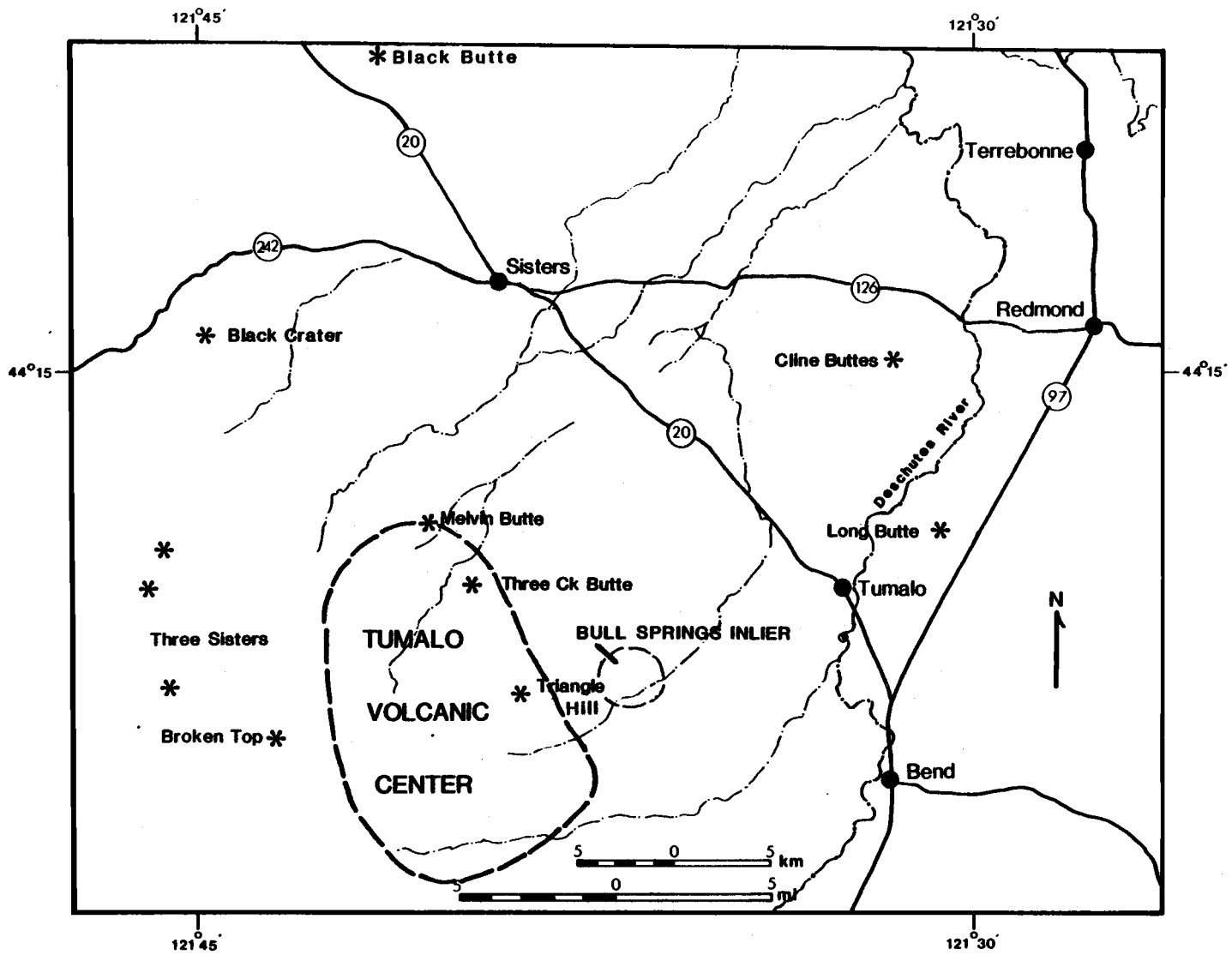
Figure 23. Location of the Tumalo Volcanic Center (TVC) and the Bull Springs inlier of Deschutes Formation rocks.

LAVAS

Deschutes Formation basalt and basaltic andesite lavas crop out over approximately 45km^2 in the Tumalo quadrangle and are the most extensively exposed Deschutes Formation rock type. These lavas form part of the lava plateau mapped by Stensland (1970) to the north and northwest, where similar lavas are also interbedded with the underlying sedimentary and pyroclastic rocks. The lavas erupted from local small shield volcanoes and cinder cones. Lava flows consistently followed the northeast paleoslope and typically formed thin units 2 - 7 m thick and up to 9 km long.

Five basalts and numerous basaltic andesites were identified in the study area. Of these lavas, eight form mappable units (Plate 1) which are described in a following section. The basalts include an aphyric, a diktytaxitic, and three porphyritic lavas. The basalts have an average silica value of 52 wt.% and are high in alumina. Phenocrysts form up to 41% of the rock in the porphyritic basalts. The predominant phenocryst phase is plagioclase, with much smaller amounts of olivine. Alteration of the basalts is minor and includes zeolites lining vesicle walls and minor carbonate in the groundmass.

Basaltic andesites form the bulk of the lavas. In outcrop they are dense and have well developed platy jointing (Figures 24 and 25). The basaltic andesties are characteristically fine grained, aphyric to sparsely porphyritic, with phenocrysts of plagioclase, olivine, clino-pyroxene, and, less commonly, Fe-Ti oxides. The most common form of

Figure 24. Typical outcrop of basaltic andesite lava (approximately 4 m thick). Hammer for scale in lower left of photo.

Figure 25. Platy basaltic andesite lava.

alteration in the basaltic andesites is a slight yellow-green or red staining along joint planes which is undetectable in thin section.

Aphyric to sparsely porphyritic lavas typically overlie the sedimentary and pyroclastic rocks and form the top of the formation. In some locations the lavas overlie paleosols, elsewhere they overlie widespread laminated sandstone. Contacts between the sedimentary rocks and the lavas which cap them are usually horizontal planar. However, an aphyric lava exposed in the canyon wall near the northeast end of the study area filled a broad channel approximately 30 m deep. The widespread laminated sandstones and predominance of horizontal contacts suggests only a brief hiatus between the end of sedimentation and eruption of the lavas. A porphyritic basaltic andesite in the river bed at Awbrey Falls appears to have been deposited during sedimentation, as sedimentary lithologies which crop out from beneath the alluvial deposits adjacent to the lava are at a higher stratigraphic level. Lavas are not found interbedded with sedimentary rocks exposed in the canyon walls. Field relationships suggest that the porphyritic basalts were erupted prior to the aphyric lavas (see following section on lava ages). The basalts were likely erupted during sedimentation, although there is no direct evidence to support this assumption.

Stratigraphic relationships between many of the lavas are uncertain due to their low relief and because a sandy soil commonly obscures flow tops and contacts. Individual basaltic andesite flows are often difficult to distinguish and follow as many of the flows are similar in appearance and original flow topography has been disrupted

by normal faults. Fault scarps and canyon walls offer the best exposures of the lavas. In the canyon walls, exposures of two or three superposed lava flows are common. Contacts between the lavas are usually roughly horizontal and are marked by an oxidized, scoraceous flow breccia 1 to 1.5 m thick. The absence of eroded surfaces or soil horizons between flows indicates the lavas were deposited over a short period of time.

Source vents

There are seven known eruptive sites in the Tumalo quadrangle (Figure 26). The basaltic shield volcano known as Long Butte lies in the southeast part of the study area and is the largest of the volcanoes. The remainder are best described as small shield volcanoes and low-lying cinder cones, typically less than 1km^2 in area and with slopes of ten degrees or less. None have slopes or height-to-width ratios characteristic of "fresh" cindercones (Porter, 1972; Wood, 1980). The original morphology of many volcanoes has been modified by erosion, faulting and mining of cinder. However, the present form of these volcanoes should not be attributed mainly to the effects of exploitation or degradation. Their flanks have not been deeply incised by erosion and they have remained roughly symmetrical, suggesting that much of their original shape has been preserved. The morphology of these small volcanoes is likely a reflection of their eruptive process and history. Even at cinder cones the
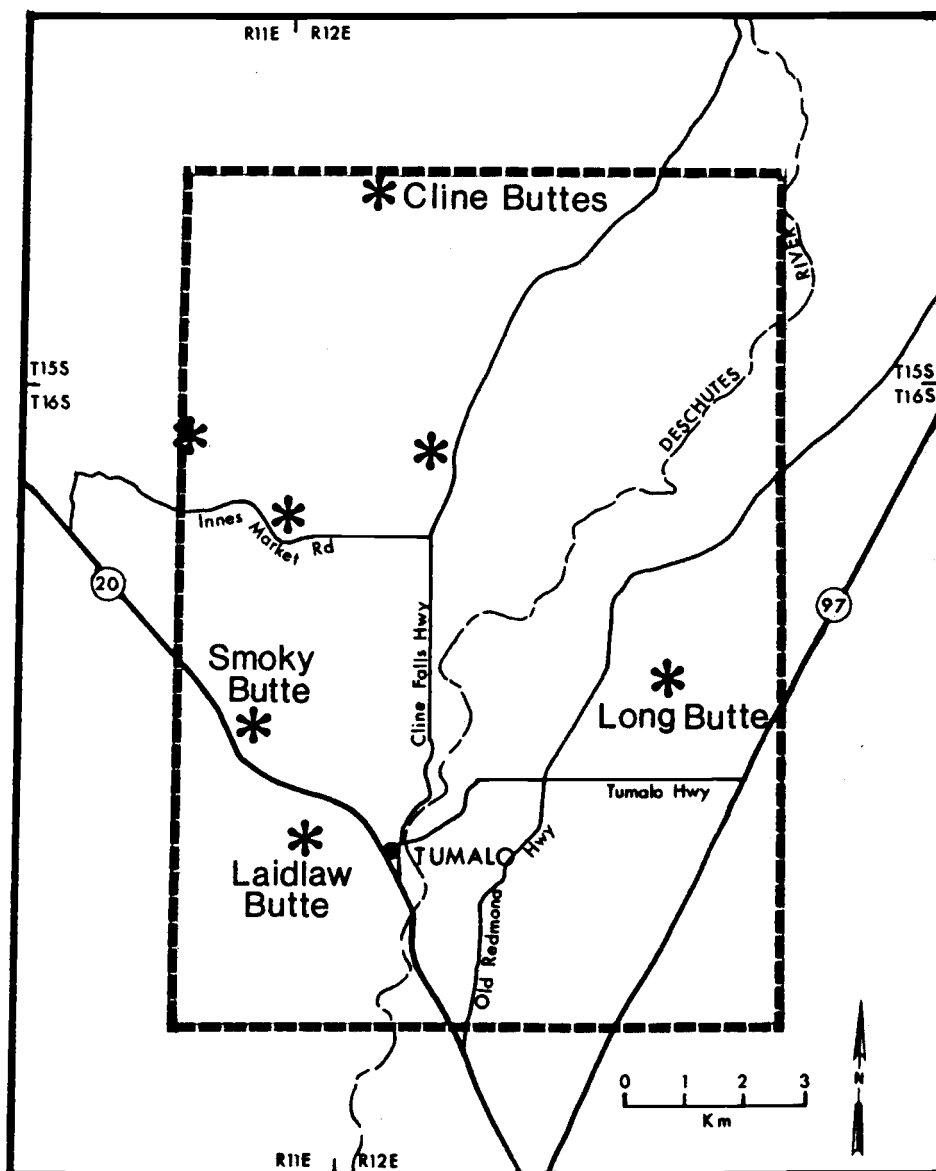
Figure 26. Location of Deschutes Formation source vents in the Tumalo quadrangle. Vents are represented by asterisks. Dashed line marks quadrangle boundaries.

volume of pyroclastic material is generally equal to or subordinate to
lava. Pyroclastic ejecta is usually absent at the small shield
volcanoes. The low-profile structure of the volcanoes and the
preponderance of lava over pyroclastic material suggests that although
volcanic eruptions may have included explosive Strombolian activity,
the effusive outpouring of low viscosity lava was probably more
characteristic of the eruptions. The small size of the volcanoes and
the small volume of the lava which they erupted suggest short-lived,
monogentic eruptive histories.

Age of lavas

The absence of paleosols or erosion surfaces between the basaltic
andesite lavas suggests that they were deposited over a relatively
short period of time. A brief depositional history for the basaltic
andesites is also suggested by the fact that they all posess a reverse
magnetic polarity. A late Miocene Ar/Ar age of 5.4 $\pm$ 0.10 Ma
(L. Snee, pers. comm.) was obtained from a lava near the top of the
volcano in section 2 and 11, T16S, R11E which erupted lava Tdba3.
This date coincides with chron 3r, a reverse polarity interval between
4.79 and 5.41 Ma (Harland and others, 1984). Plateau-capping lavas in
the more northerly part of the Deschutes basin have ages similar to
that obtained from the Deschutes Formation lava in the Tumalo quad-
rangle. A compositionally and petrographically similar lava north of
the study area at Steamboat Rock has an Ar/Ar age of 5.1 $\pm$ 0.2 Ma
(G. Smith, 1986a). A K/Ar date of 4.9 $\pm$ 0.4 (Armstrong and others,

1975; recalculated by Fielbekorn and others, 1982) was obtained from a Deschutes Formation lava on the west rim of Deep Canyon at highway 126, approximately 5km north of the study area.

Stratigraphic relationships suggest that the porphyritic basalt lavas are older than the fine grained basaltic andesites. At contacts between the two lava types, basaltic andesite invariably ramped against or flowed over the basalt. Oriented samples from Cline Buttes and Long Butte basalts have normal magnetic polarities, futher suggesting their eruption was not contemporaneous with those of the basaltic andesites. None of the basalts has been isotopically dated. Smith (1986a) described porphyritic, high-alumina basalts in the central Deschutes basin similar to the ones in the Tumalo area and assigned them a stratigraphic position in the "lower half" of the Deschutes Formation.

Unit Descriptions of lavas

More than 15 separate basalt and basaltic andesite lavas were identified in the Tumalo quadrangle. Most are represented by discontinuous exposures too small to map at the scale used for this study. Eight of the most widespread and prominent lavas (Table 7) were divided into mappable units. The remainder were grouped into a single unit. A description of these units and their source vents follows.

TABLE 7. SUMMARY OF DESCHUTES FORMATION LAVAS IN THE TUMALO QUADRANGLE

Lava	Source	Texture	Mineralogy		An content*
			Phenocryst	Groundmass	
Tdb1	Long Butte	porphyritic	plag 34% ol 4%	plag, cpx, ol, Fe ox glass	An60-68
Tdb2	Smoky Butte	sub-ophitic to intergranular, diktytaxitic		plag 52% ol 10% aug 15% Fe ox 8% glass 15%	An66
Tdb3	Cline Buttes	porphyritic	plag ol	plag, cpx Fe ox, ol	An50
Tdb4	unknown	coarsely porphyritic	plag 40% ol 1%	plag, cpx, Fe ox, ol, glass	An64
Tdba1	Laidlaw Butte	aphyric	<1% plag, aug, ol, Fe ox	plag, cpx	An75 (core) An65 (rim)
Tdba2	Innes Mkt Rd. cone	aphyric	<1% plag, aug, ol, Fe ox	plag, cpx, Fe ox, glass	An60-62
Tdba3	unnamed vent, sec. 2, 11, T16S, R11E	sparsely porphyritic	<5% plag, ol, aug, Fe ox	plag, cpx, ol, Fe ox, glass	An51-59
Tdba4	unnamed vent, sec. 7, 8, T16S, R12E	aphyric	no data available		

* compositions determined petrographically

Tdbl

A single basalt lava, Tdbl, forms the shield volcano known as Long Butte (Figure 27). It covers approximately 4.8km^2 in sections 15, 22, 23, and 26, T16S, R12E. With a maximum relief of 123 m, Long Butte is the largest Deschutes Formation volcano in the area. A small cinder cone on the lower southwest side of Long Butte has been obliterated by mining. Cinder from the cone has the same composition as the lava which forms the shield volcano. Lava approximately 8 m thick forms a tabular cap atop the remains of the cinder cone and appears to have solidified in the crater of the cone.

Long Butte lava has a distinctive appearance. It is coarsely porphyritic, forms crude polygonal joints, and often is weathered, oxidized and reddish, particularly near the summit. Phenocrysts of plagioclase (34%) and olivine (4%) commonly form glomerocrysts in Tdbl. Phenocrysts lie in an intergranular to intersertal groundmass of plagioclase (42%), clinopyroxene (25%), olivine (10%), Fe-Ti oxide (8%), and brown glass (15%) (Figure 28). Optical determinations of phenocryst plagioclase yield a labradorite composition (An60-An68). Labradorite crystals form two size groups: 0.4 - 0.75 mm, and 2 mm and larger. Most of these are somewhat resorbed, particularly at crystal margins. Cores and certain compositional zones commonly were resorbed and the ensuing voids were filled by groundmass clinopyroxene, glass, and Fe-Ti oxide. Crystals are normally zoned and may have faint oscillatory zoning. Olivine phenocrysts range in size from 0.4 to 1.5 mm and are subhedral to anhedral. They have been
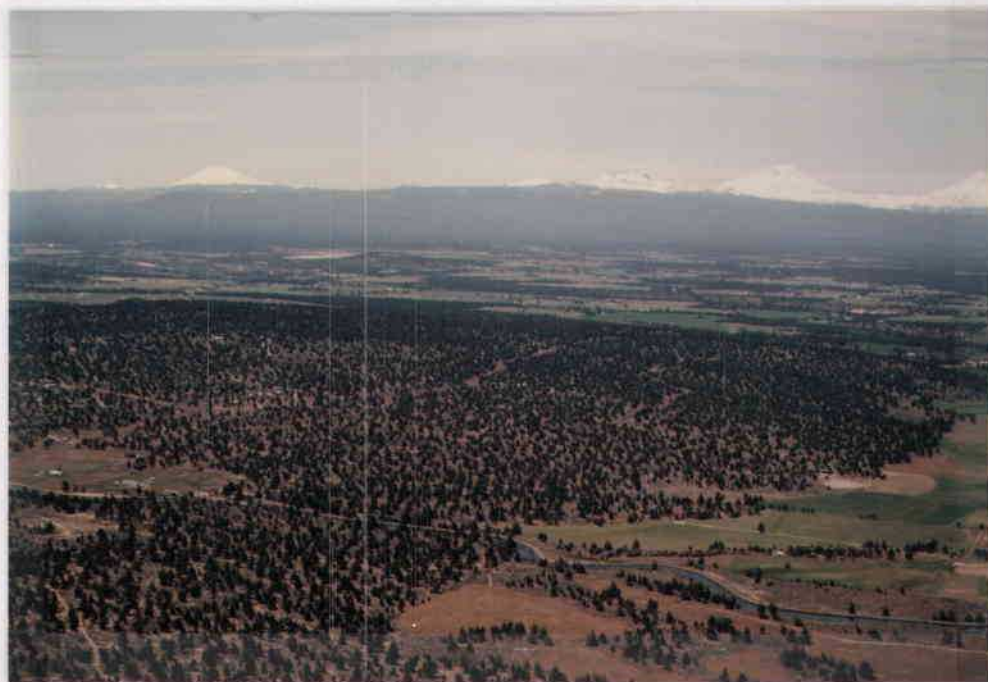
Figure 27.   The low-lying forested shield volcano Long Butte lies in center foreground.   High Cascade Range is on the horizon.
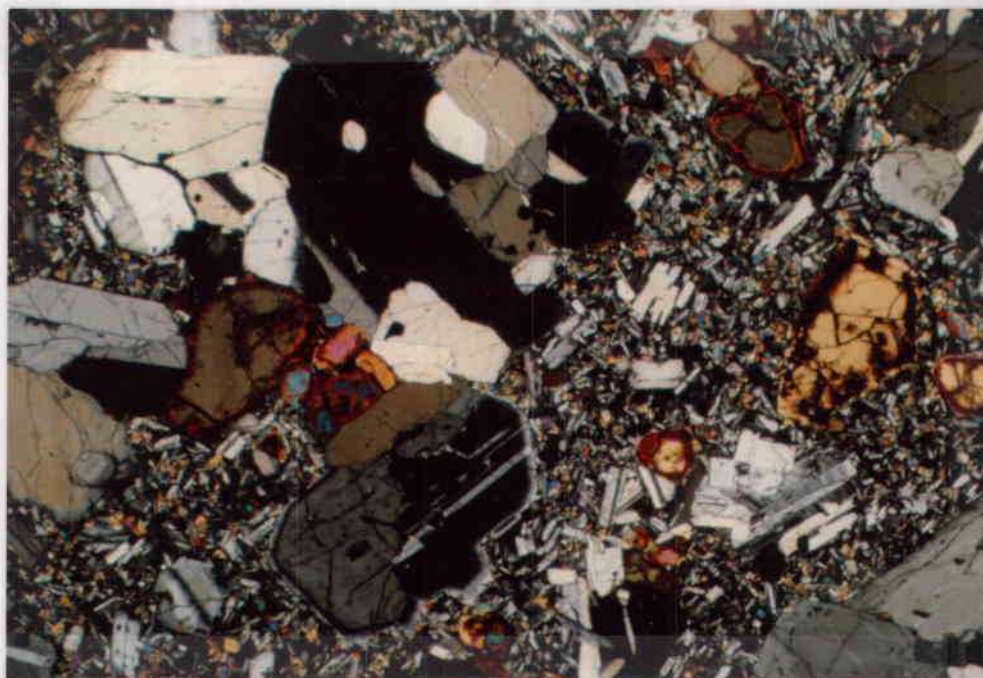
Figure 28.   Glomerocryst and phenocrysts of plagioclase and olivine
             lie in an intergranular groundmass of plagioclase,
             clinopyroxene, olivine, and Fe-Ti oxide in lava Tdbl.
             Crossed nichols at 40x.

partially to totally altered to iddingsite. Often a thin, unaltered
zone of olivine forms crystal rims. In samples collected near the
summit of Long Butte (Figure 29) olivine phenocrysts have been
completely altered and their crystal outlines are pseudomorphed
by Fe-Ti oxide. Olivine is absent in the groundmass and clino-
pyroxene is less abundant and smaller than in unaltered samples of
this lava. Numerous small crystals of a dark red translucent hydrous
iron oxide (iddingsite?) are in the groundmass. Such alteration
products are typical of the high temperature, deuteric oxidation of
forsteritic olivine.

Tdb2

Tdb2 is a basalt lava erupted from a small shield volcano in
sections 23, 24, 25, and 26, T16S, R12E, locally known as Smoky
Butte. The volcano and part of a lava flow on its eastern side are
exposed over an area slightly greater than $1km^2$. Height of the
volcano is only 33 m and its slope is between 2^0 and 3^0, making it a
nearly indiscernable topographic feature. Its eastern flank is cut
by a normal fault with an offset between 18 and 22 m.

The lava has well developed polygonal jointing. A poorly
developed diktytaxitic texture characterizes parts of the lava. The
predominant petrographic texture is subophitic to intergranular or
intersertal (Figure 30). Plagioclase is the dominant mineral,
forming 52% of the rock and ranging seriately in size from 2 mm to
less than 0.1 mm. Optical determinations of larger plagioclase
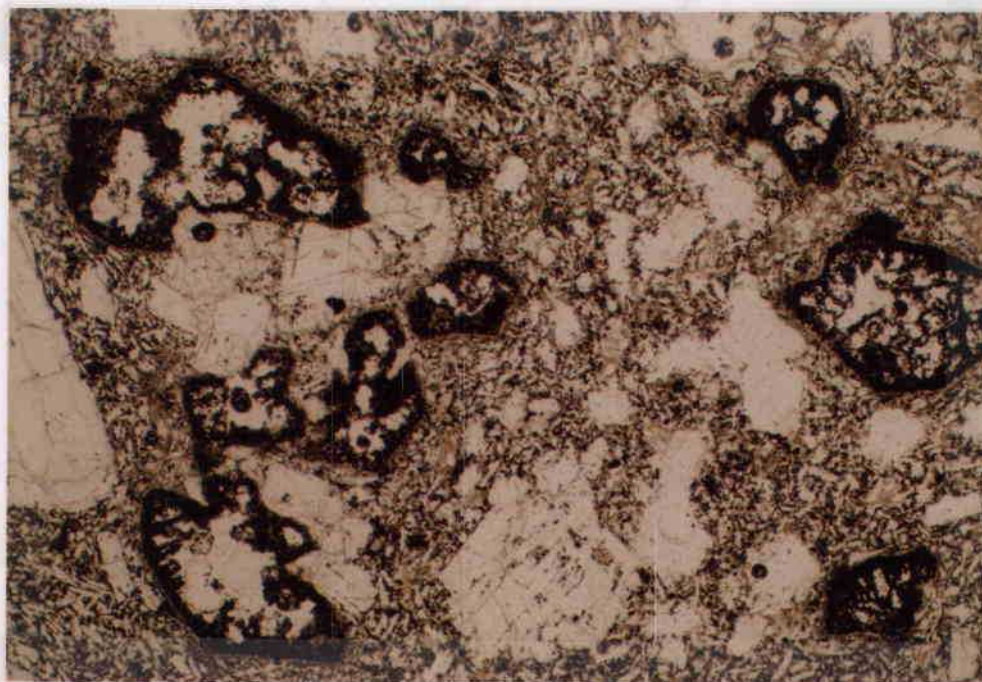
Figure 29.   Thin section of lava Tdbl from sample collected near the
summit of Long Butte.   Olivine phenocrysts have been
deuterically altered and their crystal outlines pseudo-
morphed by Fe-Ti oxide.
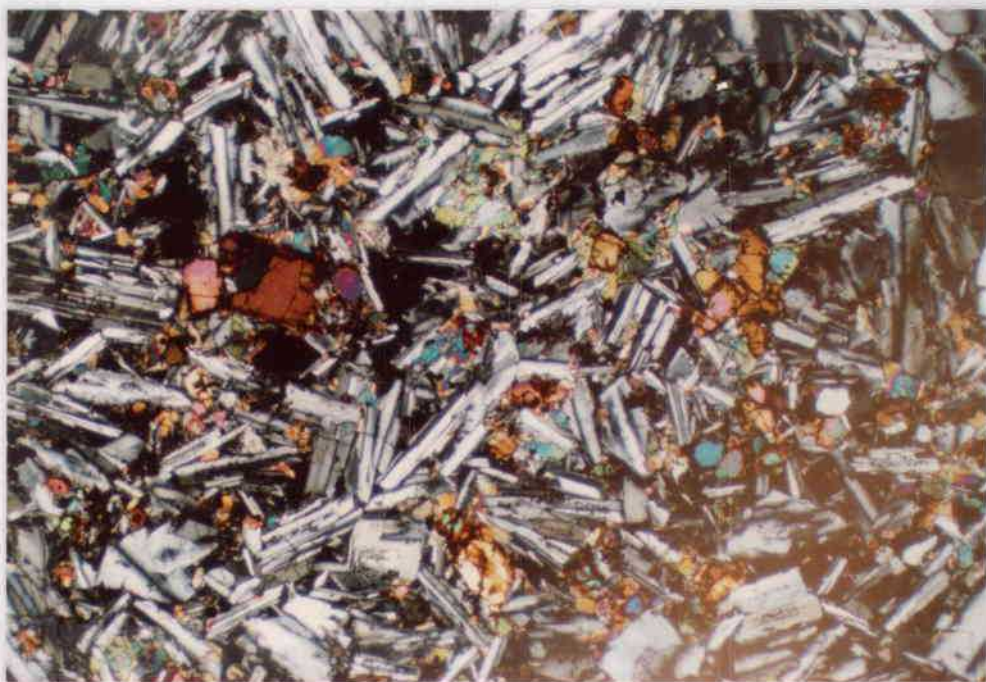
Figure 30. Basalt lava Tdb2 has poorly developed diktytaxitic texture. Plagioclase forms 52% of the rock, followd by augite, olivine, Fe-Ti oxide and glass. Crossed nichols at 20X.

crystals yield a labradorite (An66) composition. Most plagioclase crystals are normally zoned and show moderate amounts of resorption in cores or certain compositional zones. Resorbed areas are filled with groundmass clinopyroxene, glass and Fe-Ti oxide. Olivine forms 10% of the rock, ranges up to 1mm in size, and is interstitial to plagioclase. Alteration to iddingsite is common along rims and fractures in larger olivine crystals. Smaller crystals are almost completely altered to iddingsite. Augite composes 15% of the rock and forms anhedral crystals, often partially enclosing plagioclase. Hourglass zoning is well developed. Fe-Ti oxide forms 8% of the lava and appears as small subhedral crystals and inequant blebs. Dark brown glass composes 15% of the rock and forms an intersertal-to-hyalophitic texture.

Tdb3

The basalt lava Tdb3 forms a knob 1115 m high on the the south-west side of Cline Buttes and a short flow lies at its north base. The lava is vessicular and forms weathered outcrops over an area of approximately $0.5km^2$. Soft, white secondary material assumed to be zeolite, lines many of the vesicle walls. Tdb3 is included with Deschutes Formation lavas due to its similar appearance and compo-sition to other Deschutes Formation basalts, although its age remains speculative. Tdb3 appears to overlie Cline Buttes rhyodacite which pre-dates the Deschutes Formation, but is of uncertain Tertiary age (see previous discussion on Cline Buttes). An aphyric Deschutes

Formation lava laps against Tdb3 at the base of Cline Buttes.

Tdb3 is composed of 25% phenocrysts and glomerocrysts of plagioclase and olivine in a subophitic to intergranular groundmass of plagioclase, augite, Fe-Ti oxide, and olivine (Figure 31). Plagioclase phenocrysts are labradorite (An50) and are 1 to 3.5 mm long. Most plagioclase phenocrysts show corrosion parallel to cleavage and are predominantly normally zoned, with faint oscillatory zoning near crystal rims. Olivine phenocrysts range from 0.5 to 2 mm and are heavily to totally altered to iddingsite. A few olivine phenocrysts have thin rims of clinopyroxene.

Tdb4

The coarsely porphyritic basalt lava Tdb4 forms low, rounded, weathered outcrops over an area of less than 1km^2 in section 11, T16S, R11E. The lava crops out on the gentle southern slope of a small, elongate shield volcano. The volcano erupted a fine grained, sparsely porphyritic basaltic andesite (Tdba3) which appears to overlie the basalt. The basalt is overlain by another fine grained basaltic andesite to the east and disappears beneath a sandy soil to the south. No source vent for the basalt has been located.

The basalt contains 41% phenocrysts and glomerocrysts of plagioclase (40%) and olivine (1%) in a subophitic to hyalophitic groundmass of clinopyroxene, plagioclase, Fe-Ti oxide, olivine and dark brown glass (Figure 32). Plagioclase phenocrysts are labradorite (An68), 2 to 7 mm long, and show little evidence of resorption. They commonly have thin lamellar growths of Fe-Ti oxide parallel
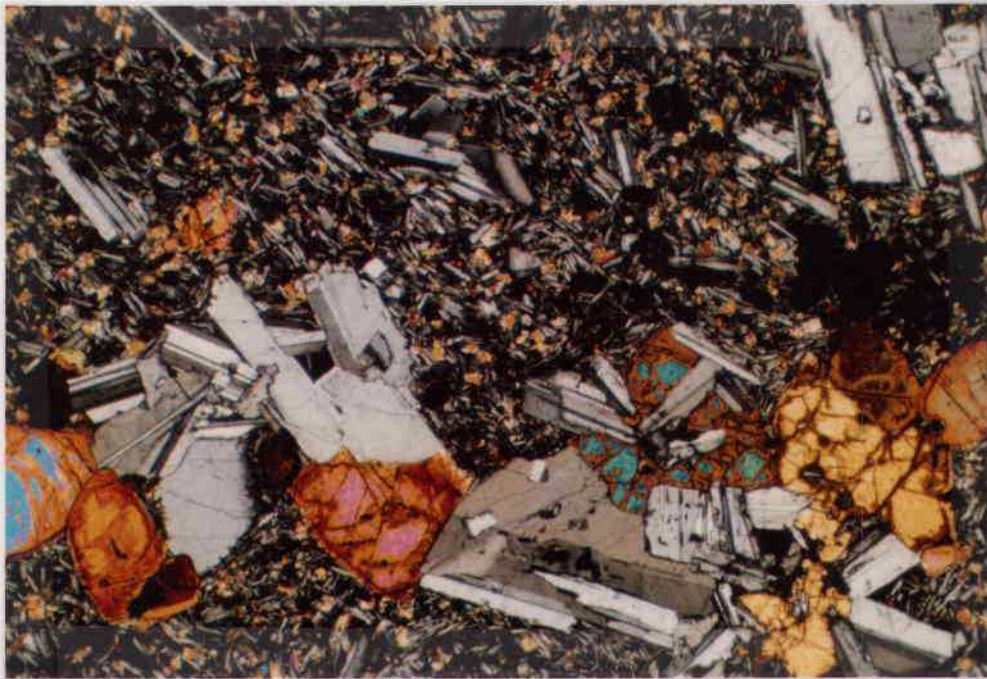
Figure 31. Lava Tdb3 is characterized by glomerocrysts and pheno-
            crysts of plagioclase and olivine in a aubophitic to
            intergranular groundmass of plagioclase, clinopyroxene,
            Fe-Ti oxide, olive and glass. Crossed nichols at 40X.

Figure 32.   Coarsely porphyritic lava Tdb4 contains phenocrysts of
             oscillatory zoned plagioclase and minor olivine in a
             subophitic to hyalophitic groundmass of clinopyroxene,
             plagioclase, Fe-Ti oxide, olivine, and glass. Crossed
             nichols at 20X.

to cleavage and glass fills minor fractures. Olivine phenocrysts are strongly altered to iddingsite, usually leaving only a rim of fresh olivine. Brownish, highly birefringent clay and minor carbonate are found as alteration products in the groundmass.

Tdbal

The fine grained, aphyric basaltic andesite lava Tdbal erupted from Laidlaw Butte (Figure 33), a cinder cone which lies a kilometer west of Tumalo. The lava flowed northeast for a distance of 8 km, wrapping around the west, southwest and north sides of Long Butte. The proximal part of the lava was subsequently downfaulted and covered by Quaternary pyroclastic deposits and alluvium, leaving only sparse, isolated islands of lava exposed at the surface. However, the lava is well exposed in canyon walls immediately north of Tumalo. It has an undulating base and a thickness which ranges between 4 and 7 m. Tdbal is dark gray and has platy jointing.

With a height of 70 m and a slope as great as 10°, Laidlaw Butte is more conspicuous than most of the small volcanoes. A large volume of coarse pyroclastic material is associated with this cinder cone and forms much of its southwest side. Volcanic bombs measuring more than a meter in diameter are common. A large cinder pit has been developed on the south side of the cone and most of the pyroclastic material has been removed. Agglutinate is prevalent on the upper part of the cone. Scoriaceous and oxidized lava covers the lower western half of the cone and marks the point of origin for the flow.
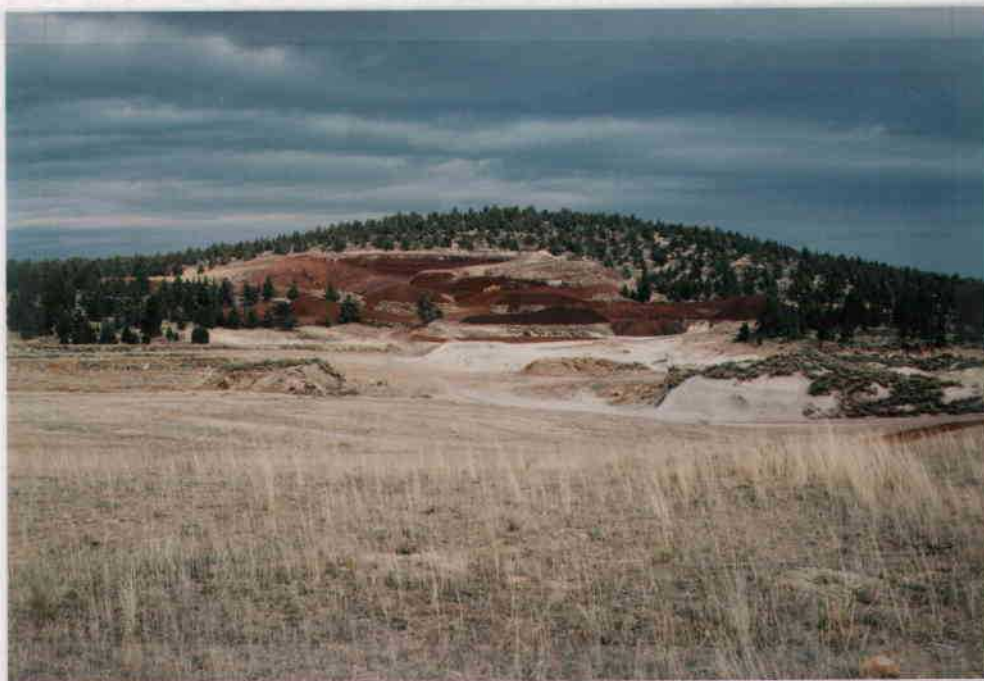
Figure 33. Cinder pit on the west side of Laidlaw Butte.

Phenocrysts and glomerocrysts of plagioclase (0.5-2 mm), augite (0.75 mm), and rare olivine (0.4-2 mm) and euhedral Fe-Ti oxide (0.2-0.4 mm) compose less than 1% of the rock (Figures 34a and 34b). Plagioclase is normally zoned, ranging in composition from bytownite (An75) at crystal cores to labradorite (An65) at crystal rims. The largest plagioclase phenocrysts are embayed and resorbed, and frequently have a seive texture. Groundmass and glass commonly fill the voids created by resorption. Crystals contain apatite inclusions and euhedral crystals of Fe-Ti oxide assumed to have filled resorbed areas.

Clinopyroxene phenocrysts were identified as augite by their high optic angle. Fe-Ti oxide forms inclusions in some augite crystals. Olivine phenocrysts are partially to totally altered to iddingsite. Some crystals are a deep red color, with corroded cores replaced by groundmass. Olivine crystals rimmed by Fe-Ti oxide are also common. Small isotropic inclusions in some of the olivine crystals may be picotite.

Groundmass constituents are plagioclase (70%), clinopyroxene (15%), and Fe-Ti oxide (15%). Groundmass plagioclase is labradorite (An 50) and forms a strongly trachytic texture. Clinopyroxene and Fe-Ti oxide are intergranular to plagioclase. The groundmass is often very dark due to concentrations of opaque Fe-Ti oxide, commonly as swirls and bands.
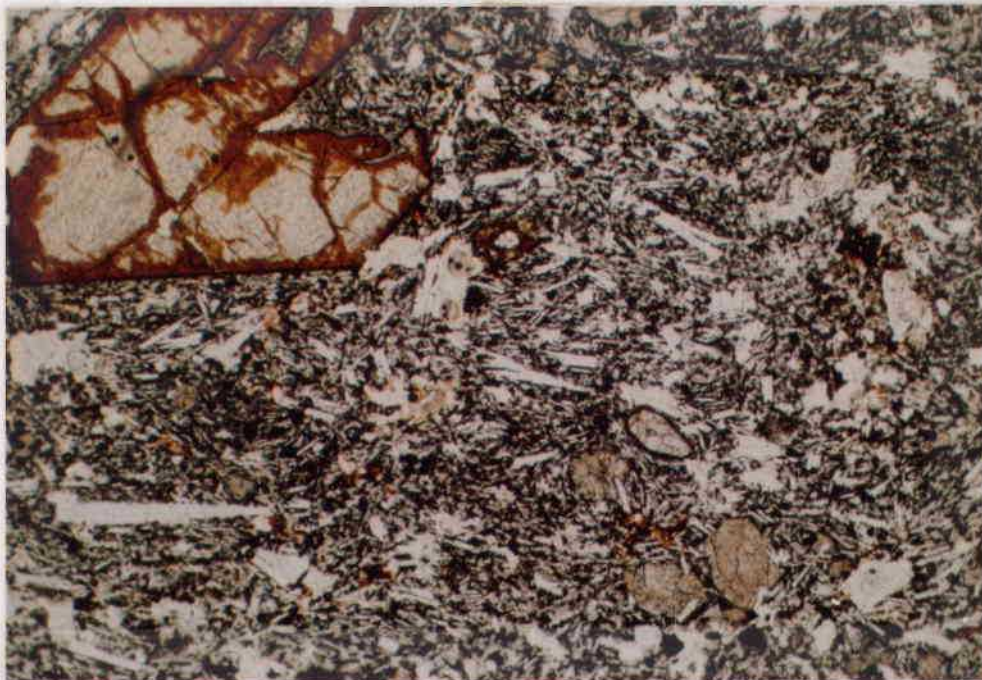
Figure 34a. Rare olivine phenocryst (upper left) in lava Tdbal.
Small olivine with resorbed margins (right center)
contains small inclusion identified as picotite.
Groundmass includes plagioclase, clinopyroxene, and
abundant Fe-Ti oxide. Plane light at 40X.
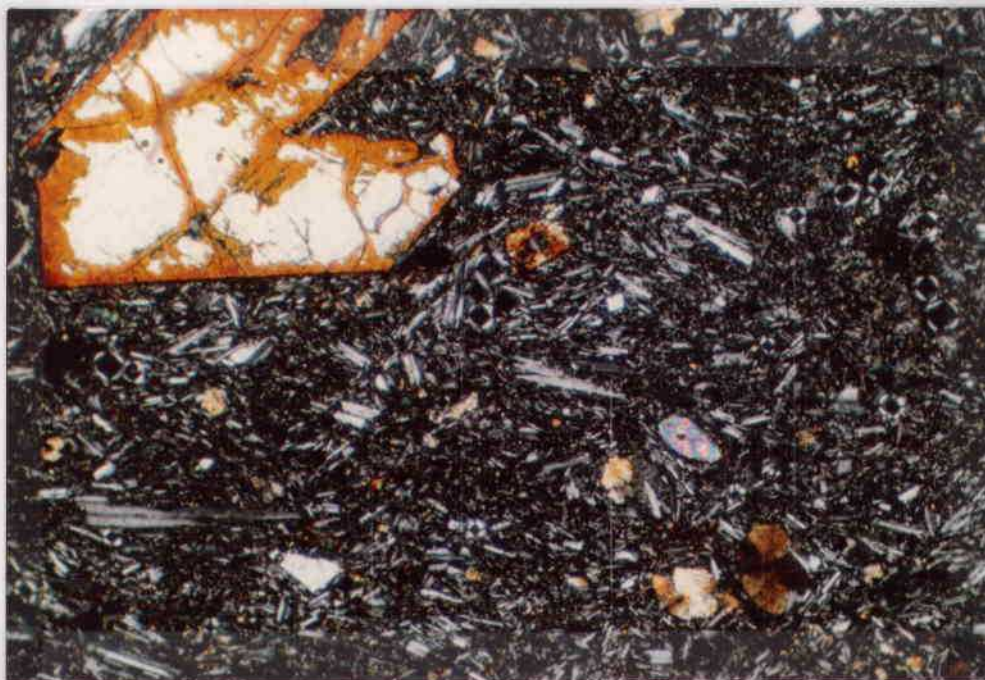
Figure 34b. As above, with crossed nichols.

Tdba2

The fine grained, aphyric basaltic andesite lava Tdba2 erupted from a small cinder cone on Innes Market Road, section 12, T16S, R11E (Figure 35). The flow issued from the north side of the cone and traveled northeast a distance of 9 km. Where exposed in the walls of the Deschutes canyon (Figure 36), the flow varies from a relatively uniform thickness of 5 m to approximately 30 m where it filled a broad topographic depression near its terminus. Platy jointing is apparent throughout most of the flow.

The area of the cinder cone is slightly greater than 0.5 km^2. Much of the cone appears to be composed of lava, or is at least mantled by lava, which is scoriaceous near its top. Sufficient cinder was available on the west side of the cone for the development of a small cinder pit, although the resource appears marginal and the pit is currently idle.

Phenocryst and glomerocrysts of plagioclase (0.5-1.75 mm), augite (0.5-1.0 mm), rare olivine (0.5-0.75 mm), and Fe-Ti oxide (0.2 mm) compose less than 1% of the lava (Figure 37). Plagioclase composition is labradorite (An60-An62). Minor voids created by resorption in cores has been filled by clinopyroxene, Fe-Ti oxide or glass is common. Extreme resorption of crystals is rare. Crystals are normally zoned but commonly have oscillatory bands at their rims. Olivine crystals are altered to iddingsite along fractures and at crystal margins. Plagioclase laths in the groundmass form a trachytic texture with intergranular clinopyroxene, Fe-Ti oxide, and intersertal glass.

Figure 35. Basaltic andesite cinder cone on Innes Market Road
(center skyline) erupted lava Tdba2.

Figure 36. Basaltic andesite lava Tdba2 exposed in the wall of
Deschutes River canyon. Lava appears to have filled
wide, east to northeast trending channel. Maximum flow
thickness approximately 30 m.

Figure 37. Lava Tdba2 contains glomerocrysts of augite, plagioclase, and euhedral Fe-Ti oxide in a trachyitic groundmass of plagioclase, with intergranular clinopyroxene, Fe-Ti oxide and glass. Crossed nichols at 40X.

Tdba3

Tdba3 is a fine-grained, sparsely porphyritic lava which origi-
nated from a small shield-like volcano in sections 2 and 11, T16S,
R11E. The volcano is a topographically inconspicuous feature approx-
imately 60 m high which covers an area of approximately 1.5 km^2.
Only the eastern half of this volcano is located in the Tumalo quad-
rangle. Its western part is located on the Tumalo Dam quadrangle and
is flanked by two smaller volcanoes. No pyroclastic deposits are
associated with the volcano. It is composed wholly of lava which is
oxidized and scoriaceous at its summit. A lava flow poured from the
north side of the volcano and traveled nearly 5.5 km northeast to the
base of Cline Buttes. The flow is cut by numerous normal faults but
offsets are not great enough to reveal the bottom of the flow in its
thicker parts. Where cut by a fault near its southern flow margin,
the lava is 2m thick, appears to overlie a sandy soil and has a thin
flow breccia at its base. Topographic relationships suggest that
Tdba3 overlies Tdba2.

Tdba3 has less than 5% phenocrysts and glomerocrysts of plagio-
clase, olivine, rare augite, and Fe-Ti oxide (Figure 38). Plagio-
clase crystals (0.5-2 mm) are normally zoned from labradorite
(An51-An59) cores to andesine (An42) rims. Reverse zoning is rare,
although faint oscillatory zoning is common at cystal rims. Minor
resorption is common in plagioclase cores and margins. Resorbed
areas contain clinopyroxene, Fe-Ti oxide, and glass. Elongate and
doubly terminated cross sections of olivine (0.3-2 mm) are common.
In samples with large quantites of Fe-Ti oxide in the groundmass,
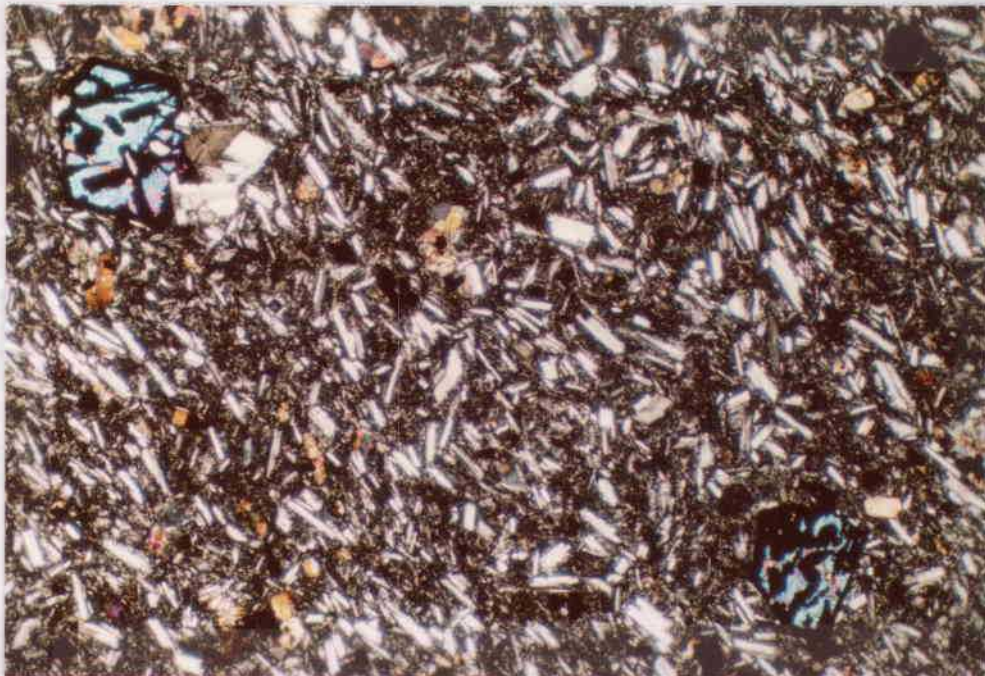
Figure 38. Phenocrysts of olivine with intergrowths of Fe-Ti oxide
in basaltic andesite lava Tdba3. Groundmass texture is
trachytic with intergranular clinopyroxene, olivine, and
abundant Fe-Ti oxide. Crossed nichols at 40X.

olivine is extensively altered to iddingsite or may be rimmed by and intergrown with Fe-Ti oxide. Clinopyroxene (pigeonite?) commonly rims olivine when quantities of Fe-Ti oxide are less abundant. Rare augite phenocrysts (0.5-0.75 mm) may have inclusions of Fe-Ti oxide, suggesting Fe-Ti oxide began crystallizing before augite. A small, isotropic mineral tentatively identified as picotite is visible in some olivine crystals. Groundmass plagioclase (55%) forms a trachytic texture. Clinopyroxene (33%), olivine (less than 1%), and Fe-Ti oxide (6%) are integranular to plagioclase, and glass (5%) is intersertal. The groundmass of some samples is unusually dark due to a concentration of fine Fe-Ti oxide which may form swirls or bands. Minor brownish-red hydrous iron oxide is scattered throughout the groundmass.

Tdba4

Lava Tdba4 is an aphyric, highly oxidized and scoriaceous lava from a small, obscure cinder cone west of Cline Buttes highway in the north part of sections 7 and 8, T16S, R12E. The cone is less than 0.5 km in diameter and is 14 m high. Alluvium covers the lower slope of the remains of this vent. A small cinder pit has been developed in its northeast side. No flows are associated with this vent.

Td1

Unit Td1 includes numerous fine grained basaltic andesite
lavas and a fine grained basalt which are too limited in exposure
to map as individual units. These lavas are petrographically and
compositionally similar to the above described basaltic andesites.
In outcrop they are dark gray and platy jointed. The porphyritic
lavas contain 3 - 15% phenocrysts and glomerocrysts, with plagioclase
the dominant phase. Plagioclase phenocrysts are normally zoned, with
labradorite cores and andesine rims, but may show minor oscillatory
zoning. Resorption of plagioclase phenocrysts is light to moderate
and common. Olivine phenocrysts typically are more common than
clinopyroxene phenocrysts, although neither is usually present in
amounts greater than 1%. Olivine phenocrysts are usually smaller
than 1 mm and are variably altered to iddingsite. They may have
Fe-Ti oxide rims or inclusions. Euhedral microphenocrysts of Fe-Ti
oxide are common in some of the lavas. Groundmass phases are
plagioclase, clinopyroxene, Fe-Ti oxide, minor olivine, and glass.
Groundmass plagioclase forms a strong trachytic texture. Other
groundmass minerals are intergranular, and glass is intersertal to
plagioclase.

Aphyric lavas contain less than 1% phenocrysts. Plagioclase is
the dominant phase, with subordinate olivine and/or clinopyroxene.
Fe-Ti oxide may be present in amounts up to 15%. Plagioclase
typically forms a strong trachytic texture, with intergranular
clinopyroxene, olivine, and opaque iron oxide, and intersertal glass.

Geochemistry

Major element oxide analyses of Deschutes Formaton lavas were completed as part of this study. Nine lavas were also analysed for trace elements. Analyses are presented in Appendix IIb.

Five basalt and at least eleven basaltic andesite lavas (Table 8) lie in the Tumalo quadrangle and erupted either from local or nearby small monogenetic volcanoes. With the exception of a single aphyric basalt, the basalts are typically porphyritic and contain up to 40% plagioclase phenocrysts ranging in composition from An60-68, and small amounts of olivine phenocrysts.

In contrast to the basalts, most basaltic andesites are fine grained and aphric to sparsely porphyritic. Common phenocryst phases in these lavas are plagioclase, clinopyroxene, olivine, and euhedral Fe-Ti oxides. Plagioclase is the dominant phase and ranges in anorthite content from An75-50. Petrographic relationships suggest that Fe-Ti oxide phenocrysts were on the liquidus before or simultaneously with clinopyroxene. Two basaltic andesites are porphyritic and contain up to 22% phenocrysts of plagioclase (approximately An50) and very sparse olivine.

There appears to be a temporal as well as a petrographic distinction between basalt and basaltic andesite lavas, as field evidence (see section on lavas) suggests the basalts were erupted prior to the basaltic andesites.

TABLE 8.   REPRESENTATIVE ANALYSES OF DESCHUTES FORMATION BASALTS
AND BASALTIC ANDESITES IN THE TUMALO QUADRANGLE

Unit	Tdb4	Tdb1	Tdb3	Tdb2	Td1	Td1	Tdba1	Tdba4
Sample	TQ279	TQ72	TQ9	TQ122	TQ49	AM251	TQ300	AM264
SiO_2	51.9	52.0	52.5	52.9	53.4	52.9	55.4	54.4
Al_2O_3	18.1	20.1	18.2	17.57	18.9	17.7	15.6	17.9
TiO_2	1.98	1.13	1.55	1.26	1.32	1.13	1.87	1.26
FeO*	10.2	7.4	9.0	8.7	8.0	8.8	10.3	9.1
MgO	3.8	4.8	5.2	5.8	4.2	5.9	3.6	4.7
CaO	9.1	10.0	8.6	8.9	9.1	9.3	7.4	9.8
K_2O	0.86	0.74	0.81	0.78	0.88	0.46	1.06	0.50
Na_2O	3.4	3.2	3.5	3.4	3.6	3.7	4.2	3.5
MnO	0.17	0.13	0.15	0.15	0.14		0.17	
P_2O_5	0.32	0.30	0.41	0.30	0.36		0.36	
Total	99.78	99.80	99.91	99.97	99.90	99.95	99.96	101.16

	Tdb4	Tdb1	Tdb3	Tdb2	Td1	Td1	Tdba1	Tdba4
Ni	28	61	87	10	44		46	
Cr	37	134	122	132	77		0	
Sc	25	18	26	27	20		31	
V	313	197	248	242	226		216	
Ba	367	370	377	426	406		492	
Rb	12	8	11	10	11		15	
Sr	515	748	576	685	684		524	
Zr	140	129	130	114	143		148	
Y	33	22	24	23	23		36	
Nb	7	7	9	4	8		5	
Ga	22	20	21	22	19		20	
Cu	76	71	98	101	84		140	
Zn	104	75	98	89	86		106	

* Total Fe as FeO

TABLE   8.   Continued

Unit	Tdba3	Td1	Tdba2	Td1	Td1	Td1	Td1	Td1
Sample	TQ34	AM54	TQ219	TQ47	AM304	AM284	AM269	AM127
SiO_2	55.3	54.9	56.7	56.7	56.1	56.4	56.9	57.2
Al_2O_3	16.5	17.5	16.1	16.7	15.6	16.4	16.1	16.6
TiO_2	1.72	1.37	1.91	1.29	1.97	1.87	1.59	2.05
FeO*	9.5	8.8	9.3	7.6	10.9	10.3	9.7	9.0
MgO	3.6	4.4	3.1	4.3	4.8	3.0	3.7	2.4
CaO	7.9	8.2	6.9	7.9	7.8	7.1	7.4	6.4
K_2O	1.09	0.84	1.33	1.03	0.90	0.99	1.00	1.03
Na_2O	3.8	3.8	4.1	4.0	3.5	4.3	4.0	4.6
MnO	0.17		0.18	0.14				
P_2O_5	0.34		0.31	0.28				
Total	99.92	99.81	99.93	99.94	101.57	100.36	100.39	99.28

Ni	10		29	25
Cr	23		0	58
Sc	32		24	25
V	283		192	224
Ba	448		522	392
Rb	19		23	17
Sr	518		485	559
Zr	154		175	160
Y	32		38	28
Nb	8		10	8
Ga	20		21	20
Cu	56		22	59
Zn	104		114	87

* Total Fe as FeO

On an AFM diagram (Figure 39a) most of the lavas plot close to
the boundary separating the calc-alkaline and tholeiitic fields. Four
basalts, prophyritic basaltic andesites and three aphyric basaltic
andesites fall into the calc-alkaline field. The coarsely prophy-
ritic, high Fe and Ti basalt Tdb4 and the remainder of the basaltic
andesites (6) lie on the boundary or close inside the tholeiitic
field. When plotted on the FeO*/MgO vs SiO$_2$ diagram (Miyashiro,
1974) (Figure 39b) to illustrate Fe enrichment with increasing SiO2,
and thus distinguish between calc-alkaline and tholeiitic trends, all
the basalts and all but one basaltic andesite lie in the tholeiitic
field. On this diagram, the lavas do not form a smooth, gradual
increase in FeO*/MgO, but abruptly increase in FeO*/MgO at approxi-
mately 55.5% SiO$_2$ and steeply increase in FeO*/MgO until reaching
57.3% SiO$_2$, the maximum silica value of the lavas.

Basalt and basaltic andesite lavas overlap somewhat in both
major and minor element compositions, however basalts tend to
have less differentiated compositions, i.e. higher MgO, CaO, and Ni
values. Alumina values between 17 and 21 wt. % characterize the
basalts as high-alumina basalts. Very low Ni and Cr values in the
basaltic andesites suggest that they represent a liquid that has
undergone significant fractionation of mafic phases. Both lava types
have relatively evolved compositions based on their Fe' values (the
molar ratio of FeO*/FeO*+MgO). Primitive Deschutes Formation and
High Cascade basalts generallly have FeO' values of < 0.4. With the
exception of Tdb3, which has a Fe' value of 0.6, Deschutes Formation
basalts in the Tumalo area have Fe' values between 0.45 and 0.49.
Basaltic andesites range between 0.50 to 0.66.
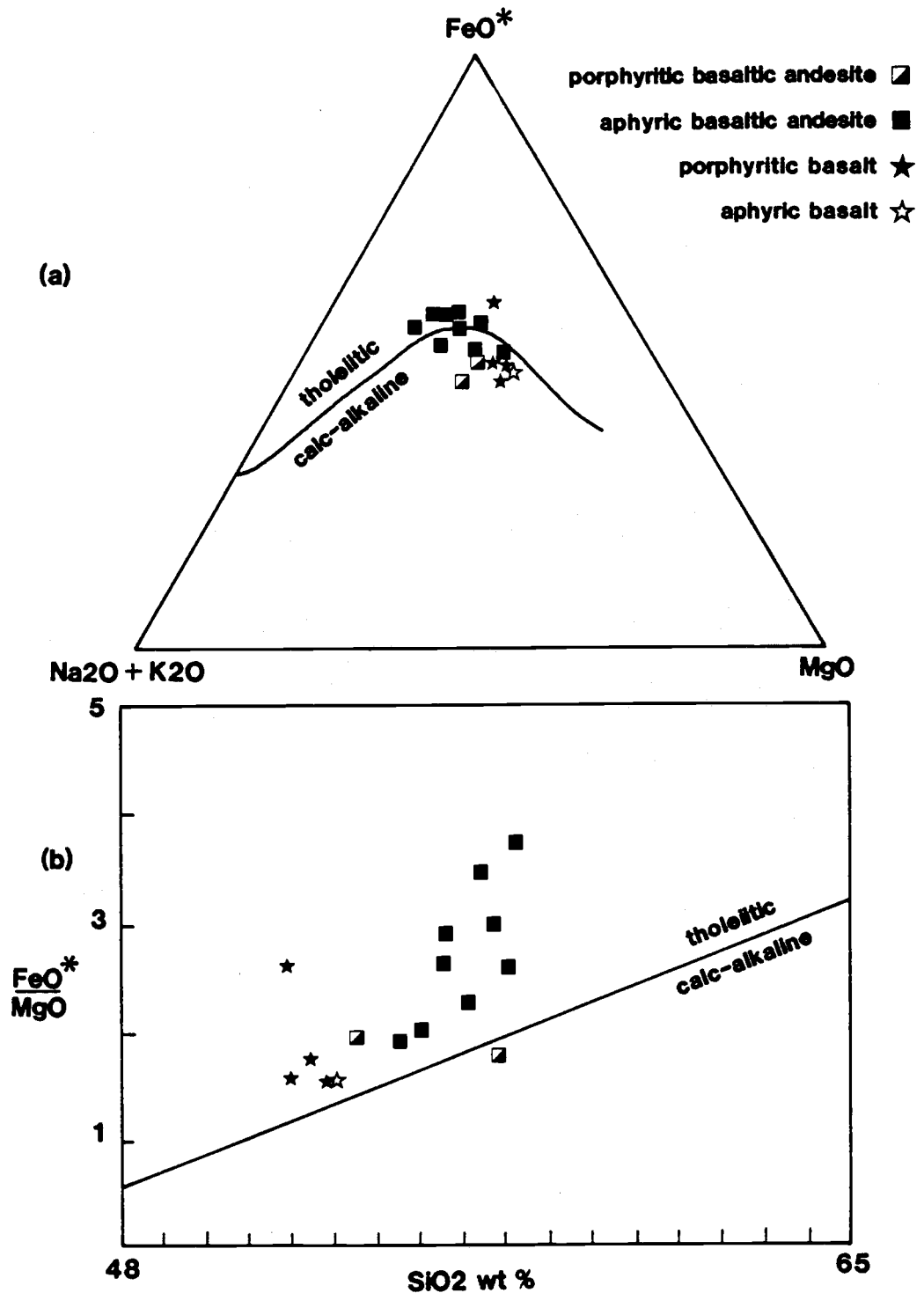
Figure 39. a) AFM diagram of Deschutes Formation lavas in the Tumalo
quadrangle. Tholeiitic and calc-alkaline fields after
Irvine and Baragar (1970); b) FeO*/MgO vs SiO$_2$ diagram,
after Miyashiro (1974).

Major element variation diagrams (Figure 40) show substantial scatter and few smooth, coherent trends. Values at the more differentiated (e.g. less MgO rich) end of the diagrams often show less scatter and form tighter trends. This tendency, coupled with an absence of values near 4 wt. % MgO, appears to divide some oxide values into two groups, one with more linear trends at lower MgO values, and another with greater scatter at higher MgO values. Lavas in the group with higher MgO values include four of the basalts, the porphyritic basaltic andesites and two aphyric lavas. The lower MgO group is composed of aphyric to sparsely porphyritic basaltic andesites and is generally lower in Al_2O_3 and CaO, higher in FeO and TiO_2, and slightly higher in K_2O than the samples in the higher MgO group.

Twenty-one out of 22 analyses (Conrey, 1985; Yogodzinski, 1984; Dill, 1989) of aphyric basaltic andesites which erupted from Deschutes Formation volcanoes in the Cascade Range, plot in the lower MgO group described above. Aphyric, high Fe and Ti basaltic andesites and andesites are common among Deschutes Formation lavas. Typically, the FeO* and TiO_2 in these lavas form an enrichment trend until reaching a SiO_2 value of approximately 57 wt. %. The appearance of Fe-Ti oxides on the liquidus, and thus their availability to form part of a fractionating assemblage, at approximately 57 wt. % SiO_2 is assumed to be responsible for the absence of an Fe and Ti enrichment trend at higher SiO_2 values. All aphyric, high Fe-Ti lavas in the Tumalo area contain microphenocrysts of Fe-Ti oxide suggesting that this phase had not undergone significant
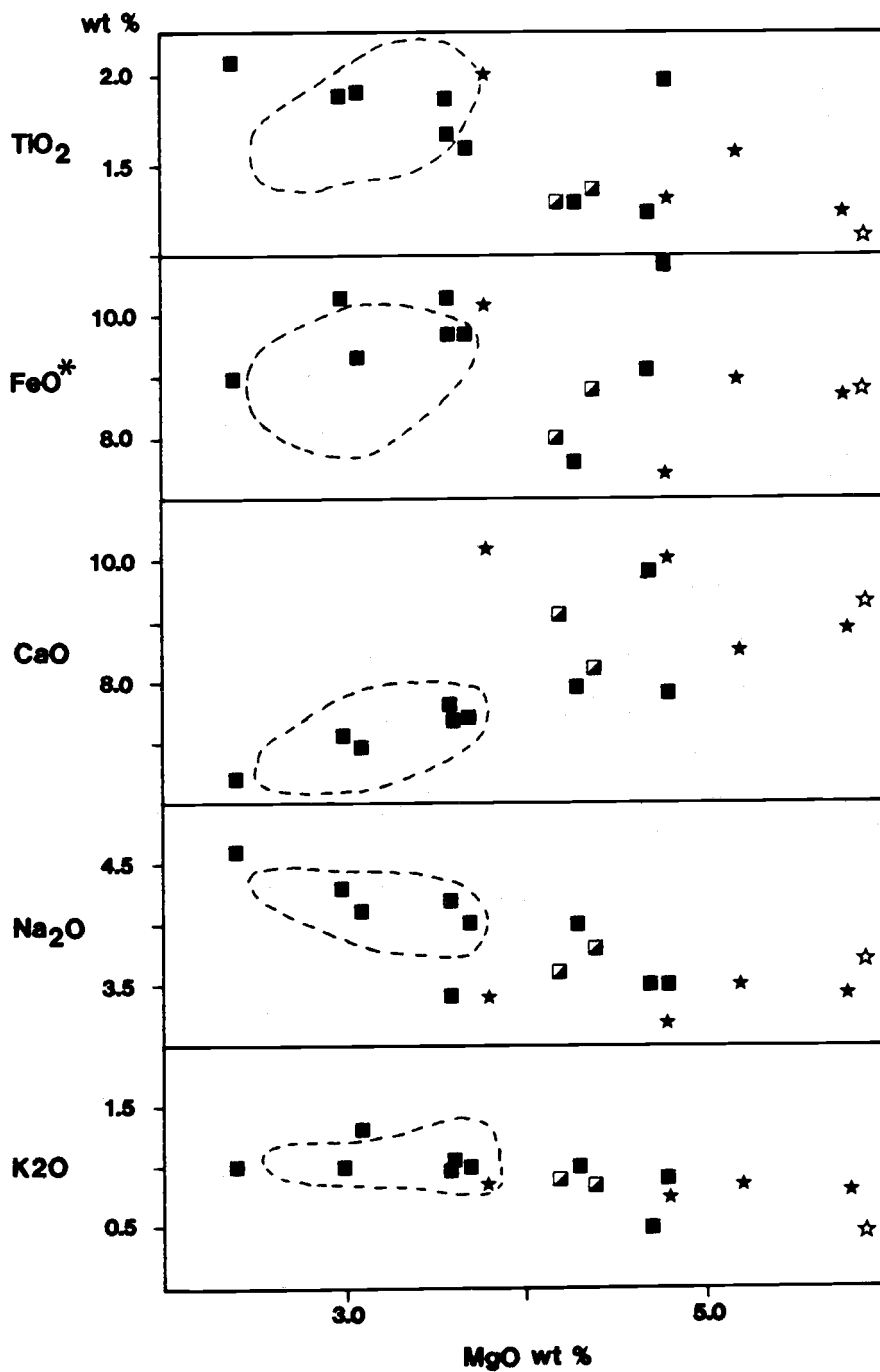
Figure 40. Major element variation diagrams of Deschutes Formation
lavas in the Tumalo quadrangle. Field defined by dashed
line represents composition of aphyric Deschutes
Formation lavas erupted from Cascade Range. Symbols as
in Figure 39.

fractionation from the melt. There appears to be a slight decline in FeO* with decreasing MgO in the high Fe and Ti basaltic andesites, but the small number of data points make this observation inconclusive. In contrast, TiO_2 values continue to increase with decreasing MgO.

Close geographic proximity of the lavas and the apparent progression with time from a basalt to basaltic andesite composition, suggests that the lavas have a similar source and may be related to one another through the differentiation process of crystal fractionation. Relationships between the lavas can be evaluated mineralogically and chemically. Petrographically determined anorthite content of the plagioclase in the lavas suggests that the aphyric basaltic andesites were not derived from the porphyritic basalts, as the anorthite content of the basaltic andesites is similar or higher than those of the basalts. Evolution of the aphyric basaltic andesites from the porphyritic basalts would require a very effecient method of removing all of the phenocryst phases in the basalts.

Despite the large amount of scatter on variation diagrams, general trends in major element chemistry supports an evolution of the basaltic andesites from the basalts via olivine and plagioclase fractionation, based on decreases in CaO, Al_2O_3 and MgO, and an increase in FeO*. Na_2O and K_2O show a relative increase with decreasing MgO, as they are less significant components of calcic plagioclase and olivine. Increasing FeO*/MgO ratios with increasing SiO_2 suggests that olivine is being progressively removed from the melt, although the trend among the lavas is not smooth or gradual.

Ni values up to 110 ppm in the less evolved basalts and as low as 6
ppm in the high Fe and Ti basaltic andesites suggest substantial
olivine fractionation has occured in evolution of the basaltic
andesites. The ratio CaO/FeO* plotted against MgO (Figure 41) is
useful to detect plagioclase fractionation, as progressive removal of
plagioclase from the melt would cause a decrease in the ratio. The
diagram shows an overall decrease in the ratio, although there is a
large amount of scatter among the more Mg-rich lavas. The nearly
flat trend this ratio forms in the high Fe and Ti basaltic andesites
does not support plagioclase fractionation among these lavas.

Clinopyroxene fractionation decreases the melt in CaO relative
to Al_2O_3. The ratio of these two oxides does not decrease between
basalts and basaltic andesites, but decreases slightly among the
basaltic andesites (Figure 41). Clinopyroxene is a common phenocryst
phase in the basaltic andesites, although it is present only in small
amounts. A plot of CaO/Al_2O_3 against Cr or Sc, trace elements
preferentially partitioned into clinopyroxene, does not indicate that
the lavas are related via clinopyroxene fractionation.

Incompatable trace elements such as K and Ba have very low and
similar partition coeffecients for ferromagnesian minerals and calcic
plagioclase. The K/Ba ratio should remain constant at variable MgO
values in lavas related by closed system fractionation from a common
parent. A plot of K/Ba (Figure 41) ratios for nine of the lavas
does not exhibit the horizontal trend expected by lavas which are
related by fractionation of a primary melt. The K/Ba ratios of the
lavas generally increase with decreasing MgO, requiring an addition
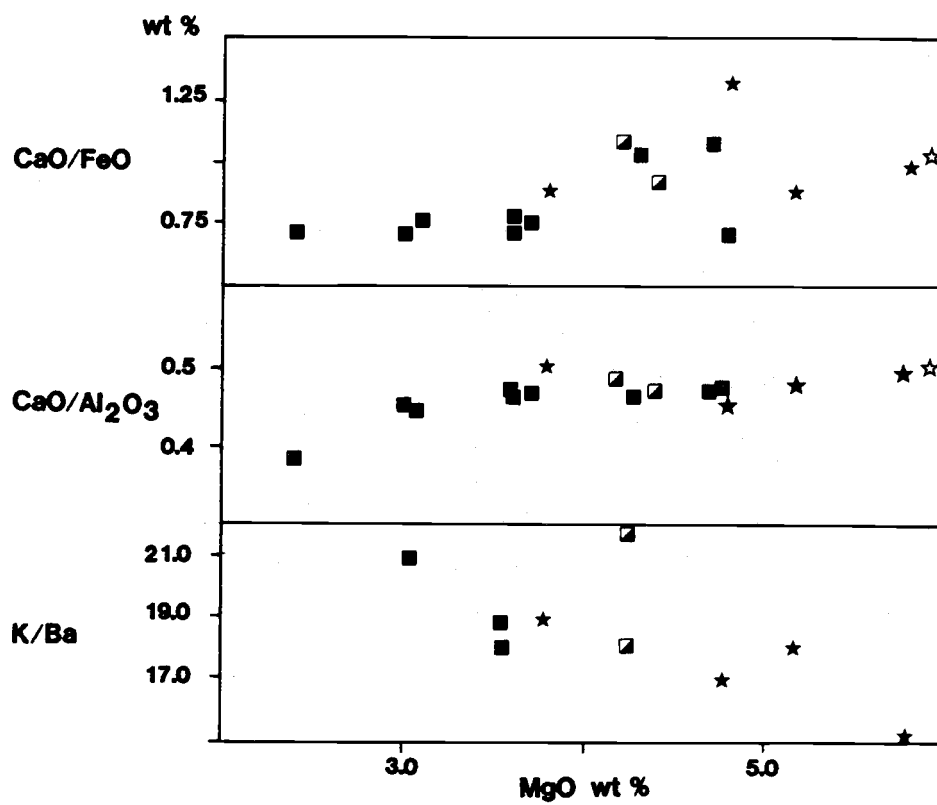
Figure 41. Variation diagrams of Deschutes Formation lavas in the
            Tumalo quadrangle. See text for explanation. Symbols as
            in Figure 39.

of K or depletion in Ba during differentiation. This may reflect mixing of lavas or assimilation of more K-rich material during evolution. Alternatively, the variation among the lavas in K/Ba ratios could reflect different primary melt compositions.

The most likely explanation for the distinctive compositions among the lavas is that they represent evolution from small amounts of discrete melts. The coherent major element trends formed by the aphyric high Fe-Ti basaltic andesite lavas and their similar trace element composition suggest that they may have followed similar evolutionary paths from a similar starting composition. A possible starting composition for the aphyric basaltic andesites is the aphyric basalt (sample AM251). This basalt has the most primitive composition of any lava in the study. It is the only lava that contains normative olivine and has the lowest Fe' (0.45). Further evaluation of the relationship between any of the lavas in the Tumalo area requires mineralogical and trace element data beyond the scope of this study.

STRATIGRAPHIC CORRELATION

The localized nature of most volcanic units and the discontinuity
of individual sedimentary units hampers stratigraphic correlation
within the Deschutes Formation. Smith (1986a) developed a strati-
graphic framework for the Deschutes Formation based on 27 widespread
volcanic units and informally assigned them member status. These
marker beds are helpful in establishing local stratigraphy, but do
not permit unambiguous stratigraphic correlation of units through-
out the basin.

None of the units designated as Deschutes Formation stratigraphic
markers are exposed in the Tumalo area. The Tetherow Buttes debris
flow deposit marks the bottom of the sedimentary section exposed in
the Tumalo area and is the only Deschutes Formation unit which can be
unequivocally identified north of the area. However, the limited
size and exposure of the Tetherow debris flow deposit restricts its
use in stratigraphic correlation.

Correlation of sedimentary units in the southern reaches of the
basin near Tumalo, with units in the central and northern parts of
the Deschutes basin is hampered by relatively shallow incision of
the sedimentary section in the south and the tendency for the units
there to form poor outcrops. Although direct correlation of units
near Tumalo and more northerly parts of the basin is precluded at
this time, similarities between their deposits suggests depositional
processes and environments were pervasive throughout the basin and
permit a general correlation between the north and south parts of

the basin. The sheetflood and high sediment concentration flood-flow processes which dominated deposition onto the arc-adjacent alluvial plain in the western two-thirds of the central and northern Deschutes basin (Smith, 1987) also dominated deposition in the southern part of the basin. Smith (1986a) notes an abrupt basin-wide shift from sheetflood, hyperconcentrated flood flow, debris flow, and ignimbrite facies to paleosol and thick lapillistone dominated facies in the upper 50 m - 100 m of the sedimentary section. A number of air-fall lapillistones are in the 50 m thick section of sedimentary rocks exposed near Tumalo, suggesting that the Tumalo rocks correlate with the upper part of the formation as identified elsewhere in the basin. However, ignimbrites are also in the Tumalo section, and extensive beds of laminated, tuffaceous sandstone immediately below the basaltic andesite lavas suggests that sheetflood deposition remained active in the upper part of the Tumalo section, making the correlation with the upper part of the formation ambiguous based on the criteria of Smith (1986a). Development of a stratigraphic framework which allows correlation of the southern part with the central and north parts of the Deschutes basin will necessarily include correlation of the numerous widespread air-fall lapilli-stones and further data on the trace element composition of ignim-brites that are very similar in major element composition.

Radiometric dating of Deschutes Formation plateau- and rim-forming lavas throughout the basin permits a time stratigraphic correlation of units erupted during late stage and intrabasinal vol-canism. Tetherow Buttes lavas, including those which form Agency

Plains north of Madras, erupted approximately 5.5 + 0.2 Ma (L. Snee, unpub. data). Steamboat Rock basaltic andesites west and northwest of Terrebonne, have an age of 5.1 + 0.2 Ma (L. Snee, unpub. data). These ages correspond closely to those of rim-forming lavas further south in the basin. A basaltic andesite at the top of the Deschutes section in the Tumalo area has an age of 5.4 + 0.10 Ma (L. Snee, unpub. data).

The Canadian Bench and Fly Creek basalts (Conrey, 1986; Dill, 1989) erupted from Green Ridge and flowed east into the basin. They form the rimrock along the Metolius and Deschutes River canyons. The Canadian bench flow, reported by Armstrong and others (1975) (recalculated by Fiebelkorn and others, 1983) to have an age of 5.5 + 0.5 Ma, overlies Tetherow Butte lavas at Agency Plains. These basalt lavas are in turn overlain by younger Deschutes Formation lavas on the east side of Green Ridge (Conrey, 1986). The youngest Deschutes Formation lava was erupted at Round Butte, east of Madras, and has an age of 4.0 + 0.1 Ma (L. Snee, unpub. data).

With the exception of Round Butte, the plateau-forming Deschutes Formation lavas were erupted over a relatively short period of time and form the top of the Deschutes Formation. Intrabasin basaltic and basaltic andesite volcanism appear to have been comtemporaneous with the basalt to basaltic andesite lavas which characterize the top of the volcanic pile at Green Ridge.

QUATERNARY UNITS

The contact between the Deschutes Formation and overlying
Pleistocene volcanic units marks the boundary of the Deschutes basin.
Although the contact is not exposed in the Tumalo area, the
Pleistocene units disconformably overlie the Deschutes Formation.
Two silicic pyroclastic flows, a pyroclastic fall, and at least three
basaltic andesite lavas entered the Tumalo area from High Cascade
sources to the southwest. A younger basalt lava from Newberry
volcano flowed into the area from the southeast.

PYROCLASTIC UNITS

Two ignimbrites, the Desert Spring Tuff and the Tumalo Tuff, and
one airfall lapillistone, the Bend Pumice, form the bulk of the
Pleistocene section in the Tumalo area. All three units are well
exposed in roadcuts and stream channels near Tumalo State Park,
and along the Deschutes River in section 17, T16S, R12E, where they
form exposures up to 30 m thick. This is a minimum collective
thickness of the units, as the bottom of the section is not locally
exposed and the top has been subject to erosion.

The source and age of the pyroclastic deposits have been the
subjects of recent interest and investigation. Based on geographic
proximity, direction of increasing thickness and welding of the
units, and trace element analyses, the source of the Pleistocene

pyroclastic units is hypothesized to be the Tumalo volcanic center
(TVC) (Hill, 1988; see Figure 23). The TVC is approximately 20 km
southwest of Tumalo and 17 km east of the High Cascade axis and is
synonymous with the area of silicic volcanism referred to by Taylor
(1978) as the "silicic highland". The TVC is characterized by
andesitic cinder cones and dacitic to rhyodacitic domes which predate
and are unrelated to the magmatism which generated the nearby Three
Sisters and Broken Top stratovolcanoes.

Recently, the pyroclastic deposits have been correlated with
pluvial and marine ash beds in Nevada, California, and deep sea
drill cores (Sarna-Wojcicki and others, 1987, in press). Through the
combined use of tephrachronology, magnetostratigraphy, major and
trace element analyses, and isotopic dating, the pyroclastic units in
the Tumalo-Bend area have been assigned much younger and more precise
mid-Pleistocene ages than those suggested by earlier investigators
(0.5+0.9 Ma, Armstrong and others, 1975; 2.5+2.0, 2.6+2.2, and
3.98+1.9 Ma, Fiebelkorn and others, 1983).

Desert Spring Tuff

The Desert Spring Tuff (Figure 42) is a poorly to firmly welded
dacitic ignimbrite (Appendix IId) and represents the first of five
distinctive Pleistocene pyroclastic flows (Hill and Taylor, in press)
that reached the low-lying area east and northeast of the High
Cascades. It is easily distinguished from other High Cascade ignim-
brites by its orange color, crystal-rich matrix, and honeycomb
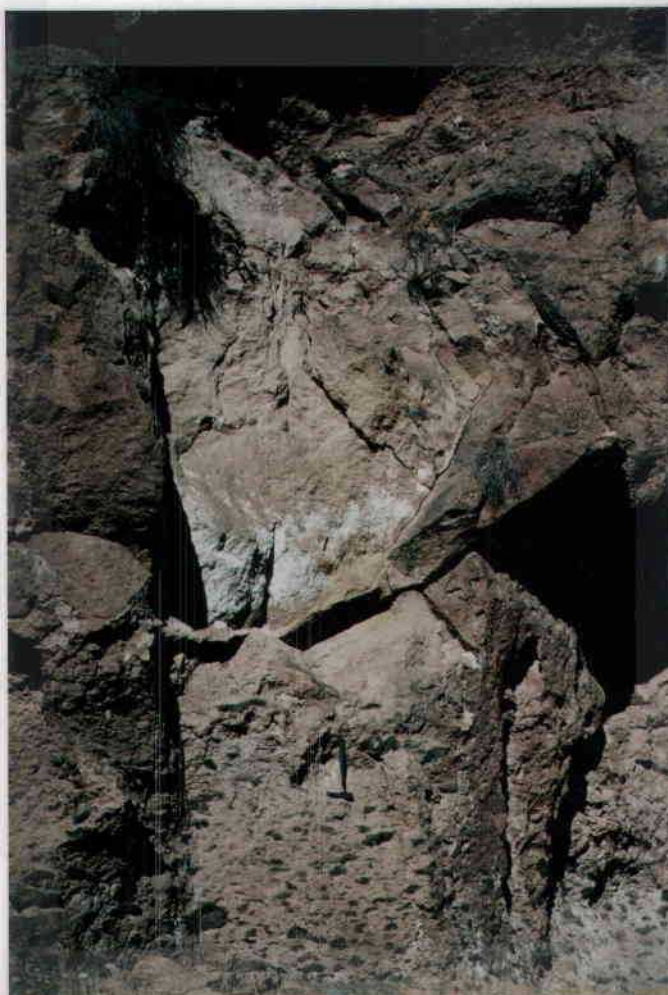
Figure 42. Outcrop of welded Desert Spring Tuff, the oldest Pleistocene unit exposed in the Tumalo area. Note collapsed black pumice bombs and lapilli in lower half of photo.

weathering texture. Although the base is not locally exposed and the top of the unit has been removed by erosion, good outcrops of the Desert Spring Tuff are in and adjacent to Tumalo State Park. A stream channel in the north half of section 6, T17S, R12E, exposes a 9 m thick section of Desert Spring Tuff. The lower 2 m of the ignimbrite contains 20 - 25% devitrified and partly collapsed black pumice lapilli and bombs with conspicuous feldspar and pyroxene phenocrysts. The orange, crystal-rich, welded matrix contains approximately 5% lithic fragments which are generally less than 1 cm in diameter. A subtle break and change in the appearance of the ignimbrite above this level represents the contact between two flow lobes. The overlying 3 m is characterized by partly collapsed, orange, vapor phase altered pumice lapilli (approximately 8%), sparse black pumice (approximately 2%), and an increase in the size of lithic fragments to 2.5 cm. Unflattened, orange and black pumice lapilli (15 - 20%) in an orange, poorly welded matrix characterize the upper 2 m of the exposure. Reverse grading is apparent in the upper flow lobe. Increase in the size of the pumice is particularly conspicuous in the upper 2 m of the unit, where there is a concentration of pumice bombs up to 80 cm long. Based on major element analyses, the Desert Spring Tuff has been correlated with an ash bed in northwest Nevada (Sarna-Wojcicki and others, in press). Correlation of this ash bed to ash units of known age in northern California, suggests the Desert Spring Tuff has an age of approximately 0.63 Ma (Sarna-Wojcicki and others, in press).

Bend Pumice

A white, air-fall lapillistone known as the Bend Pumice overlies the Desert Spring Tuff. The two units are separated by an erosional unconformity and local thin deposits of alluvium. The Bend Pumice is dacitic and represents the airfall deposit of Plinian eruption. Collapse of the eruption column initiated the pyroclastic flow which deposited the overlying Tumalo Tuff (Hill, 1985).

The Bend Pumice is divided into two subunits (Hill, 1985): a 1 - 3 m thick, rarely exposed, lower reworked zone which consists of bedded pumice and ash from an early eruption stage, and an upper air-fall zone which represents the climactic eruption. Both units are exposed in a roadcut along Tumalo Market Road (SW 1/4 Sec. 6, T18S, R12E). The upper airfall zone is composed of unsorted angular pumice lapilli (approximately 80%) and ash (15%) with small amounts of rock fragments and free crystals. Local exposures of the Bend Pumice range to approximately 8 m thick. The unit appears subtly stratified near the top due to a 0.5 m layer of slightly finer pumice interspersed between coarser pumice lapilli characteristic of the unit.

K-Ar ages from the overlying Tumalo Tuff and an undisturbed airfall lapillistone immediately below the Bend Pumice, bracket the age of the Bend Pumice between 0.3 and 0.4 Ma (Sarna-Wojcicki and others, in press). A marine ash bed in northern California with an age of about 0.35 to 0.39 Ma, has been correlated with the Bend

Pumice using major and trace element analyses (Sarna-Wojcicki and others, 1987).

Tumalo Tuff

The Tumalo Tuff is a pink, unwelded to poorly welded, rhyodacitic ignimbrite (Figure 43) which is widely distributed in the Tumalo area. It was deposited by the pyroclastic flow component of the eruption that produced the Bend Pumice airfall lapillistone (Hill, 1985). Southwest of Tumalo, the Deschutes River has cut through the Tumalo Tuff creating exposures of the ignimbrite up to 30 m thick. Such an uncharacteristically thick section of Tumalo Tuff near its northernmost extent, suggests the pyroclastic flow locally filled a topographic depression. The top of the Tumalo Tuff has been removed by erosion and is overlain by alluvium.

A white to pink, ashy, coarse-pumice-depleted layer at the base of the Tumalo Tuff represents the 2a layer of the standard ignimbrite unit (see Figure 20) of Sparks and others (1973). Thickness of the 2a layer ranges from 0.1 to 1 m. The 2a layer grades upward into the 2b layer, the massive and unsorted main body of the ignimbrite. Local sections of the 2b layer range to approximately 4.5 m thick. Components of the 2b layer are pumice lapill (20%), ash (70%), rock fragments (9%), and free crystals (1%). In more proximal locations (outside of the Tumalo area), the Tumalo Tuff contains mixed composition pumice believed to represent the incomplete mixing of unrelated rhyodacitic and dacitic magmas (Hill, 1985).
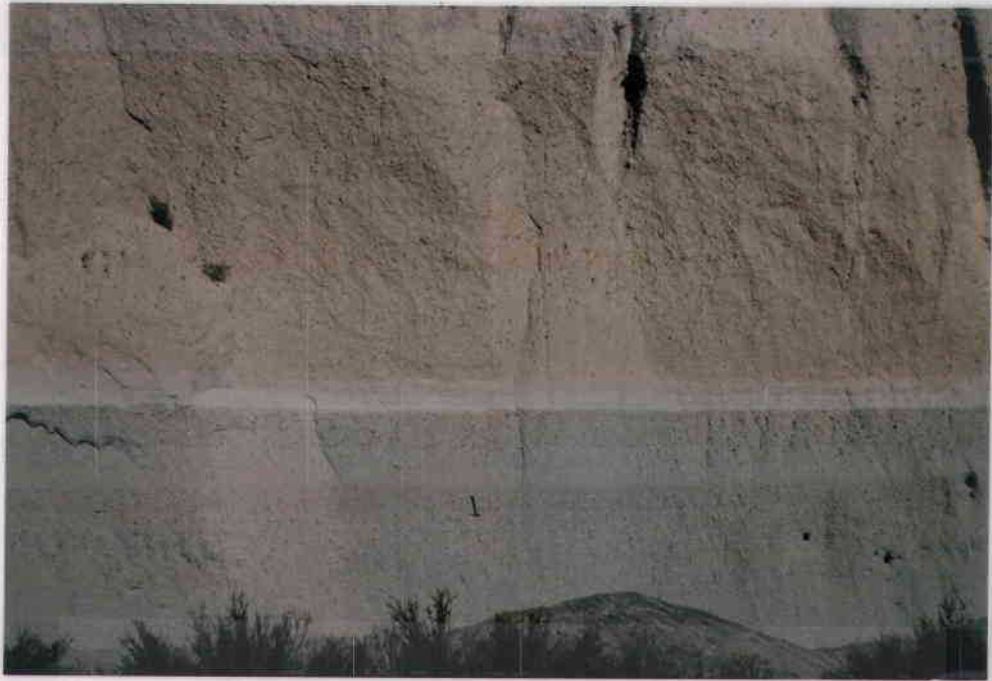
Figure 43. The Bend Pumice airfall lapillistone and the overlying
Tumalo Tuff ignimbrite are the products of the same High
Cascade eruption. Exposure in quarry north of Tumalo
State Park.

A weighted average of four K-Ar ages on feldspars extracted from homogeneous Tumalo Tuff pumice, gives the unit an age of 0.29 ± 0.12 Ma (Sarna-Wojcicki and others, 1987).

LAVAS

Pleistocene lavas exposed in the Tumalo area appear to have two origins. At least three basaltic andesite lavas flowed into the area from the southwest, suggesting sources in or on the flanks of the High Cascades. A distinctive and extensive basaltic lava originated from Newberry shield volcano to the southeast.

High Cascade lavas

A small outcrop of basaltic andesite lava lies in a drainage at the southwest corner of the study area (SW 1/4 of section 1, T17S, R11E). Another basaltic andesite is exposed in a roadcut north of Tumalo State Park (NE 1/4 of section 6, T17S, R12E) and in a gravel pit approximately 300 m southwest of this roadcut. Both lavas have a normal polarity and appear to have filled small channels eroded into Desert Spring Tuff. Both lavas are finely porphyritic. The latter contains approximately 5 - 8% phenocrysts of partially resorbed plagioclase and red, iron oxide stained clinopyroxene in a trachytic groundmass of plagioclase and minute grains of intergranular clino-pyroxene and magnetite.

The southeast tip of a basaltic andesite lava of unknown extent overlies the Tumalo Tuff in the southwest corner of the study area (sec. 2, T17S, R11E). The lava is finely porphyritic with approximately 10% phenocrysts and glomerocrysts of plagioclase (approximately An46) and augite in a trachytic groundmass of plagioclase and intergranular clinopyroxene and magnetite.

Newberry lava

Newberry shield volcano, a center of Pleistocene and Holocene bimodal volcanism some 40 kilometers south of Tumalo, is the source of a basaltic lava which covers approximately 16 km^2 of the study area. Local exposures represent only the easternmost extent of a lava which covered much of the Bend area as it flowed from the flanks of Newberry volcano north toward Redmond. The basalt flowed over and filled erosional depressions in the Tumalo Tuff and lapped against Deschutes Formation lavas. The present course of the Deschutes River along the western margin of the lava suggests that the river was forced westward by the lava flow.

The Newberry lava is topped by thin soil and sparse vegetation. Tumuli and pressure ridges are common features on the irregular, hummocky surface of the lava (Figure 44). In outcrop the lava has well developed polygonal jointing. In hand sample it appears fresh and fine grained and has a conspicuous diktytaxitic texture. The rock has a subophitic to intergranular microscopic texture (Figure 45). The constituents of the lava are labradorite (approximately

Figure 44. Tumuli in polygonally jointed diktytaxitic basalt flow from Newberry volcano.
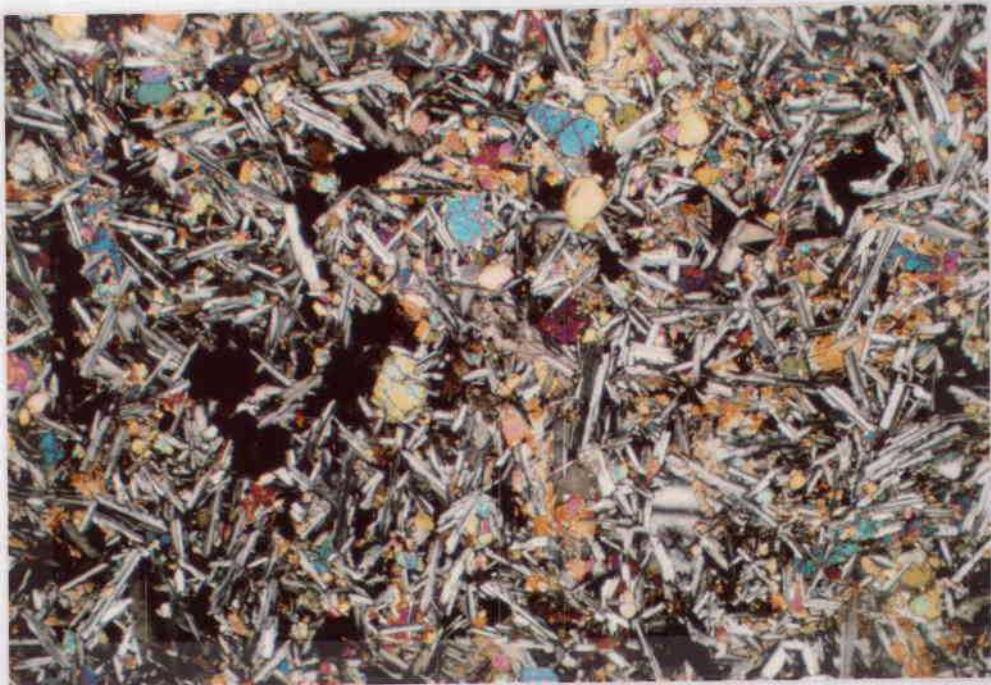
Figure 45. Subophitic to intergranular microscopic texture of Newberry basalt. Macroscopic diktytaxitic texture is represented in photo by large, dark angular void spaces.

65%), augite (approximately 20%), olivine (approximately 9%) and void space (approximately 6%).

Newberry mafic and intermediate lavas are divided into two chemical types, one tholeiitic and the other calc-alkaline (Higgins, 1983; Beyer, 1983). The basalt lava in the Tumalo area is the calc-alkaline type (Appendix IId).

ALLUVIAL DEPOSITS

An estimated 16 km^2 of bedrock in the Tumalo area is obscured by alluvium. Alluvial deposits are common and widespread west and northwest of Tumalo and appear to lie approximately parallel to the eastern slope of the High Cascades (Peterson and others, 1976).

The bulk of the alluvium in the Tumalo area is in a northeast trending zone over 2 km wide in the center of the map area (see Plate I). Water well drill logs suggest the alluvium here is tens of meters thick. Exposures in the alluvium range from 4 m to greater than 7 m thick.

Two types of alluvium have been identified in the Tumalo quadrangle: alluvium associated with the present Deschutes River channel (Qal), and an older, widespread alluvium (Qoa) which lies topographically above river level. The two types appear compositionally and genetically distinct from one another. Qal is predominately coarse, clast supported, imbricated gravel and sand which occupy the stream bed and channel margins of the Deschutes River. These deposits lie on the eroded surfaces of Pleistocene ignimbrites,

where they are most widespread, or fill channels cut into the Deschutes Formation. Pebbles and cobbles in the gravels are rounded to subrounded and originiated from fine to medium grained aphyric and porphyritic mafic lavas. Qal deposits clearly have their origin in normal stream channel processes within a mafic volcanic provenance.

Qoa (Figures 46 and 47) is composed predominately of sand and gravelly sands. Rarely, gravel fills shallow channels cut into Qoa sands. Boulders commonly litter the top of the unit, particularly in the southern half of the map area. Clast supported pebble and cobble gravels in Qoa are most common on terraces adjacent to the present course of the Deschutes River. Sands are generally medium to coarse grained, moderately to poorly sorted and may contain out-sized clasts. Predominate structures are planar horizontal laminae and beds and low-angle crossbeds. Massive beds are less common. Tabular cross-beds and ripples are locally present. The principal constituent of the sands is mafic volcanic material (cinders, rock fragments), with lesser amounts of crystal fragments, reworked ash and pumice lapilli, and a trace of black glass fragments. Clast composition is predominately mafic lavas, but banded rhyolite and grey to black obsidian are also common, suggesting a silicic as well as mafic volcanic provenance.

The character of most Qoa deposits does not suggest deposition by normal stream flow. Facies suggestive of a shallow braided stream are locally present, but the widespread thin planar beds, and massive, poorly sorted beds are more typical of sheetflood and high sediment concentration floods. Paleosols commonly cap Qoa deposits
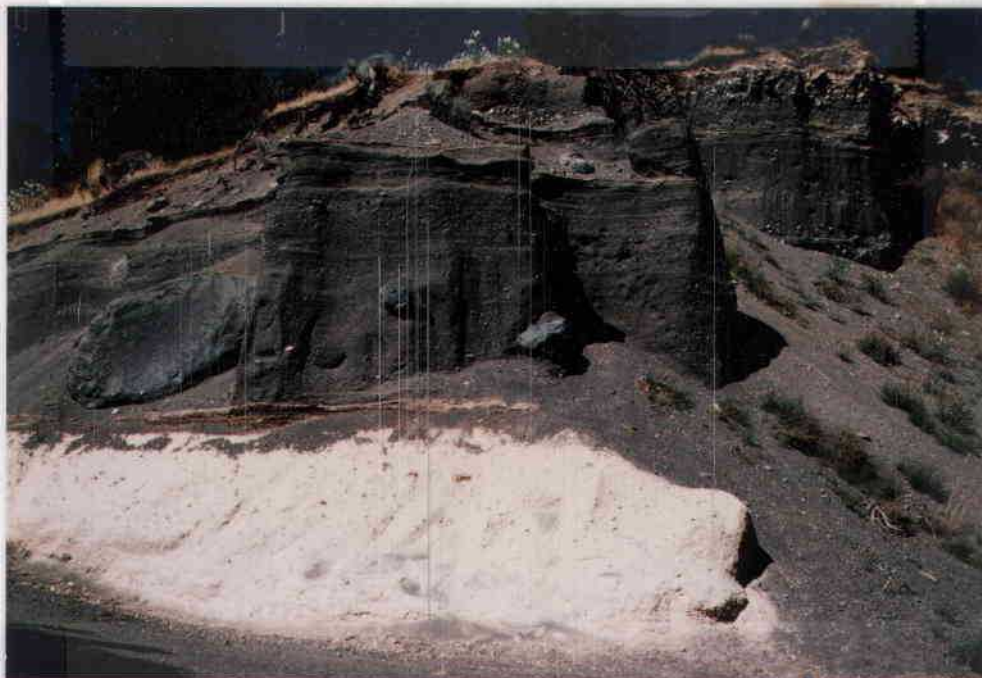
Figure 46. Qoa deposits above Tumalo Tuff. Large boulder at left center is 2 m in diameter. Note horizontal bedding and coarse gravel at top of unit. Outcrop on Swalley Road.

Figure 47. Horizontal beds and laminae are the predominant structures in Qoa sands and gravels. Note shallow cut and fill structure in upper right of photo. Exposure in gravel pit on highway 20 northwest of Tumalo.

but do not appear within the unit, suggesting that the alluvium was deposited over a relatively brief period of time and was not subject to long periods of subaerial exposure.

Discussion

In the Tumalo area, the hiatus between the close of the Deschutes Formation and deposition of the first Pleistocene unit was approximately 4.5 million years. Volcanism was active in the Cascade Range and areas adjacent to the Deschutes Basin during the late Pliocene and early Pleistocene, but it did not affect the Tumalo area. When local deposition did resume, pyroclastic flows and lava flows, and later a large quantity of alluvium, entered the area from sources to the southwest, in or on the flanks of the High Cascades. The same source area originated much of the Deschutes Formation.

Much of the alluvium capping the Pleistocene section appears to have originated from deposition during floods. Although the purpose of this study does not include careful analysis of Quaternary alluvial deposits, similarity between many Qoa deposits and some of the facies in the Deschutes Formation warrants brief discussion. High Cascade volcanism, and in particular pyroclastic volcanism, was closely linked with the widespread flooding and aggradation that produced the Deschutes Formation. Large volumes of loose pyroclastic material overwhelmed established drainages, causing flooding and resulting in thick deposits of volcaniclastic sediment. Subsequent thick alluvial deposits such as those deposited during the

Quaternary, might be assumed to have an origin similar to that of the Deschutes Formation.

Established drainages were no doubt disrupted by channel filling lavas and pyroclastic flows during the mid-Pleistocene, a process which could have caused local, periodic flooding. However, the absence of significant amounts of widespread alluvium between Quaternary volcanic units suggests that this was not a controlling factor in sediment deposition. Unlike the Deschutes Formation, pyroclastic debris does not dominate Quaternary alluvial deposits. This suggests that pyroclastic volcanism and processes related to pyroclastic volcanism did not play the part in Quaternary aggradation that they did during the Miocene.

Rather than interrupting normal stream flow via volcanic processes, the High Cascades may have contributed unusually high water and sediment discharge onto adjacent plains as a result of glacial melting. Sandy, glacial outwash plains, known as sandurs, are characterized by deposits (i.e. Ruegg, 1977) similar in appearance to those in Qoa. Three periods of Pleistocene glaciation have been documented in the High Cascades (Taylor, 1968; Scott, 1977). Moraines and outwash east of Middle and North Sister volcanoes record the advance of Pleistocene glaciers to elevations close to 1500 m and probably were emplaced during Wisconsin glaciation sometime between 75,000 - 12,000 years ago (Scott, 1977).

STRUCTURE AND TECTONICS

The Deschutes Formation has experienced only minor structural deformation since its deposition during the late Miocene and early Pliocene. Deschutes Formation units are generally flat-lying and undisturbed. The gentle eastward dip of units on the east flank of Green Ridge and the subtle northward tilt of the plateau-forming lavas reflect depositional paleoslopes. A gentle, southward dip of $1°$ among lower units in the northern part of the Deschutes basin (Smith, 1986a) suggests that early deposition was coincident with minor uplift of the Mutton Mountains. Main structural features of the Deschutes basin are the north-south trending Green Ridge fault scarp and the northwest trending Tumalo fault zone (Figure 48). The faults which cut the southernmost Deschutes basin are part of the Tumalo fault zone.

TUMALO FAULT ZONE

The Tumalo fault zone (TFZ) is a 16 km wide northwest trending zone of en echelon faults that stretches between the north flank of Newberry volcano and Green Ridge. Some thirty normal faults in this zone were mapped during the study of the Tumalo quadrangle. The zone trends approximately N32°W; the strike of individual faults ranges between N15°W and N35°W. Dip of the faults is steep to vertical (Figure 49). Offset is small, typically less than 5 m and rarely up
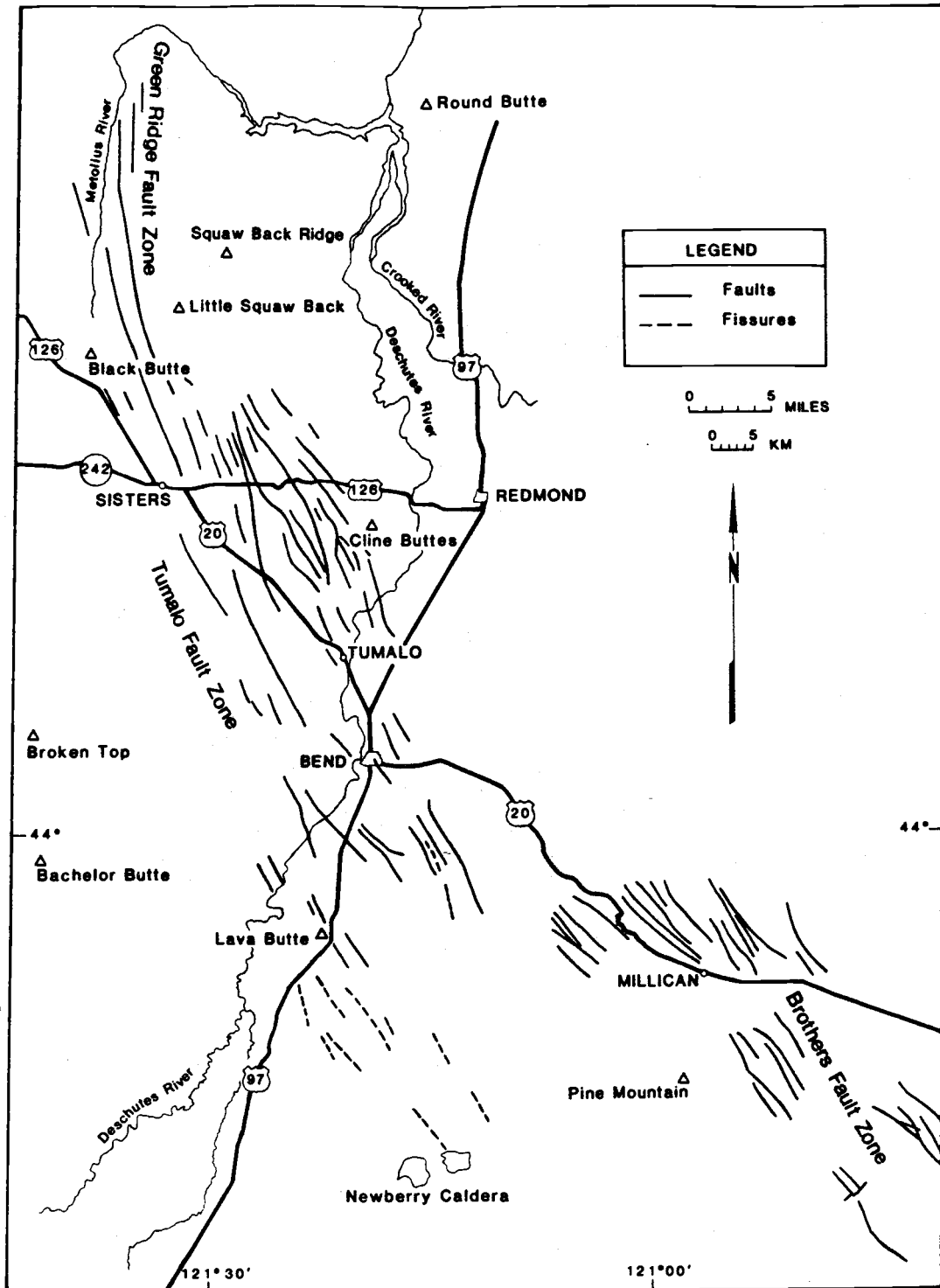
Figure 48. Location of the Green Ridge, Tumalo, and Brothers fault
zones.

Figure 49. High-angle normal fault of the Tumalo fault zone offsets
Deschutes Formation basaltic andesite lava in the wall of
the Deschutes River canyon. Offset is approximately 2 m.
Downdropped block lies on the southwest side of the
fault.

to 20 m with an average of 5 m. Amount of offset may vary along the length of a fault. Length of individual faults varies between less than 0.5 km to over 10 km. The longest fault, the Tumalo fault, near the western boundary of the zone, can be traced for 40 km (Taylor, 1981a).

Relative motion along the faults is most often down to the southwest, particularly in the north part of the zone. To the south, as exhibited by the faults in the Tumalo area, the northeast or southwest block may be downdropped, creating small horst and graben.

Faults cutting Cline Buttes rhyodacite, the only locally exposed rocks older than the Deschutes Formation, show about the same amount of offset as younger rocks. Numerous small Deschutes Formation volcanoes which erupted the plateau-capping lavas that cover the south end of the Deschutes basin are localized in the TFZ (Figure 50), which suggests the lavas were channeled along structural pathways.

Although vent alignments in the zone are rare, the concentration of vents in the TFZ suggests that the stresses expressed by faulting were in place at least as early as 5.4 Ma, the approximate time of volcanic activity. Tetherow Buttes and Steamboat Rock, Deschutes Formation vents approximately 13 km northeast of the TFZ, are aligned on northeast trends that parallel the TFZ, suggesting a similar structural control on their activity.

Mid-Pleistocene pyroclastic flows filled topographic lows created by faults in Deschutes Formation lavas. In the Tumalo area this is
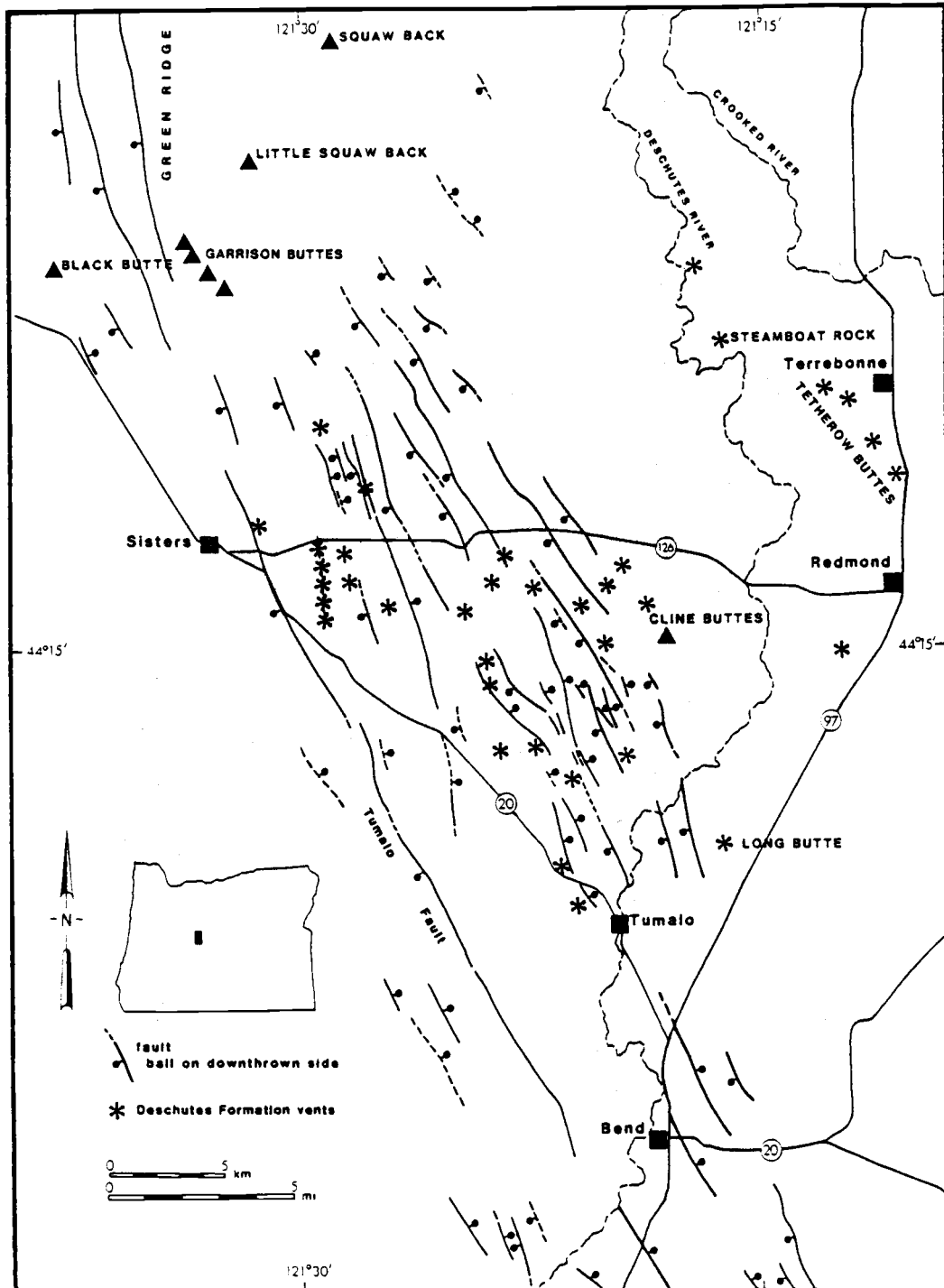
Figure 50. Deschutes Formation vents are concentrated in the Tumalo fault zone.

evidenced by the outcrop of pyroclastic units adjacent to the fault

in sections 17 and 20, T16S, R12E. The Tumalo Tuff, the youngest

Pleistocene ignimbrite in the Tumalo area, is offset by faulting

(Figure 51). The youngest Pleistocene unit in the Tumalo area, a

basalt flow from Newberry volcano, does not appear faulted. However,

exposures of the same lava near Bend are cut by faults of the TFZ.

Holocene age lavas of Newberry volcano (MacLeod and others, 1982) are

not cut by the TFZ, but northwest trending fissures on the flanks of

the volcano have erupted Holocene age basaltic andesites.

REGIONAL STRUCTURAL RELATIONSHIPS

The TFZ terminates against two other major fault zones that

shaped the central Oregon landscape during the Neogene: the Brothers

fault zone and the Green Ridge fault zone. The east end of the TFZ

appears to merge with the Brothers fault zone (BFZ) (Figure 52) on

the northeast flank of Newberry volcano. Newberry volcano also marks

the juncture of the Walker Rim fault zone of Basin and Range

Province, with the TFZ and the BFZ. Vent alignments and fissures on

the south side of the volcano are parallel to the northeast trending

Walker Rim fault zone. MacLeod and Sherrod (1988) suggest that the

Walker Rim fault zone and the TFZ form one fault zone that curves

beneath Newberry volcano.

The BFZ is a 25 to 50 km wide zone of en echelon normal faults

which trends N60°W across the High Lava Plains province between the

Harney basin and the northeast side of Newberry volcano, a distance
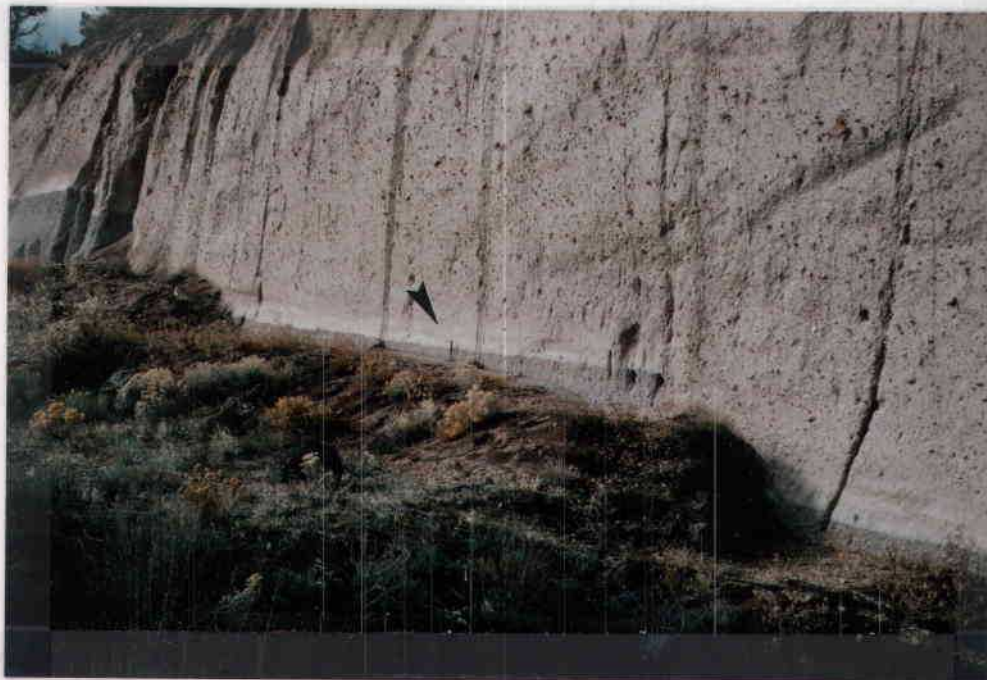
Figure 51. Parallel normal faults cut the Pleistocene age Tumalo Tuff and Bend Pumice. Cumulative offset in photo is 4.5 m. Blocks are downdropped to the southeast. Exposure is in quarry north of Tumalo State Park. Hammer for scale at photo center.
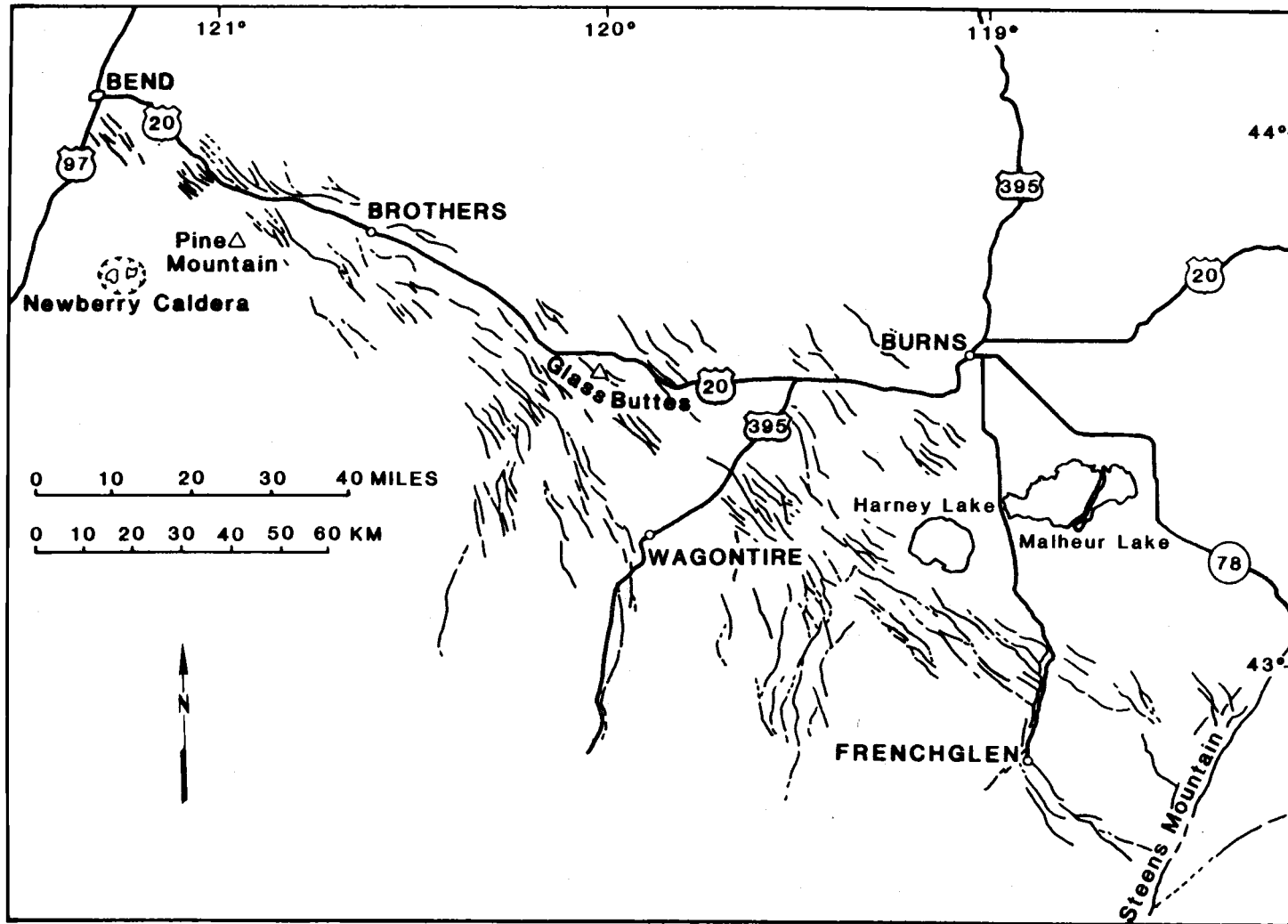
Figure 52. Location of the Brothers fault zone. After Walker and Nolf, 1981.

of approximately 240 km (Walker and others, 1967; Greene and others,
1972). Most faults in the zone strike between N30-40°W, are between
3 and 16 km long, and typically have offsets between 10 and 100 m.
Crossfaults approximately 80° to the direction of the enechelon
faults are common and are typically less than 1 km long (Tucker,
1975). Net displacement across the BFZ does not appear to be greater
in one direction than the other. The BFZ offsets Pliocene and older
rocks but does not offset Pleistocene rocks on the flanks of Newberry
volcano (MacLeod and others, 1982).

At its eastern margin, the BFZ terminates against Steens Mountain
fault, a north-south trending fault of the Basin and Range province.
South of the BFZ, north-south trending normal faults terminate
against or turn to assume the northwest trend of the zone. Lawrence
(1976) suggested that the BFZ is the surface manifestation of a
deeply buried right lateral fault which terminates Basin and Range
faulting. The pattern of faulting in the BFZ is interpreted to
represent the early deformation stages of strike-slip faulting.
En echelon faults, most of which lie at an acute angle to the overall
trend of the fault zone, are interpreted as Riedel shears and the
shorter crossfaults are interpreted as conjugate Riedel shears.
Absence of fractures with a strike-slip motion is interpreted to
mean that little motion has occured along the BFZ.

Numerous late Miocene and Pliocene basaltic and silicic vents are
concentrated in the BFZ. The progressive westward decrease in age of
silicic domes in and adjacent to the BFZ (Walker, 1974) might suggest
that motion along the BFZ has migrated from east to west, and

perhaps, that motion was subsequently taken up along the TFZ. However, basaltic lavas have a much greater volume than silicic lithologies in the BFZ and do not appear to have an eastward age progression (MacLeod and others, 1975). Limited age data on basaltic rocks (Parker and others, 1972) suggests volcanism in the BFZ began prior to but was in part coincident with volcanism in the TFZ. Motion along the TFZ appears to have continued past the time of last motion along the BFZ, as the BFZ does not cut Pleistocene lavas on the flanks of Newberry volcano.

The prevalence of volcanic vents in the TFZ and BFZ indicates that they both represent deep structural features that facilitated the passage of magma to the surface. Other similarities between the two zones, such as northwest trend and en echelon normal faulting, as well as their proximity to one another, has often lead to the assumption that the TFZ and BFZ are extensions of the same fault zone. However, faulting patterns suggest that they represent different stress environments. Characteristics of the BFZ that are attributable to right lateral shear are absent in the TFZ. In the TFZ, the trend of the faults closely parallels the overall trend of the fault zone, and there is no evidence of crossfaulting. Instead, the TFZ appears to represent faulting in a tensional environment.

The western margin of the TFZ is the Green Ridge fault zone (GRFZ). Green Ridge is a prominent north-south trending and steeply dipping fault scarp some 32 kilometers long that forms the eastern boundary of the volcano tectonic depression known as the central Oregon High Cascade graben. Deschutes Formation lavas and ignim-

brites dip gently toward the Deschutes basin on the east side of Green Ridge and younger High Cascade basaltic lavas lie west of the scarp. Absence of Deschutes Formation vents among younger High Cascade volcanoes, and the abrupt westward termination of the Deschutes Formation at Green Ridge, suggests that Deschutes Formation source volcanoes were downdropped along the west side of Green Ridge and were subsequently buried by younger lavas (Taylor, 1981a). Based on isotopic ages from lavas at Green Ridge and the stratigraphic relationship between units in the basin, faulting is dated at approximately 5.4 Ma (Smith and others, 1987).

Offset along the GRFZ has been across a narrow zone of near parallel faults (Conrey, 1985). Faults at the south end of the zone trend N5-15°W and exhibit stratigraphic offset of only 18 - 20 m. In more northerly latitudes the faults trend north-south and reach an offset of 600 to 670 m. Further north, offset again decreases until faulting appears to terminate at the north end of Green Ridge (Yogodzinski, 1985; Wendland, 1989).

Graben bounding faults along the High Cascades appear discontinuous. (See Priest and others, 1983, for a summary of High Cascade graben faulting). The gradual decrease in offset south along the GRFZ, coupled with the low topographic relief and the depositional contact between Deschutes Formation and younger High Cascde lavas in the Sisters area, suggests that graben faulting did not extended south of the GRFZ. Some TFZ faults appear to assume a more northward trend and merge with north-northwest trending GRFZ faults at the south end Green Ridge; other TFZ faults continue on their original

northwest trend and end abruptly south of Green Ridge. There is no evidence for continuation of the TFZ west of Green Ridge across Quaternary High Cascade lavas. However, there is a north-northwest alignment of Quaternary cinder cones approximately 2 km west of the south end of Green Ridge, which were interpreted by Conrey (1985) to overlie a major fault of the GRFZ.

Early faulting along Green Ridge approximately coincides with the initiation of volcanism in the TFZ. Tensional stresses in both the the TFZ and the GRFZ appear to have originated at about the same time. The steep angle of the faults and the absence of significant tilting among the fault blocks does not suggest that lateral extension across the zones was significant.

DISCUSSION

The relationship between the TFZ, GRFZ and the BFZ is not clearly understood. The TFZ appears to have remained active longer than either the GRFZ or the BFZ, but motion along all three zones probably overlapped in time. Both ends of the BFZ terminate in a zone of normal faulting. The TFZ appears to represent a transition from the strike-slip faulting of the BFZ to normal faulting at Green Ridge (Lawrence, 1976). The GRFZ and TFZ responded to tensional stress at approximately the same time. The difference in the orientation of the TFZ and GRFZ suggests that the stress field was oriented slightly different in each zone or that the local response to a similar stress orientation was slightly different.

The accumulation of numerous airfall lapillistones and paleosols and the absence of pyroclastic flow deposits at the top of the Deschutes Formation sedimentary section in the central part of the Deschutes basin suggests that pyroclastic flows and volcaniclastic sediment that once freely entered the basin from the west were impounded by the increasing offset along Green Ridge (Conrey, 1985; Smith, 1986a; Dill 1989). Smith (1986a) invoked "displacment across a wide zone" in the TFZ to facilitate structural isolation of Deschutes Formation source volcanoes from the Deschutes basin south of the latitude of Green Ridge. However, stratigraphic evidence in the southernmost Deschutes basin does not support the hypothesis that the Deschutes basin was completely cut off from volcanic sources to the south. As well as abundant lapillistone beds and paleosols, there are at least two and perhaps three ignimbrites near or at the top of the sedimentary section in the southern Deschutes basin. The White Rock ignimbrite caps the sedimentary section in the Tumalo area, and another ignimbrite lies less than 2 m below plateau-forming lavas. A Deschutes Formation ignimbrite near the top of the sedimentary section is also exposed in a roadcut along highway 126 near Cline Falls.

SUMMARY AND CONCLUSIONS

The Tumalo quadrangle lies behind the Cascade volcanic arc and at the southernmost extent of the Deschutes basin. Local and High Cascade volcanism have alternately controlled deposition in the area from the late Miocene to late Pleistocene. Cline Buttes was a local center of silicic volcanism at some undetermined time during the mid- to late Tertiary, prior to deposition of the Deschutes Formation. Other silicic volcanic centers in and adjacent to the Deschutes basin have yielded radiometric ages coincident with John Day volcanism (between 36 - 22 Ma) and others have younger mid-Miocene ages.

Deposition of the Deschutes Formation in the Tumalo area occurred during the latest Miocene and may have continued into the early Pliocene. A radiometric age from one of the numerous basaltic andesite lavas which locally form the top of the formation places volcanic activity at 5.4 $\pm$ 0.1 Ma, close to the Pliocene-Miocene boundary and within the error limits of ages obtained for similar lavas adjacent to the Tumalo area. Field evidence suggests that deposition of the lavas took place over a relatively brief period of time.

Both local and High Cascade volcanism contributed to deposition of the Deschutes Formation. The bottom of the formation is not exposed in the Tumalo area. Exposures in the walls of the Deschutes River canyon reveal that locally the formation is more than 70 m

thick and is dominated by interbedded volcaniclastic sedimentary rocks, pumice lapillistones, and ignimbrites. Volcaniclastic sediment, debris flows, and pyroclastic flows entered the area from the southwest, following the northeast paleoslope, from sources in the Early High Cascade volcanic arc. The large amount of silicic pyroclastic material in the sedimentary rocks and the dominance of silicic compositions among pyroclastic units indicates that silicic volcanism had a controlling influence on deposition. High discharge events, often accompanied by high sediment concentration, controlled sediment deposition. These events were likely triggered when large quantities of loose pyroclastic and other volcaniclastic material exceeded the transporting capacity of established drainages and caused widespread flooding. Depositional events were episodic and interspersed with periods of subaerial exposure during which thick air-fall pumice lapillistones and tuffs were deposited. The horizontal, widespread nature of many units suggests deposition onto a broad, nearly flat-lying alluvial plain.

Sedimentation appears to have ceased shortly before eruption of basaltic andesite lavas from local, small, monogenetic shield volcanoes and cinder cones at approximately 5.4 Ma. The termination of sedimentation in the central Deschutes basin has been attributed to structural isolation of the basin from sources west of the growing fault scarp at Green Ridge. This hypothesis is not easily invoked to explain the termination of sedimentation in the southern reaches of the basin. There is no topographic evidence of graben faulting south of Green Ridge and offset along structural zones in the

southern basin appears insufficient to isolate the area from sources which lay to the southwest. Despite prolonged periods of exposure and slow sedimentation, field evidence suggests that ignimbrites and sheetfloods were still able to reach the southern part of the basin until shortly before eruption of lavas from local vents.

Deschutes Formation basaltic lavas are typically porphyritic, with phenocrysts of plagioclase and olivine, and are high in Al_2O_3. They are less numerous than basaltic andesites and appear to be older, based on field relationships between the two lava types. Analytical data does not suggest that the basaltic andesites evolved from the basalts by a simple fractionation process, a suggestion that is supported by the fine grained, aphyric to sparsly porphyritic character of the basaltic andesites, and plagioclase compositions in the basaltic andesites which are similar or higher in anorthite content than those of the basalts. Both lava types have tholeiitic compositional tendencies, although the high $FeO-TiO_2$ basaltic andesites have a stronger tholeiitic character than the basalts. Both lava types have relatively evolved compositions based on Fe'.

After a 4 million year hiatus, deposition in the Tumalo quadrangle resumed at approximately 0.6 Ma when rhyodacitic pyroclastic flows, erupted from the High Cascades west and southwest of Tumalo, spread into the area. Pleistocene age basaltic andesite lavas which erupted from High Cascade sources between and after the pyroclastic flows, typically form small localized outcrops in the quadrangle. One of the voluminous diktytaxitic basalt lavas erupted from Newberry volcano flowed into the Tumalo area subsequent to

deposition of the High Cascade units, forcing the Deschutes River to a more westerly course along the margin of the flow.

More than thirty high-angle en echelon normal faults which trend between N15°-35°W over a 6 km wide zone, offset the rocks of the Tumalo quadrangle. These faults are part of the Tumalo Fault zone which trends approximately N35°W between the Green Ridge fault zone and the Brothers fault zone. The faults typically have small offsets; the average offset in the Tumalo area is 5 m. Deschutes Formation volcanoes are localized in the fault zone, suggesting eruption of the basalts and basaltic andesites was structurally controlled. There is no evidence for faulting prior to eruption of the lavas, suggesting that the stresses responsible for faulting were initiated shortly before eruption of the lavas in the late Miocene. Faulting continued into the late Pleistocene, offsetting the youngest ignimbrite (approximately 0.3 Ma) in the Tumalo area. A local tensional stress regime with a northeast-southwest least compressive stress orientation appears to have been established late in Deschutes Formation time and remained active until the late Pleistocene. The coincidence of normal faulting along the Tumalo fault zone and the Green Ridge fault zone at approximately 5.4 Ma suggests they responded to closely related, although slightly differently oriented, tensional stresses.

BIBLIOGRAPHY

Allen, J.E., 1966, The Cascade Range volcano-tectonic depression of
    Oregon, in, Staples, L.W., and Green, J. eds., Transactions
    of the lunar geological field conference: Oreg. Dept. Geol
    Min. Ind., p. 21-23.

Armstrong, R.L., Taylor, E.M., Hales, P.O., and Parker, D.J., 1975,
    K-Ar dates for volcanic rocks, central Cascade Range of Oregon:
    Isochron/West, no. 13, p. 5-10.

_____, 1978, Cenozoic igneous history of the U.S. Cordillera
    from latitude 42° to 49°N: Geol. Soc. Amer. Mem. 152,
    p. 265-282.

Beyer, R.L., 1973, Magma differentiation at Newberry crater in
    central Oregon: Eugene, University of Oregon Ph.D. dissertation
    (unpub.), 93 p.

Blissenbach, E., 1954, Geology of alluvial fans in semi-arid regions:
    Geol. Soc. Amer. Bull., v. 65, p. 175-190.

Bull, W.B., 1972, Recognition of alluvial fan deposits in the strat-
    igraphic record, in, Rigby, J.B. and Hamblin, W.K., eds., Recog-
    nition of ancient sedimentary environments: Soc. Econ. Paleon.
    Min. Spec. Pub. 16, p. 63-83.

Cannon, D.M., 1985, The stratigraphy, geochemistry and mineralogy of
    two ash-flow tuffs in the Deschutes Formation, central Oregon:
    Corvallis, Oregon State Univ. M.S. thesis (unpub.), 142 p.

Chaney, R.W., 1938, The Deschutes flora of eastern Oregon: Carnegie
    Inst. Washington, Contrib. to Paleo., v. 476, p. 185-216.

Conrey, R.M.. 1985, Volcanic stratigraphy of the Deschutes Formation,
    Green Ridge to Fly Creek, north-central Oregon: Corvallis,
    Oregon State Univ. M.S. thesis (unpub.) 349p.

Dill, T.E., 1989, Stratigraphy of the Neogene volcanic rocks along
    the lower Metolius River, Jefferson County, Oregon: Corvallis,
    Oregon State Univ. M.S. (unpub.), 345 p.

Dingus, L.W. 1979, The Warm Springs Fauna (Mammalia, Hemmingfordian)
    from the western facies of the John Day Formation, Oregon:
    Riverside, University of California M.S. thesis (unpub.).

Enlows, H.E., and Parker, D.J., 1972, Geochronology of the Clarno
    igneous activity in the Mitchell quadrangle, Wheeler County,
    Oregon: The Ore Bin, v. 34, p. 104-110.

Evernden, J.F., and James, G.T., 1964, Potassium-Argon dates and the Tertiary floras of North America: Amer. Jour. Sci., v. 262, p. 945-974.

Farooqui, S.M., Bunker, R.C., Thoms, R.E., Clayton, D.C., and Bela, J.L., 1981, Post-Columbia River Basalt Group stratigraphy and map compilation of the Columbia Plateau, Oregon: Oregon Dept. Geol. and Min. Ind. Open-File Rept. 0-81-10, 79p.

Fiebelkorn, R.B., Walker, G.W., MacLeod, N.S., McKee, E.H., and Smith, J.G., Index to K-Ar determinations for the state of Oregon: Isochron/West, no. 37, p. 3-60.

Fisher, R.V., 1961, Proposed classification of volcaniclastic sediments and rocks, Geol. Soc. Amer. Bull., v.72, p. 1409-1414.

_____, 1966, Rocks composed of volcanic fragments and their classification, Earth Sci. Rev., v. 1, p. 287-298.

_____, 1967, Early Tertiary deformation in north-central Oregon: Amer. Assoc. Petrol. Geol. Bull. v. 51, p. 111-123.

Frostick, L.E., and Reid, I., 1977, The origin of horizontal laminae in ephemeral stream channel fill: Sedimentology, v. 24, p. 1-10.

Greene, R.C., Walker, G.W., and Corcoran, R.E., 1972, Geologic map of the Burns quadrangle, Oregon: U.S. Geol. Surv. Misc. Geol. Invest. Map I-680, scale 1:250,000.

Hales, P.O., 1975, Geology of the Green Ridge area, Whitewater River quadrangle, Oregon: Corvallis, Oregon State Univ. M.S. thesis (unpub.) 90p.

Hammond, P.E., 1979, A tectonic model for evolution of the Cascade Range, in, Armentrout, J.M., and others, eds., Cenozoic Paleo-geography of the western United States: Pacific Coast Paleo-geography symposium no. 3: Los Angeles, SEPM Pacific Section, 335 p.

Harland, W.B., Cox, A.V., Llewellyn, A.C. Pickton, C.A.G., Smith, A.G., and Walters, R., 1982, A geologic time scale: Cambridge, Cambridge University Press, 131p.

Harms, J.C., and Fahnstock, R.K., 1965, Stratification, bed forms, and flow phenomena (with an example from the Rio Grande), in, Middleton, ed., Primary sedimentary structures and their hydro-dynamic interpretation: Soc. Econ. Paleo. Min. Spec. Pub. 12, p. 84-115.

Harms, J.C., Southard, J.B., Spearing, D.R., and Walker, R.G., 1975, Depositional environments as interpreted from primary sedimentary structures and stratification sequences: Soc. Econ. Paleo. Min. Short Course 2, 161p.

Hay, R.L., 1962, Origin and diagenetic alteration of the lower part of the John Day Formation near Mitchell, Oregon: Geol. Soc. Amer. Buddington Memorial Memoir, p. 191-216.

Hayman, G.A., 1983, Geology of a part of the Eagle Butte and Gateway quadrangles, east of the Deschutes River, Jefferson County, Oregon: Corvallis, Oregon State Univ. M.S. thesis (unpub.), 97 p.

Hewitt, S.L., 1970, Geology of the Fly Creek quadrangle and the north half of the Round Butte Dam quadrangle, Oregon: Corvalllis, Oregon State Univ. M.S. thesis (unpub.), 69p.

Higgins, M.W., 1973, Petrology of Newberry volcano, central Oregon: Geol. Soc. Amer. Bull., v. 84, p. 455-488.

Hill, B.E., 1985, Petrology of the Bend pumice and Tumalo tuff, a Pleistocene Cascade eruption involving magma mixing: Corvallis, Oregon State Univ. M.S. thesis (unpub.), 101p.

_____, 1988, The Tumalo volcanic center: A large Pleistocene vent complex on the east flank of the Oregon central High Cascades, Geol. Soc. Amer. Abst. Pgms., p. A398.

_____, and Taylor, E.M., in press, Oregon central High Cascade pyroclastic units in the vicinity of Bend, Oregon: in Scott, W.E., Gardner, C.A., Sarna-Wojcicki, A.M., eds., Field trip guide to the central Oregon High Cascades, U.S. Geol. Surv. Open File Report.

Hodge, E.T., 1928, Framework of the Cascade Mountains in Oregon: Pan-Amer. Geol., v. 49, p.341-355.

_____, 1940, Geology of the Madras quadrangle: Oregon State Monographs, Studies in Geology no. 1.

_____, 1942, Geology of north central Oregon: Oregon State Mono., Studies in Geology no. 3, 76 p.

Hooke, R.L., 1964, Processes in arid-region alluvial fans: Jour. Geol., v.75, p. 438-460.

Jay, J.B., 1982, The geology and stratigraphy of the Tertiary Vol-
     canic and volcaniclastic rocks, with special emphasis on the
     Deschutes Formation, from Lake Simtustus to Madras in Central
     Oregon: Corvallis, Oregon State Univ. M.S. Thesis (unpub.),
     119p.

Johnson, A.M., 1970, Physical processes in Geology: San Francisco,
     Freeman, Cooper, 577 p.

Kay, S.M., Kay, R.W., and Citron, G.P., 1982, Tectonic Controls on
     tholeiitic and calc-alkaline magmatism in the Aleutian Arc:
     Jour. Geophys. Res., v. 87, p. 4051-4072.

Kuenzi, W.D., Horst, O.H., and McGehee, R.V., 1979, Effect of
     volcanic activity on fluvial-deltaic sedimentation in a modern
     arc-trench gap, south-western Guatemala: Geol. Soc. Amer. Bull.,
     v. 90, pt. 1, p. 827-838.

Lawrence, R.D., 1976, Strike-slip faulting terminates the Basin and
     Range province in Oregon: Geol. Soc. Amer. Bull., v. 87,
     p. 846-850.

MacLeod, N.S., and others, 1975, Geothermal significance of east-
     ward increase in age of upper Cenozoic rhyolite domes in south-
     eastern Oregon: Proceedings of the 2nd U.N. symposium on the
     development and use of geothermal resources. v. 1, p. 465-474.

MacLeod, N.S., and others, 1982, Geologic map of Newberry Volcano,
     Deschutes, Klamath and Lake counties, Oregon: U.S. Geol. Surv.
     Open File Rept. 82-847, scale 1:62,500.

_____, and Sherrod, D.R., 1988, Geologic evidence for a magma
     chamber beneath Newberry Volcano, Oregon: Jour. Geophys. Res.,
     v. 92, no. B9, p. 10,067-10,079.

Martin, R.F., and Piwinskii, A.J., 1972, Magmatism and tectonic
     setting: Jour. Geophys. Res., v. 77, p. 4966-4975.

Mathisen, M.E., and Vondra, C.F., 1983, The fluvial and pyroclastic
     deposits of the Cagayan basin, northern Luzon, Phillipines -
     an example of non-marine volcaniclastic sedimentation in an
     interarc basin: Sedimentology, v. 2, p. 585-589.

McKee, E.D., Crosby, E.J., and Berryhill, H.L., Jr., 1967, Flood
     deposits, Bijou Creek Colorado, June 1965: Jour. Sed. Pet., v37,
     p. 829-851.

McKee, E.H., Swanson, D.A., and Wright, T.L.,1977, Duration and
     volume of Columbia River Basalt volcanism; Washington, Oregon,
     and Idaho: Geol. Soc. Amer. Abs. Prog., v. 9, p. 463-464.

Miall, A.D., 1977, A review of the braided river depositional environment: Earth Sci. Rev., v. 13, p. 1-62.

_____, 1978, lithofacies types and vertical profile models in braided river deposits: a summary, in, Miall, A.D., ed., Fluvial Sedimentology: Can. Soc. Petrol. Geol. Mem. 5, p. 597-604.

Middleton, G.V., 1967, Experiments on density and turbidity currents. III. Deposition of sediments: Can. Jour. Earth. Sci., v. 4, p. 475-505.

Noblett, J., 1981, Subduction-related origin of the volcanic rocks of the Eocene Clarno Formation near Cherry Creek, Oregon: Oregon Geology, v. 43, p. 91-99.

Obermiller, W.A., 1987, Geologic, structural and geochemical features of basaltic rocks of the Smith Rock/Gray Butte area: Eugene, Univ. of Oregon M.S. thesis (unpub.).

Osborn, E.F., 1959, Role of oxygen pressure in the crystallization and differentiation of basaltic magma: Am. Jour. Sci., v. 257, p. 609-647.

Parker, D., and Armstrong, R.L., 1972, K-Ar dates and Sr isotope initial ratios for volcanic rocks in the Harney Basin, Oregon: Isochron/West, no. 5, p. 7-12.

Peck, D.L., Griggs, A.B., Schlicker, H.G., Wells, F.G., and Dole, H.M., 1964, Geology of the central and northern parts of the Western Cascade Range in Oregon: U.S. Geological Surver Professional Paper 449, 56p.

Peterson, N.V., and Groh, E.A., 1970, Geologic tour of Cove Palisades State Park near Madras, Oregon: The Ore Bin, v. 32, p. 41-51.

_____, _____, Taylor, E.M., and Stensland, D.E., 1976, Geology and mineral resources of Deschutes County, Oregon: Oregon Dept. Geol. Min. Ind. Bull. 89, 89p.

Picard, M.D., and High, L.R., 1973, Sedimentary structures of ephemeral streams, Developments in sedimentology, 17: Elsevier, Amsterdam, 223 p.

Porter, S.C., 1972, Distribution, morphology, and size frequency of cinder cones on Mauna Kea Volcano, Hawaii: Geol. Soc. America Bull., v.83, p. 3607-3612.

Priest, G.R., Woller, N.M., and Black, G.L., 1983, Overview of the geology of the central Oregon Cascade Range, in, Priest, G.R., and Vogt, B.F., eds., Geology and geothermal resources of the central Oregon Cascade Range: Oregon Dept. Geol. Min. Ind. Spec. Paper 15, 123p.

Robinson, P.T., 1975, Reconnaissance geologic map of the John Day Formation in the southeastern part of the Blue Mountains and adjacent areas, north-central Oregon: U.S. Geol. Survey. Misc. Invest. Map I-872.

_____, and Brem, G.M., 1981, Guide to geologic field trip between Kimberly anmd Bend, Oregon with emphasis on the John Day Formation, in, Johnston, D.A., and Donnelly-Nolan, J.. eds., Guides to some volcanic terranes in Washington, Idaho, Oregon and northern California: U..S. Geol. Surv. Circ. 838, p. 55-58.

_____, and Brem, G.M., 1984, John Day Formation of Oregon: A distal record of early Cascade volcanism: Geology, v. 12. p. 229-232.

_____, and Laenen, A., 1976, Water resources of the Warm Springs Indian Reservation, Oregon: U.S. Geol. Surv. Water Res. Invest. 76-26, 85p.

_____, and Price, D., 1963, Groundwater in the Prineville area, Crook County, Oregon: U.S. Geol. Surv. Water Supply Paper 1619-P, 49p.

_____, and Stensland, D.E., 1979, Geologic map of the Smith Rock area, Jefferson, Deschutes, and Crook Counties, Oregon: U.S. Geol. Surv. Misc. Invest. Map I-1142.

Rogers, J.J.W., 1966, Coincidence of structural and topographic highs during post-Clarno time in north-central Oregon: Amer. Assoc. Petrol. Geol. Bull., v. 50, p. 390-396.

Ruegg, G.H.J., 1977, Features of middle Pleistocene sandur deposits in the Netherlands: Geol. en Mijnbouw, v. 56, p. 5-24.

Russel, I.C., 1905, A preliminary report on geology and mineral resources of central Oregon: U.S. Geol. Surv. Bull. 252, 138p.

Rust, B.R., 1978, Depositional models for braided alluvium, in, Miall, A., ed., Fluvial Sedimentology: Can. Soc. Petrol. Geol. Mem. 5, p. 605-625.

Sarna-Wojcicki, A.M., Morrison, S.D., Meyer, C.E., Hillhouse, J.W., 1987, Correlation of upper Cenozoic tephra layers between sediments of the western United States and eastern Pacific Ocean and comparison with biostratigraphic and magnetostratigraphic age data: Geol Soc. Amer. Bull., v. 98, p. 207-223.

_____, Meyer, C.E., Nakata, J.K., Scott, W.E., Hill, B.E., Slate, J.L., Russell, P.C., in press, Age and correlation of mid-Quaternary ash beds and tuffs in the vicinity of Bend, Oregon, in Scott, W.E., Gardner, C.A., and Sarna-Wojcicki, A.M., eds., Field Trip Guide to the central Oregon High Cascades, U.S. Geol. Surv. Open file report.

Scott, W.E., 1977, Quaternary glaciation and volcanism, Metolius River area, Oregon: Geol. Soc. Amer. Bull., v. 88, p113-124.

Schmid, R., 1981, Descriptive nomenclature and classification of pyroclastic deposits and fragments: Recommendations of the IUGS Subcommission of the Systematics of Igneous Rocks, Geology, v. 9, p. 41-43.

Smith, G.A., 1986a, Stratigraphy, sedimentology, and petrology of Neogene rocks in the Deschutes Basin, Central Oregon: a record of continental-margin volcanism and its influence on fluvial sedimentation in an arc-adjacent basin: Corvallis, Oregon State Univ. Ph. D. dissertation (unpub.), 467 p.

_____, 1986b, "Simtustus Formation": paleogeographic and stratigraphic significance of a newly defined Miocene unit in the Deschutes basin, central Oregon: Oregon Geology, v. 48, p. 63-72.

_____, 1986c, Coarse-grained nonmarine volcaniclastic sediment: terminology and depositional process: Geol. Soc. Amer. Bull., v. 97, p. 1-10.

_____, and Priest, G.R., 1983, A field trip guide to the central Oregon Cascades, first day: Mount Hood - Deschutes basin: Oregon Geology, v. 45, p. 119-126.

_____, and Snee, L.W., 1984, Revised stratigraphy of the Deschutes basin, Oregon: implications for the Neogene development of the central Oregon Cascades (abstr.): EOS, Trans. Amer. Geophys. Union, v. 65, p. 330.

_____, Snee, L.W., and Taylor, E.M., 1987, Stratigraphic, sedimentologic, and petrologic record of late Miocene subsidence of the central Oregon High Cascades: Geology, v. 15, p. 389-392.

_____, and Taylor, E.M., 1983, The central Oregon High Cascade graben: What? Where? When?: Trans. Geotherm. Res. Coun., v. 7, p. 275-279.

Sparks, R.S.J., and others, 1973, Products of ignimbrite eruptions: Geology, v. 1, p. 115-118.

Stearns, H.T., 1930, Geology and water resources of the middle Deschutes River basin: U.S.Geo. Surv. Water Supply Paper 737, p. 125-212.

Stensland, D.E., 1970, Geology of part of the northern half of the Bend quadrangle, Jefferson and Deschutes Counties, Oregon: Corvallis, Oregon State Univ. M.S. thesis (unpub), 118 p.

Surdam, R.C. and Boles, J.R., 1979, Diagenesis of volcanic sandstones: Soc. Econ. Paleo. Min. Spec. Pub. 26, p. 227-242.

Swanson, D.A., 1969, Reconnaissance geologic map ot the east half of the Bend quadrangle, Crook, Wheeler, Jefferson, Wasco, and Deschutes counties, Oregon: U.S. Geol. Surv. Misc. Geol. Invest. Map I-568, scale 1:250,000.

_____, and Robinson, P.T., 1968, Base of the John Day Formation in and near the Horse Heaven mining district, north-central Oregon: U.S. Geol. Surv. Prof. Paper 600-D, p. 154-161.

Taubeneck, W.H., 1970, Dikes of Columbia River Basalt in northeastern Oregon, western Idaho, and southeastern Washington, in, Gilmore, E.H., and Stradling, D., eds., Proceedings of the second Columbia River Basalt symposium: Cheney, Eastern Washington State College Press, 333p.

Taylor, E.M., 1968, Roadside geology, Santiam and McKenzie Pass Highways, Oregon, in, Dole, H.M., ed., Andesite Conference Guidebook: Oregon Dept. Geol. Min. Ind. Bull. 62, p. 3-33.

_____, 1973, Geology of the Deschutes basin, in, Beaulieu, J. D. and others, eds., Geologic field trips in northern Oregon and southern Washington: Oregon Dept. Geol. and Min. Ind. Bull. 77, p. 29-32.

_____, 1978, Field geology of the S. W. Broken Top quadrangle, Oregon: Oreg. Dept. Geol. Min. Ind. Spec. Pap. 2, 50p.

_____, 1980, Volcanic and volcaniclastic rocks on the east flank of the central Cascade Range to the Deschutes River, Oregon, in, Oles, K.F. and others, eds., Geologic tield trips in Western Oregon and Washington: Oregon Dept. Geol. and Min. Ind. Bull. 101, p. 1-7.

_____, 1981a, Central High Cascade roadside geology - Bend,
Sisters, McKenzie Pass, and Santiam Pass, Oregon, in, Johnston,
D.A., and Donnelly-Nolan, J., eds., Guides to some volcanic
terranes in Washington, Idaho, Oregon, and Northern California:
U.S. Geol. Survey. Circ. 838, p. 55-58.

_____, 1981b, A mafic dike system in the vicinity of Mitchell,
Oregon, and its bearing on the timing of Clarno-John Day vol-
canism and early oligocene deformation in central Oregon: Oregon
Geology, v. 43, p. 107-112.

_____, 1987, Field geology of the northwest quarter of the
Broken Top 15' quadrangle, Deschutes County, Oregon: Oregon
Dept. Geol. Min. Ind. Spec. Paper 21, 17 p.

Thayer, T.P., 1936, Structure of the North Santiam River section of
the Cascade Mountains in Oregon: Jour. Geol., v. 44, p. 701-716.

Tucker, E.R., 1975, Geology and structure of the Brothers fault
zone in the central part of the Millican SE quadrangle,
Deschutes County, Oregon: Corvallis, Oregon State Univ. M.S.
thesis (unpub.) 88p.

Tunbridge, I.P., 1981, Sandy high-energy flood sedimentation - some
criteria for recognition, with an example from the Devonian of
S.W. Endland: Sedimentary Geology, v. 28, p. 79-95.

Uppuluri, V.R., 1974, Prineville chemical type: a new basalt type in
the Columbia River Group: Geol. Soc. Amer. Bull., v. 85,
p. 1315-1318.

Vessell, R.K., and Davies, D.K., 1981, Nonmarine sedimentation in an
active fore arc basin: Soc. Econ. Paleon. Min. Spec. Pub. 31,
p. 31-45.

Walker, G.W., 1974, Some implications of late Cenozoic volcanism to
geothermal potential in the High Lava Plains of south-central
Oregon: Ore Bin, v. 36, no. 7, p. 1-11.

_____, 1981, Geologic map of the Deschutes Canyon further
planning area (Rare II), Jefferson and Deschutes counties, Ore-
gon: U.S. Geol. Surv. Misc. Field Studies Map MF-1303A.

_____, and Nolf, B., High Lava Plains, Brothers fault zone to
Harney Basin, Oregon, in, Johnston, D.A., and Donnelly-Nolan,
J., eds., Guides to some volcanic terranes in Washington, Idaho,
Oregon and northern California, U.S. Geol. Surv. Circ. 838,
p. 105-118.

_____, Peterson, N.V., and Green, R.C., 1967, Reconnaissance geologic map of the east half of the Crescent quadrangle; Lake, Deschutes, and Crook Counties, Oregon: U.S. Geol. Surv. Misc. Geol. Invest. Map I-493, scale 1:250,000.

Waters, A.C., 1961, Stratigraphic and lithologic variations in the Columbia River basalt: Amer. Jour. Sci., v. 259, p. 283-311.

_____, 1968, Reconnaissance geologic map of the Madras quadrangle, Jefferson and Wasco Counties, Oregon: U.S. Geol. Surv. Misc. Geol. Invest. Map I-555.

Weidenheim, J.P., 1981, The petrography, structure and stratigraphy of Powell Buttes, Crook County Central Oregon: Corvallis, Oregon State Univ. M.S. thesis (unpub.), 95p.

Wendland, D.W., 1989, Castle Rocks: a late Miocene eruptive center at the north end of Green Ridge, Jefferson County, Oregon: Corvallis: Oregon State Univ. M.S. thesis (unpub.) 189p.

Wentworth, C.K., and Williams, H., 1932, The classification and terminology of the pyroclastic rocks, Natl. Acad. Sci. - Natl. Res. Council, v. 89, p. 19-53.

White, C.M., 1980a, Geology and geochemistry of Mt. Hood volcano: Oreg. Dept. Geol. Min. Ind. Spec. Pap. 9, 26p.

_____, 1980b, Geology and geochemistry of volcanic rocks in the Detroit area, western Cascade Range, Oregon: Eugene, University of Oregon Ph. D. dissert. (unpub.) 178p.

Williams, G.E., 1971, Flood deposits of the sand-bed ephemeral streams of central Australia: Sedimentology, v. 17, p. 1-40.

Williams, H., 1924, Geology of the Pelton Dam site: Report to the Federal Power Commission (unpub.)

_____, 1957, A geologic map of the Bend quadrangle, Oregon, and a reconnaissance geologic map of the central portion of the High Cascade Mountains: Oregon Dept. Geol. Min. Ind.

Wood, C.A., 1979, Morphometric evolution of cinder cones: Jour. Volcan. Geotherm. Res., v. 7, p. 387-413.

Woodburne, M.O., and Robinson, P.T., 1979, A new late Hemmingfordian mammal fauna from the John Day Formation, Oregon, and its stratigraphic implications: Jour. Peleo., v. 51, p. 750-757.

Yogodzinski, G.M., 1986, The Deschutes Formation – High Cascade
    transition in the Whitewater River area, Jefferson County,
    Oregon: Corvallis, Oregon State Univ. M.S. thesis (unpub.),
    165p.

APPENDICES

APPENDIX I

DESCHUTES FORMATION MEASURED SECTIONS

Appendix I-A: White Rock ranch measured section

Location: east wall, Deschutes River canyon, center of section
10, T 16 S, R 12 E.

Unit	Description	Thickness (m) unit	total
11	ALLUVIUM, cobbles, boulders, and sand.	2.0	27.9
10	IGNIMBRITE, unwelded, tan to light gray, white and rare medium gray pumice lapilli; 2.5 cm structureless ash layer at base; sharp base.	12.3	25.9
9	SANDSTONE, tuffaceous, fine- to coarse-grained, poorly sorted, pale yellowish brown, dispersed pumice lapilli and pebbles, crude horizontal bedding; grades into:	1.5	13.6
8	SANDSTONE, medium-grained, moderately sorted, tuffaceous, brownish tan, massive, bottom 15 cm contains reworked pumice lapilli from underlying unit:	1.0	12.1
7	LAPILLISTONE, white to tan, angular pumice lapilli to 5 cm, 2% angular pebbles to 1.5 cm; massive; sharp base.	2.0	11.1
6	SANDSTONE and CONGLOMERATE, medium- to coarse-grained pebbly sandstone, brownish tan; thin, horizontal beds and lenses of pebble conglomerate; lower 1.5m are interbeds of thin, horizontal, clast supported, angular pebble conglomerate and pebbly, laminated to massive sandstone; sharp base.	1.3	9.3
5	TUFF, light gray, massive, minor pumice lapilli and angular pebbles; accretionary lapilli; gradational to:	0.2	8.0
4	LAPILLISTONE, tan, pink and black pumice, lapilli to 5cm, angular pebbles to 1.5 cm; massive; 4 cm thick ash layer at base; sharp base.	1.3	7.8

3 SANDSTONE, medium- to coarse-grained,   1.5   6.5
   moderately sorted, dispersed pumice lapilli
   and pebbles, dark brown, friable; massive;
   sharp base.

2 SANDSTONE, SILTSTONE, and MUDSTONE   3.0   5.0
   coarse-grained, poorly sorted, thin bedded
   and laminated sandstone and laminae with
   horizontal laminae of siltstone and mudstone,
   and lenses and laminae of fine, pebble con-
   glomerate; low-angle, large scale cross-beds,
   scour-and-fill; sharp base.

1 SANDSTONE, medium- to coarse-grained, poorly   2.0   2.0
   sorted, dark brown, dispersed tan pumice
   lapilli and black cinder, massive; base not
   exposed.

Base of section at 3060 feet

Appendix I-B: 77th Avenue wayside measured section

location: West wall, Deschutes River canyon, SW 1/4, SE1/4, sec. 35,
           T 15 S, R 12 E.

Unit	Description	Thickness (m) unit	total
11	BASALTIC ANDESITE lava, aphyric.	7.0	47.6
10	SANDSTONE, coarse-grained, moderately sorted, medium gray, thinly and horizontally laminated near top grading down into massive; laminae load deformed by overlying basalt; sharp base.	0.3	40.6
9	SANDSTONE, fine- to medium-grained, moderately to well sorted, yellow brown to medium gray; dispersed pumice lapilli to 0.5 cm, horizontal and low-angle cross laminae; base gradational to:	0.6	40.3
8	SANDSTONE, fine-grained, tuffaceous, dark gray; faint horizontal laminae to massive; gradational at base to:	0.3	39.7
7	SANDSTONE, fine-grained, light to medium gray, horizontal laminae; sharp base.	0.5	39.4
6	TUFF, coarse black ash with minor cinders; gradational at base to:	0.3	38.9
5	LAPILLISTONE, angular, irridescent, black pumice and cinder; sharp base.	0.1	38.6
4	SANDSTONE (paleosol?) with pumice lapilli interbed; coarse- to medium-grained, poorly sorted, normally graded; yellowish brown; dispersed white pumice lapilli; friable; 5-10 cm discontinuous interbed of angular to sub-rounded white pumice lapilli; base covered.	1.5	38.5
	COVERED	10	37.0
3	SANDSTONE, moderately to well sorted, coarse to medium-grained, light gray to tan, massive; sharp base.	1.0	27.0
2	IGNIMBRITE, unwelded, light gray; sharp base.	2.0	26.0
1	CONGLOMERATE, very coarse-grained, matrix supported, massive; base not exposed.	24.0	24.0

Base of section at 2940 feet

APPENDIX II

CHEMICAL ANALYSES OF VOLCANIC ROCKS

Most major element oxide analyses in this study were performed by the author at Oregon State University. Oxides of Si, Al, Ti, Fe, and Ca were obtained by X-ray fluorescence; oxides of Mg and Na were obtained via atomic absorption spectrometry. Selected samples were analysed for major and trace elements at Washington State University by X-ray fluorescence. Those samples analysed at WSU are prefixed by "TQ" before the sample number and include values for MnO and P_2O_5. WSU analyses have been normalized to 100%. Analytical precision (at one sigma) for the analyses are listed below:

	OSU	WSU			
SiO_2	1.0%	0.3%	Ni	2	ppm
Al_2O_3	0.5	0.3	Cr	5	ppm
FeO*	0.2	0.2	Sc	3	ppm
CaO	0.1	0.1	V	10	ppm
TiO_2	0.05	0.02	Ba	20	ppm
K_2O	0.05	0.02	Rb	2	ppm
MgO	0.2	0.1	Sr	4	ppm
Na_2O	0.2	0.1	Zr	4	ppm
MnO	–	0.02	Y	2	ppm
P_2O_5	–	0.02	Nb	1	ppm
			Ga	2	ppm
			Cu	3	ppm
			Zn	5	ppm

t

158

Appendix IIa

Cline Buttes Silicic Lavas

Unit	Tcbr	Tcbr	Tcbr	Tcbr
Sample	B29	B28	AM290	TQ3
SiO_2	73.5	72.8	76.1	74.1
Al_2O_3	14.3	14.5	13.8	14.1
TiO_2	0.16	0.18	0.19	0.20
FeO*	2.0	2.3	1.4	1.9
CaO	1.0	0.9	0.8	1.0
MgO	0.2	0.2	0.2	0.00
Na_2O	5.3	5.1	4.2	5.1
K_2O	3.05	3.06	3.44	3.47
MnO				0.05
P_2O_5				0.02
Total	99.51	99.04	100.13	99.94

Ni	21	(ppm)
Cr	0	
Sc	2	
V	20	
Ba	939	
Rb	81	
Sr	74	
Zr	253	
Y	31	
Nb	18	
Ga	18	
Cu	12	
Zn	53	

B29   Rhyodacite, east summit, NW1/4 SE1/4 sec. 21, T15S, R12E.
        (E. M. Taylor, unpublished data)
B28   Rhyodacite, summit, NE1/4 SW1/4 sec. 21, T15S, R12E.
        (E. M. Taylor, unpublished data)
AM290   Rhyodacite, NE1/4 NE1/4 sec. 30, T15S, R12E.

TQ3   Rhyodacite, NW1/4 SW1/4 sec. 21, T15S, R12E.

* Total Fe as FeO

Appendix IIb

Deschutes Formation Basalt and Basaltic Andesite Lavas

Unit	Tdb1	Tdb1	Tdb1	Tdb2	Tdb3	Tdb3	Tdb4	Tdb4
Sample	TQ72	AM72	B108	TQ122	AM9	TQ9	TQ279	B142
SiO_2	52.0	53.6	52.6	52.9	52.2	52.5	51.9	50.3
Al_2O_3	20.1	19.4	20.8	17.7	18.3	18.2	18.1	19.2
TiO_2	1.13	1.03	1.00	1.26	1.63	1.55	1.98	2.05
FeO*	7.4	7.4	7.1	8.7	10.0	9.0	10.2	10.0
CaO	10.0	9.2	10.0	8.9	8.2	8.6	9.1	9.7
MgO	4.8	4.9	4.1	5.8	5.7	5.2	3.8	3.9
Na_2O	3.2	3.1	3.5	3.4	3.5	3.5	3.4	3.6
K_2O	0.74	0.76	0.66	0.78	0.81	0.81	0.86	0.70
MnO	0.13			0.15		0.15	0.17	
P_2O_5	0.30			0.30		0.41	0.32	
Total	99.80	99.39	99.76	99.97	100.34	99.91	99.78	99.45
Ni	61 (ppm)			104		87	28	
Cr	134			132		122	37	
Sc	18			27		26	25	
V	197			242		248	313	
Ba	370			426		377	367	
Rb	8			10		11	12	
Sr	748			685		576	515	
Zr	129			114		130	140	
Y	22			114		24	33	
Nb	7			4		9	7	
Ga	20			22		21	22	
Cu	71			101		98	76	
Zn	75			89		98	104	
Q	0.88			1.05		1.28	1.34	
or	4.37			4.61		4.79	5.08	
ab	27.08			28.77		29.62	28.77	
an	38.30			30.73		31.56	31.59	
di	7.66			9.38		6.51	9.58	
hy	16.89			20.16		20.00	17.21	
mt	1.78			2.10		2.17	2.46	
il	2.15			2.39		2.94	3.76	
ap	0.70			0.70		0.95	0.74	

* Total Fe as FeO
Normative calculations assume $Fe_2O_3/FeO = 0.20$

Appendix IIb (cont.)

Deschutes Formation Basalt and Basaltic Andesite Lavas

Unit	Tdba1	Tdba1	Tdba1	Tdba1	Tdba2	Tdba2	Tdba2	Tdba2
Sample	AM277	AM85	AM78	TQ300	TQ219	AM305	AM237	AM261
SiO_2	56.3	57.0	55.8	55.4	56.7	57.2	57.2	57.8
Al_2O_3	15.6	15.2	15.5	15.6	16.1	15.7	15.9	16.1
TiO_2	1.84	1.84	1.86	1.87	1.91	1.80	1.89	1.92
FeO*	10.6	10.5	10.6	10.3	9.3	9.4	9.7	9.5
CaO	7.5	7.0	7.4	7.4	6.9	6.4	6.6	6.3
MgO	3.8	3.9	3.8	3.6	3.1	3.4	3.2	2.8
Na_2O	3.8	4.3	4.2	4.2	4.1	4.1	4.1	4.3
K_2O	1.10	0.93	1.00	1.06	1.33	1.22	1.33	1.18
MnO				0.17	0.18			
P_2O_5				0.36	0.31			
Total	100.54	100.67	98.43	99.96	99.93	99.22	99.92	99.90
Ni				6	29			
Cr				0	0			
Sc				31	24			
V				216	192			
Ba				492	522			
Rb				15	23			
Sr				524	485			
Zr				148	175			
Y				36	38			
Nb				5	10			
Ga				20	21			
Cu				140	22			
Zn				106	114			
Q				4.41	6.9			
or				6.26	7.86			
ab				35.54	34.69			
an				20.58	21.6			
di				11.50	8.86			
hy				14.78	13.42			
mt				2.49	2.25			
il				3.55	3.63			
ap				0.83	0.72			

* Total Fe as FeO
Normative calculations assume $Fe_2O_3/FeO = 0.20$

Appendix IIb (cont.)

Deschutes Formation Basalt and Basaltic Andesite Lavas

Unit	Tdba3	Tdba3	Tdba3	Tdba3	Tdba4	Td1	Td1	Td1
Sample	AM30	AM34	TQ34	AM211	AM264	AM251	TQ49	AM127
SiO_2	55.0	55.5	55.3	57.9	54.4	52.9	53.4	57.2
Al_2O_3	16.1	16.6	16.5	16.2	17.9	17.7	18.9	16.6
TiO_2	1.67	1.68	1.72	1.7	1.26	1.13	1.32	2.05
FeO*	9.6	9.7	9.5	9.8	9.1	8.8	8.0	9.0
CaO	7.6	7.6	7.9	7.4	9.8	9.3	9.1	6.4
MgO	3.8	3.6	3.6	3.7	4.7	5.9	4.2	2.4
Na_2O	3.7	3.4	3.8	3.7	3.5	3.7	3.6	4.6
K_2O	1.02	1.05	1.09	0.99	0.50	0.46	0.88	1.03
MnO			0.17				0.14	
P_2O_5			0.34				0.36	
Total	98.49	99.53	99.92	101.39	101.16	99.95	99.90	99.28
Ni			10				44	
Cr			23				77	
Sc			32				20	
V			283				226	
Ba			448				406	
Rb			19				11	
Sr			518				684	
Zr			154				143	
Y			32				23	
Nb			8				8	
Ga			20				19	
Cu			56				84	
Zn			104				86	
Q			5.33		2.96	–	2.30	7.23
or			6.44		2.95	2.72	5.20	6.09
ab			32.15		29.62	31.31	30.46	38.92
an			24.75		31.66	30.33	32.81	21.61
di			10.18		13.99	12.93	8.22	8.52
hy			14.86		15.38	17.19	15.63	10.84
ol			–		–	1.14	–	–
mt			2.35		2.20	2.13	1.93	2.17
il			3.27		2.39	2.15	2.51	3.89
ap			0.79		–	–	0.83	–

* Total Fe as FeO
Normative calculations assume $Fe_2O_3/FeO = 0.2$

Appendix IIb (cont.)

Deschutes Formation Basalt and Basaltic Andesite Lavas

Unit	Td1	Td1	Td1	Td1	Td1	Td1	Td1
Sample	AM304	AM260	AM54	AM269	AM55	TQ47	AM284
SiO_2	56.1	54.5	54.9	56.9	57.3	56.7	56.4
Al_2O_3	15.6	17.5	17.5	16.1	16.1	16.7	16.4
TiO_2	1.97	1.40	1.37	1.59	1.59	1.29	1.87
FeO*	10.9	8.9	8.8	9.7	9.8	7.6	10.3
CaO	7.8	8.0	8.2	7.4	7.6	7.9	7.1
MgO	4.8	4.5	4.4	3.7	4.1	4.3	3.0
Na_2O	3.5	3.8	3.8	4.0	4.1	4.0	4.3
K_2O	0.90	0.80	0.84	1.00	0.99	1.03	0.99
MnO						0.14	
P_2O_5						0.28	
Total	101.57	99.30	99.81	100.39	101.58	99.94	100.36
Ni						25	
Cr						58	
Sc						25	
V						224	
Ba						392	
Rb						17	
Sr						559	
Zr						160	
Y						28	
Nb						8	
Ga						20	
Cu						59	
Zn						87	

	AM304	AM54	AM269	AM55	TQ47
Q	6.13	3.60	6.44	5.74	5.53
or	5.32	4.96	5.91	6.09	5.85
ab	29.62	32.15	33.85	33.85	36.39
an	24.20	28.21	23.02	24.57	22.53
di	11.99	10.28	11.39	10.51	10.65
hy	17.93	15.86	14.41	14.24	13.37
mt	2.64	2.13	2.35	1.84	2.49
il	3.74	2.60	3.02	2.45	3.55
ap	-	-	-	0.65	-

* Total Fe as FeO

TQ72   Porphyritic basalt, Long Butte, NW1/4 sec. 22, T16S, R12E.

AM72   Porphyritic basalt, Long Butte, NW1/4 sec. 22, T16S, R12E.

B108   Cinder, Long Butte cindercone, SW1/4 sec. 22, T16S, R12E,
     (E. M. Taylor, unpublished data).

TQ122   Basalt, Smoky Butte, NE1/4 sec. 25, T16S, R11E.

AM9   Porphyritic basalt, Cline Buttes, NE1/4 sec. 30, T15S, R12E.

TQ9   Porphyritic basalt, Cline Buttes, NE1/4 sec. 30, T15S, R12E.

TQ279   Porphyritic basalt, SE1/4 NW1/4 sec. 11, T16S, R11E.

B142   Porphyritic basalt, SW1/4 sec. 11, T16S, R11E.
     (E. M. Taylor, unpublished data).

AM277   Aphyric basaltic andesite, SE1/4 SE1/4 sec. 20, T16S, R12E.

AM85   Aphyric basaltic andesite, SE1/4 NW1/4 sec. 30, T16S, R12E.

AM78   Aphric basaltic andesite, gravel pit, SE1/4 NW1/4 sec. 27,
     T16S, R12E.

TQ300   Aphyric basaltic andesite, Laidlaw Butte, SE1/4 SE1/4
     sec. 25, T16S, R11E.

TQ219   Aphyric basaltic andesite, fault scarp, center sec. 6,
     T16S, R12E.

AM305   Aphyric basaltic andesite, cindercone on Innes Market Rd.,
     NW1/4 SE1/4 sec.12, T16S, R11E.

AM237   Aphyric basaltic andesite, near power line, NE 1/4 NE 1/4
     sec. 33, T15S, R12E.

AM261   Aphyric basaltic andesite, top of east wall, Deschutes River
     canyon, NE1/4 SW1/4 sec. 35, T15S, R12E.

AM30   Sparsely porphyritic basaltic andesite, SW1/4 SW1/4 sec. 30
     T15S, R12E.

AM34   Sparsely porphyritic basaltic andesite, vent in NW1/4 NE1/4
     sec. 11, T16S, R11E.

TQ34   Sparsely porphyritic basaltic andesite, vent in NW1/4 NW1/4
     sec. 11, T16S, R11E.

AM211   Sparsely porphyritic basaltic andesite, NW1/4 NW1/4 sec. 33,
     T15S, R12E.

AM264   Cinder from low-lying vent on Cline Falls highway, NW1/4
     SW1/4 sec. 5, T16S, R12E.

AM251   Aphyric basalt, southwest wall Deschutes River canyon, SW1/4
     NE1/4 sec. 26, T15S, R12E.

TQ49   Porphyritic basaltic andesite, Awbrey Falls, SE1/4 NW1/4
     sec. 16, T16S, R15E.

AM127   Aphyric basaltic andesite, NE1/4 NE1/4 sec. 14, T16S, R11E.

AM304   Aphyric basaltic andesite, SE1/4 NW1/4 sec. 30, T15S, R12E.

AM260   Porphyritic basaltic andesite, east side Deschutes River
     canyon, SW1/4 SE1/4 sec. 35, T15S, R12E. Same as AM54.

AM54 Porphyritic basaltic andesite, middle flow, west side Deschutes River canyon, NE1/4 SE1/4 sec. 9, T16S, R12E.

AM269 Aphyric basaltic andesite, near fault, north side Deschutes River canyon, SE1/4 SE1/4 sec. 17, T16S, R12E. Same as AM55.

AM55 Aphyric basaltic andesite, top flow, north side Deschutes River canyon, NE 1/4 SE 1/4 sec. 9, T16S, R12E.

TQ47 Aphyric basaltic andesite, top flow, west wall, Deschutes River canyon, NW1/4 SE1/4 sec. 9, T16S, R12E.

AM284 Aphyric basaltic andesite, capping plateau, SW1/4 NW1/4 sec. 14, T16S, R11E.

Appendix IIc

Deschutes Formation Ignimbrites and Debris Flow Deposits

Unit	Tdi	Tdi	Tdi	Tds	Tds	Tds	Tds	Tds	Tds
Sample	TQ57	AM57	AM57a	AM255	AM282	TQ601	AM295	AM303	AM253
SiO_2	67.8	68.2	71.1	71.1	62.6	60.4	67.0	65.3	65.3
Al_2O_3	16.3	16.2	14.7	14.6	16.5	16.8	16.3	15.5	15.9
TiO_2	0.74	0.69	0.33	0.30	1.14	1.37	0.83	0.87	0.89
FeO	4.1	3.9	3.8	3.2	5.4	6.5	4.4	5.7	5.3
CaO	2.8	2.6	1.5	1.6	4.3	5.8	3.0	3.2	3.4
MgO	0.9	1.0	0.2	0.8	1.8	2.3	1.3	1.1	1.3
Na_2O	4.6	4.6	5.4	4.4	5.0	4.6	4.8	4.8	4.5
K_2O	2.33	2.21	2.68	3.63	1.74	1.50	1.87	2.52	2.47
MnO	0.16					0.18			
P_2O_5	0.17					0.50			
Total	99.90	99.44	99.71	99.63	98.48	99.95	99.50	98.99	99.06

Ni	36					11			
Cr	4					1			
Sc	9					18			
V	28					105			
Ba	793					604			
Rb	50					33			
Sr	350					516			
Zr	272					202			
Y	51					44			
Nb	17					14			
Ga	21					20			
Cu	19					35			
Zn	111					115			

TQ57   Rhyodacite pumice, light grey, White Rock ignimbrite, SW1/4 SE1/4 sec. 10, T16S, R12E.

AM57   Rhyodacite pumice, light grey, White Rock ignimbrite, SW1/4 SE1/4 sec. 10, T16S, R12E.

AM57a   Rhyodacite pumice, medium grey, White Rock ignimbrite, SW1/4 SE1/4 sec. 10, T16S, R12E.

AM255   Rhyodacite pumice, white, from ignimbrite in west wall, Deschutes River canyon, NW1/4 SE1/4 sec. 35, T15S, R12E.

AM282   Andesite pumice, black, from ignimbrite in SW1/4 SE1/4 sec. 14, T16S, R11E.

TQ601   Andesite pumice, black, from ignimbrite in SW1/4 SE1/4 sec. 14, T16S, R11E.

AM295   Dacite pumice, pink, from ignimbrite in roadcut, Dayton Rd., SW1/4 NW1/4 sec. 24, T16S, R11E.

AM303   Dacite vitrophyre boulder, southwest flank Cline Buttes, NE1/4 SW1/4 sec. 30, T15S, R12E.

AM253   Dacite vitrophyre clast, Tetherow debris-flow deposit, NE1/4 NE1/4 sec.26, T15S, R12E.

* Total Fe as FeO

Appendix IId

Pleistocene Lavas and Ignimbrites

Unit	Qba	Qba	Qnb	Qdt	Qbp	Qtt
Sample	AM114	AM287	B-1	B-54	Qbp	Qtt
SiO_2	57.05	54.5	49.7	68.8	74	75
Al_2O_3	17.1	18.3	16.9	15.2	14	15
TiO_2	1.51	1.43	1.57	0.65	0.14	0.15
FeO*	8.64	9.97	9.2	3.60	1.9	2.0
CaO	7.32	8.64	9.4	2.2	0.9	0.9
MgO	4.87	4.55	8.4	0.8	0.1	0.1
Na_2O	3.98	3.6	3.5	4.89	4.9	4.6
K_2O	0.83	0.57	0.45	2.95	3.4	3.6
Mn						
P_2O_5						
Total	101.3	101.56	99.12	99.09	99.34	98.35

AM114   Basaltic andesite above Tumalo Tuff in sec. 2, T17S, R11E.

AM287   Basaltic andesite, channel fill in Desert Spring Tuff, sample from roadcut in NE1/4, sec. 6, T17S, R12E.

B-1   Basalt from Newberry volcano, roadcut on highway 20, NE1/4 sec. 6, T17S, R12E (E. M. Taylor, unpublished data).

B-54   Desert Spring Tuff, no location given (Hill and Taylor, in press).

Qbp   Bend Pumice, average of 19 analyses (Hill, 1985).

Qtt   Tumalo Tuff, average of 7 analyses (Hill, 1985).

* Total Fe as FeO